Master's thesis

NTNU
Norwegian University of Science and Technology
Faculty of Information Technology and Electrical Engineering
Department of Electric Power Engineering

Tormod Habbestad Aarnes

High-Power Electric Charging in the Norwegian Distribution Grid

Master's thesis in Electric Power Engineering
Supervisor: Magnus Korpås NTNU and Bendik Nybakk Torsæter SINTEF Energi AS

June 2020

NTNU
Norwegian University of
Science and Technology

Tormod Habbestad Aarnes

High-Power Electric Charging in the Norwegian Distribution Grid

Master's thesis in Electric Power Engineering
Supervisor: Magnus Korpås NTNU and Bendik Nybakk Torsæter
SINTEF Energi AS
June 2020

Norwegian University of Science and Technology
Faculty of Information Technology and Electrical Engineering
Department of Electric Power Engineering

NTNU
Norwegian University of
Science and Technology

Problem Description

This master's thesis is written in collaboration with and is a part of KPN FuChar [30]. FuChar is a KPN project funded by The Research Council of Norway and industry partners (grant no. 295133/E20). The aim of the FuChar project is to minimise investment and operating costs related to the grid integration of electric transport. For that purpose, essential topics like charging behavior of electric vehicles, methods related to the utilization of flexibility of charging infrastructure, as well as strategies for optimal charging infrastructure, are all significant elements toward reaching the goal of FuChar.

The purpose of this thesis is to investigate the grid impacts of a large charging demand from stationary high-power charging stations in the medium-voltage (MV) grid, and also to investigate problems that could interfere with optimal charging infrastructure. In addition to that, strategies that could be implemented to mitigate the impacts of high-power charging will also be examined. The tasks to be performed are the following:

- Develop a MATLAB-based simulation model for analysing different scenarios related to the future grid integration of high-power charging interfaces
- Investigate potential challenges related to grid integration of high-power charging of electric cars
- Investigate different measures to mitigate the supply voltage variations

Supervisor: Magnus Korpås, NTNU Elkraft
Co-Supervisor: Bendik Nybakk Torsæter, SINTEF Energi AS

Abstract

Norway has made a goal of reducing greenhouse gas emissions by 40% by 2030. Due to this, a significant contributor to achieving this goal is the transition to electric transportation. The purpose of this thesis was to investigate how a modelled network responded to high power consumption from high-power charging and alternatives that could be established to reduce the grid impacts, focusing on the supply voltage variations. The network was being examined through load flow analysis, which was executed in MATPOWER, a package tool in MATLAB®. The power flows were based on hourly-resolution profiles for the general loads and the charging load, thus giving a power flow result for each individual hour, simulated through one day.

Several study cases were developed in MATLAB®, represented as different scenarios of charging. The major difference between these charging scenarios was the number of charging outlets, varying from 2 to 20 outlets. Each case was equipped with individual charging outlets of 150kW. Even without any form of charging, the assumed voltage limit of -5% was exceeded for several hours considering high demand months. With the implementation of a charging station consisting of up to six outlets, the results expressed the considerably small impacts of these charging alternatives. The more interesting study case where the power system was exposed to a charging station with 20 outlets, gave an additional voltage drop of 0.92% for the most critical hour, compared to the initial case. In addition to that, the voltage threshold was exceeded for an additional six hours.

The methods used to reduce the grid impacts from electric passenger car (EV) charging were presented as battery storage for peak-shaving and increased cross-section for reducing losses. As a result of these strategies, the voltage was raised above the minimum limit of -5% for the majority of the day. It was concluded that even with a large EV scale and with its high power consumption, the voltage quality could be improved by a considerable amount by using smart and already developed strategies for grid improvements.

Sammendrag

Norge har satt seg et mål om å redusere klimagassutslippene med 40% innen 2030. En betydelig bidragsyter for å nå dette målet er overgangen til elektrisk transport. Hensikten med denne oppgaven var å undersøke hvordan et modellert nettverk responderte på høyeffekt lading med høy andel elbiler og hvordan ulike tiltak kunne redusere påvirkningen av lading av elbil, med fokus på de langvarige spenningsvariasjonene. Nettverket ble undersøkt ved hjelp av lastflytanalyser, som ble utført i MATPOWER, en pakke i MATLAB®. Analysen baserte seg på timesoppløste verdier, hvor det ble utført en lastflytanalyse for hver time, for 24 timer.

Ulike studier ble utført i MATLAB®, representert som forskjellige scenarier av lading. Forskjellen mellom disse ladescenariene var antall ladeuttak, varierende fra 2 til 20 uttak. For hver studie var ladestasjonen utstyrt med individuelle ladeuttak på 150 kW. Selv uten noen form for lading, ble den antatte spenningsgrensen på -5% overskredet flere timer for de høybelastede månedene. Med implementering av en ladestasjon bestående av opptil seks ladeuttak, ga det betydelige små utslag. Det mer interessante scenariet hvor det ble implementert en ladestasjon med 20 ladeuttak, ga et spenningsfall på 0,92% mer enn for scenario en, hvor ingen ladestasjon var tilkoblet. I tillegg til dette ble spenningsgrensen overskredet i ytterligere seks timer.

Metodene som ble brukt for å redusere påvirkningen av elbil lading ble introdusert som batterilagring og økt kabeltverrsnitt. Som et resultat av disse strategiene ble spenningen hevet over minimumsgrensen på -5% for de fleste timene. Det ble konkludert med at selv med en stor andel elbiler og med sitt høye effektbehov, kan spenningskvaliteten forbedres betydelig ved bruk av smarte og allerede utviklede strategier for nettforbedringer.

Preface

This thesis is submitted as the final part of the 2-year master's degree in Electric Power Engineering for the Department of Electric Power Engineering at The Norwegian University of Science and Technology. This work has been motivating and challenging at the same time, but it has also given me theoretical and technical insight into how real problems are approached.

I would like to share my gratitude for my supervisor Magnus Korpås for his extraordinary helpful supervision and inputs, and his motivation and knowledge within the field of research. I would also like to thank Bendik Nybakk Torsæter at SINTEF for his helping hand and guidance, and letting me be part of the FuChar project.

Tormod Habbestad Aarnes
23.06.20

Table of Contents

Problem Description i

Abstract ii

Sammendrag iii

Preface iv

Table of Contents vii

List of Tables ix

List of Figures xi

Abbreviations xii

1 Introduction 1
1.1 Motivation and Background 1
1.2 Scope of Work 2
1.3 Thesis Outline 3

2 Literature Review 4
2.1 Electric Vehicle Consumption and Grid Impacts 4
2.2 Methods to Mitigate the Grid Impacts from Implemented Fast-charging . 5
2.3 Demand Response of Various Strategies of Electric Vehicle Charging . . . 6
2.4 The Effect of Electrical Distancing of EV Charging 7
2.5 Challenges Related to Integration of Electric Taxis and Electric Busses . . 8

3 Theory 9
3.1 Voltage Quality 9
3.2 Power Flow 9
3.2.1 Newton-Raphson Power Flow 9

3.2.2 Current Injection 11

4 Power Grid Modelling in MATLAB **12**
4.1 MATPOWER 12
4.2 MATLAB Modelling Description 12
4.2.1 MATLAB Overview 12
4.2.2 Running a Power Flow 14
4.2.3 Load Modelling 14

5 System Description **15**
5.1 System Topology 15
5.2 Load Data 16
5.2.1 Charging Load 17
5.2.2 General Load Description 18
5.3 Bus Data 20
5.4 Branch Data 20
5.5 Battery Storage 21
5.6 Voltage Limit 22

6 Case Studies **23**
6.1 Case Zero - Initial Condition 23
6.2 Case One - Two Charging Outlets Connected 23
6.3 Case Two - Four Charging Outlets Connected 24
6.4 Case Three - Six Charging Outlets Connected and Increased Traffic Flow of 40% 24
6.5 Case Four - Twenty Charging Outlets Connected and Increased Traffic Flow of 335% 24
6.6 Case Five - Measures for Grid Improvement 25

7 Results **26**
7.1 Case Zero Results - Initial Condition 26
7.1.1 High Demand 26
7.1.2 Low Demand 29
7.2 Case One Results - Two Charging Outlets Connected 32
7.3 Case Two Results - Four Charging Outlets Connected 35
7.4 Case Three Results- Six Charging Outlets and 40% Increased Traffic Flow 38
7.5 Case Four Results - Twenty Charging Outlets and 335% Increased Traffic Flow 39
7.6 Case Five Results - Measures for Grid Improvement 45
7.6.1 Increased Cross-section 45
7.6.2 Implementation of Battery Storage 47

8 Discussion **53**
8.1 Validation of the Modelled Power System 53
8.2 Validation of the Results 54

9 Conclusion **57**

10 Further Work **59**

Bibliography **59**

Appendix A General FASIT Load Profiles **63**
A.1 General Load Demand 64

Appendix B Charging Load Profiles for EV and Battery Storage **65**

Appendix C MATLAB Code **66**
C.1 Load_flow.m File 66
C.2 System_description.m File 68
C.3 Runpf_new.m File 70

List of Tables

5.1 Weather data of Ranheim 16. January 2019 18
5.2 Weather data of Ranheim 16. June 2019 18
5.3 Bus types and their corresponding variables 20
5.4 Specification of BLX overhead line 21
5.5 Branch data 21

7.1 Case zero - Active loads in the system, highest demand hour - high demand 26
7.2 Case zero - Total power loss for 24 hours - high demand 28
7.3 Case zero - Total power injection for 24 hours - high demand 29
7.4 Case zero - Active loads in the system, highest demand hour - low demand 29
7.5 Case zero - Total power loss for 24 hours - low demand 31
7.6 Case zero - Total power injection for 24 hours - low demand 32
7.7 Case one - Active loads in the system, highest demand hour 32
7.8 Charging load demand with two charging outlets and 69% EV penetration 32
7.9 Case one - Total power loss for 24 hours 34
7.10 Case one - Total power injection for 24 hours 34
7.11 Case two - Active loads in the system, highest demand hour 35
7.12 Charging load demand with four charging outlets and 69% EV penetration 36
7.13 Increased current magnitude of line 1-2 for case one and two, compared to high demand of case zero. 37
7.14 Case two - Total power injection for 24 hours 37
7.15 Charging load demand with six charging outlets and 69% EV penetration, day 2 38
7.16 Charging load demand with six charging outlets and 69% EV penetration, day 7 38
7.17 Increased voltage drop of the different radials as a result of the charging load P_{ev10}. It is compared to high demand of case zero 42
7.18 Case four - Total power injection for 24 hours, day 6 44
7.19 Case four - Total power injection for 24 hours, day 10 44
7.20 Case four - Total power loss for 24 hours, day 6 45

7.21 Case four - Total power loss for 24 hours, day 10 45
7.22 Case five - Total power loss for 24 hours with modified transmission lines 46
7.23 Case five - Total power loss for 24 hours with modified transmission lines and battery storage 51

A.1 General load demand for high demand months 64
A.2 General load demand for low demand months 64

B.1 EV charging load profiles for case four, for day 6 and day 10 65
B.2 Power demand for $P_{battery}$ and P_{total} 65

List of Figures

1.1 Number of public charging points in Norway [7] 2

5.1 System overview 16
5.2 A geographical overview of the area that has been examined 19

7.1 Case zero - Voltage magnitude - high demand 27
7.2 Case zero - Current distribution - high demand 28
7.3 Case zero - Voltage magnitude - low demand 30
7.4 Case zero - Current distribution - low demand 31
7.5 Case one - Power demand for all loads excluding P1 and P6 33
7.6 Case one - Voltage magnitude 33
7.7 Case one - Current distribution 34
7.8 Case two - Power demand for all loads excluding P1 and P6 35
7.9 Case two - Voltage magnitude 37
7.10 Case three - Power demand for all loads, six charging outlets and 40% increased traffic flow 38
7.11 Case three - Voltage magnitude 39
7.12 Case four - Power demand for all loads excluding P1 and P6, twenty charging outlets and 335% increased traffic flow 40
7.13 Case four - Power demand for all loads, twenty charging outlets and 335% increased traffic flow 41
7.14 Case four - Voltage magnitude 42
7.15 Case four - Additional voltage drop as a result of charging load P_{ev10}, compared to high demand of case zero. The P_{ev10} load is related to the left y-axis, while the remaining voltage curves are referred to the right y-axis 43
7.16 Case four - Current distribution 44
7.17 Case five - Voltage magnitude comparison of case four and increased cross section 46
7.18 Case five - Power losses for transmission line 2-3 and 10-11, comparison of case four and increased cross section 47

7.19 Case five - Power demand from modified charging load, including the battery charging and discharging 48
7.20 Case five - Voltage magnitude 49
7.21 Case five - Voltage magnitude for bus 11 when the system is being exposed to EV charging and different strategies to of grid improvement 50
7.22 Case five - Current distribution with increased cross section in addition to battery storage 51
7.23 Case five - Active power losses as a result of varying current distribution for transmission line 1-2. Comparison of modified transmission lines and implementation of battery storage 52

Abbreviations

BSS	Battery Swapping Stations
DSO	Distribution System Operator
EB	Electric Buses
ET	Electric Taxis
EU	European Union
EV	Electric Passenger Car
HV	High-voltage
ICE	Internal Combustion Engine
LV	Low-voltage
MV	Medium-voltage
NVE	The Norwegian Water Resources and Energy Directorate
SoC	State of Charge

Chapter 1

Introduction

1.1 Motivation and Background

The goal of the Paris Agreements is to reduce global warming, more specifically its purpose is to reduce the temperature below 2°C. For the transport sector, this means that the focus is moving away from the internal combustion engine (ICE) and more towards low or zero-emission vehicles. Based on statistical measures from SSB [29], road traffic contributed to 56% of the total greenhouse gas emissions coming from the transport sector in 2017. Looking at the bigger picture, the transport sector contributes to almost one-third of the total greenhouse gas emissions in Norway. This emphasises the reduction that could potentially come from the transport sector when aiming towards low emission vehicles. Norway has set a target of a 40% reduction of greenhouse gas emissions by 2030 and becoming a low-emission society by 2050.

Norway is said to have taken the leading role within electric mobility, including solutions to electric transport but also for developments of electric solution within shipping. With its expertise within electric mobility, Norway has 80% electrified rail transport, introduced electric vessels or hybrid vessels, and also the highest share of electric cars considering all new sold passenger vehicles. Looking at the infrastructure of normal charging and fast-charging points, Norway has made more progress than any other nation. As a leading example, Norway's pioneering role of electrification of transport can hopefully have a vital role in the transition to electric mobility on a worldwide basis [11].

Already in 2010, the market of electric vehicles in Norway started to increase drastically, first off with the popular Nissan LEAF and Mitsubishi i-MiEV. Before the market skyrocketed, the need for public charging stations were minimal. People charged their cars at home or at work, thus the need for public charging were limited. As of today, the electric passenger car (EV) market share has boomed, which results in more vehicles that need to charge. To satisfy this increase of EVs, public charging station becomes a viable option, not only does it provide the already existing customers with an alternative way of charging, but it also makes the foundation for an even further expansion in the EV market. The high increase in the EV market in Norway has been accomplished due to several incentives that have made EV become a more viable option, compared to diesel and petrol cars. The Norwegian government has also played a more significant role in the development of charging infrastructure, where 100% of the installation cost of standard chargers for up to a total of NOK 50 million were covered by the Norwegian government, within a particular limitation per charging point [19].

In 2015, Enova came up with a scheme for implementation of fast-chargers, where it was proposed to implement these chargers every 50 km along the Norwegian main roads. It was suggested that every charging point would have a CHAdeMO and CSS fast charger, in addition to a few smaller outlets. This support scheme provoked the expansion of fast-chargers, but it also showed that fast charging operators were expanding throughout cities and along highways without any public support. Figure 1.1 illustrates how the various types of charging alternatives have increased throughout the years. As seen from this figure, the regular charging option has had a slow increase over the past years, while on the other hand, the implementation of fast-chargers has increased by a considerable amount over the last five years [19].

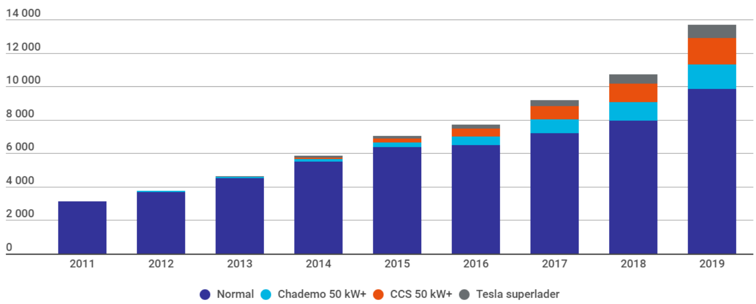

Figure 1.1: Number of public charging points in Norway [7]

A major issue related to the fast-growing EV expansion is the power grid, and how it will handle a substantial and fast increase. As of today, spare capacity in the grid is what gives EV consumers easy accessible energy, but as of a future perspective, the spare capacity might not be enough to handle a high penetration of EV.

1.2 Scope of Work

This thesis will look at how various EV charging scenarios are affecting the voltage quality of the power grid, using the package tool MATPOWER in MATLAB®. Furthermore, it investigates the current flow and power distribution, how one charging alternative is different from another, and what measures can be done to mitigate the grid impacts. In this thesis, grid impacts are more specifically referred to as the impact on the supply voltage variations. The system is modelled as a single phase network, which means that asymmetry will not be taken into account. The network that has been modelled is based on a location outside Trondheim. However, no actual customer data or specifications of this area have been retrieved, but instead assumed and simplified based on The Norwegian Water Resources and Energy Directorate's (NVE) geographical map of medium-voltage (MV) grid and general load profiles made by SINTEF. The EV charging profiles that are used to represent the charging load are modelled in another project thesis [13].

1.3 Thesis Outline

The outline of this thesis is expressed as 10 different chapters. *Chapter 1* presents the motivation and background for this thesis, in addition to its limitations. From various literature studies, challenges and strategies that can be related to implementation of EVs are reviewed in *Chapter 2*. The useful background theory for the purpose of this thesis is found in *Chapter 3*. *Chapter 4* is expressing briefly how the power system is modelled in the software that is used. The description and modelling of the system that is analysed in this thesis is shown in *Chapter 5*. *Chapter 6* is describing the variety of study cases that are being investigated in this thesis. The corresponding results from each of these study cases are presented in *Chapter 7*. The discussion of the results are found in *Chapter 8*, and the conclusion for this thesis can be reviewed in *Chapter 9*. *Chapter 10* gives suggestions for further work. This chapter discuss how this thesis could be expanded, additional studies that could be examined, and further improvements.

Chapter 2

Literature Review

The number of vehicles that could be tied up to electric mobility is constantly increasing and thus contributing to an environmentally friendly globe by reducing the CO_2 emission. Moving away from fossil fuel cars and more towards electric vehicles or hybrid mobility will help to reach the climate goals of lower greenhouse gas emissions. On the other hand, this enormous increase in electric mobility creates a never ending increase in the electric power demand. A challenge related to the electric power grid is the increasing demand, and how the infrastructure will be able to withstand this increase. When considering the charging of an EV, it can be hard to predict the outcome of this due to the dynamic complexity charging, when it takes place, how fast it charges, and the power consumption of both active and reactive power [4].

2.1 Electric Vehicle Consumption and Grid Impacts

When looking at the impacts of EVs, some factors that have to be considered like when do people tend to charge and how often do they charge, and whether these charging locations will cause necessary grid upgrades or not. These rely on the number of EVs that are present and how significant a portion this is to the total electricity demand. For instance, a study from [15] assumed that the EV penetration for an EV-high scenario of the European Union's (EU) car fleet would reach 80% in 2050. In terms of an average value for the 28-EU countries, the EV demand share would equal roughly 9.5%, compared to the total electricity demand. This number will most likely require grid upgrades from several distribution system operators (DSO), mainly if this happens during high demand hours [22].

Another study regarding a normal American highway with fast charging stations with a total demand of 1200kW showed that adjustments were needed to maintain the power balance. An additional transformer was essential in order to supply this extra power, or other grid upgrades that would compensate for this increase in power. This amount of power covered 5-10% of the rated power of a typical transmission line in the United States. China examined 27 residential communities and looked at the effect of fast-charging stations. The results showed that 21 out of 27 communities needed to upgrade the corresponding distribution transformer when considering 20% EV share [22].

In a study of Germany [27], approximately one million electric cars would increase the electricity demand with 1.5%. It was also described how a market with 42 million EVs would explode the demand by 92% of the total power supply. Combining the general load and a clean structured load from EV charging, it would still have a noticeable impact on the power grid. When that is said, EV could potentially have some good use if the power generated in the system consisted of mainly renewable sources. If a flexible scheme of charging were considered, it could somewhat outweigh the natural problems related to the variability of power sources.

A study regarding the availability of 50kW chargers based on transformers' spare capacity in an existing San Francisco grid showed some diverse results. In this study, the transformers capacity map showed San Francisco more or less divided into two separate areas. The residential area had less spare capacity of transformers, thus fast chargers were limited to less than two in most of the general locations in that area. Unlike the residential area, the central business district had in most places the capability of more than four EV fast chargers [21], although these two areas were laying only a couple of km apart.

2.2 Methods to Mitigate the Grid Impacts from Implemented Fast-charging

With the implementation of fast-charging stations, problems related to utility upgrades or transformers capacity will be the major factors determining whether the grid can handle the charging. When that is said, there are strategies to reduce these impacts, like choosing a location with lower demand, energy storage, and smart charging [22]. These strategies are briefly described below.

By implementing fast-charging stations at places where there is considerably higher spare capacity or the cost of installation is lower, it will reduce the impacts from a utility point of view. Areas with more available capacity are most likely not to provoke voltage problems or an overloaded system. However, some locations may be appropriate for the utilities but not as convenient for the consumers. Various areas with unequal distributed grid capacity can easily be mitigated by having vehicles move to places having higher spare capacity.

Secondly, the smart charging of vehicles is another way to mitigate grid impacts. Smart charging gives the opportunity for charging vehicles to be started and stopped by signals from the utility grid. The purpose of this is to have the grid and the charger communicate to not exceed any limits. By having a more extensive site consisting of several chargers where all charges are occupied at the same time, the output power will have to be limited in some way to not reach a threshold.

During the later years, energy storage is a phenomenon that has been taken more into consideration when looking at how the power can be utilized in the best possible way. Under normal conditions, the vehicles can charge as usual, through the power grid or other renewable energy sources. At periods where the demand is already high and closing in on the limits, energy storage can be used as a supply and distribute the necessary power without exceeding threshold. This backup power source will not only reduce the grid impacts, but also contribute to significantly higher savings.

At last, another strategy is to adjust the charging prices based on when the charging takes place. For instance, having a higher charging price during high demand peaks and the other way around. For transmission lines, transformers, and generators, this could be a good way to mitigate the grid impacts [10].

2.3 Demand Response of Various Strategies of Electric Vehicle Charging

From a study carried out from Perth Australia, it showed how EV would affect the power system in terms of charging the vehicles in the electric grid, assuming a high EV penetration. The study examined how much of the spare capacity that could be used for EV charging, considering both annual peak day and average peak load. The results emphasised the importance of having the EVs charge during the right period of time. Looking at the spare capacity at annual peak day it showed that it was only enough to handle 7% EV penetration, while on the other hand, it was capable of handling 59% EV penetration when considering an average peak day. Achieving a full EV penetration and with no new generation in addition to meeting the demand supply balance, 93% and 41% of the EV load had to be moved to off-peak hours, for annual and average peak, respectively [20].

Another study regarding a power grid in the UK discussed how the power grid was affected by a variety of EV home charging alternatives. Three study cases were examined where 10%, 20%, and 30% of houses were equipped with home charging, charging at 10A continuously for six hours. The strategy of no control units or incentives for demand scheduling showed an increase of 18% to the maximum demand for each 10% increase in home charging. However, if a scheduled charging system were taken into account, the highest peak demand was kept unaffected, thus EV charging had no impact on the system's capacity [25].

A study carried out by [18], it was investigated how a large deployment of EV with different strategies of charging would impact the electric grid. The different strategies were the use of dumb charging, smart charging, and dual tariffs, which is a strategy where the electricity prices are changed based on the hour of consumption. The grid investigated was a 15 kV large network consisting of two input feeders, representing a semi-urban meshed network. The charging that took place in this paper was based upon home charging with output power varying from 1.5kW to 6kW, and assuming that all charging was active for 4 hours, from start to end.

First off, the dumb charging strategy, which means that there is no controllable source of when charging takes place, had an allowable share of 10% EV. This strategy gave an additional peak value of roughly 2.0 MW on top of the already existing system peak of 18 MW, at 21:00. The buses located furthest away, hence the most critical buses concerning the voltage level, experienced an additional voltage drop of 1.0 and 1.1 %. Some of the corresponding buses had voltages as low as 0.951 pu with dumb charging, which is relatively close to the voltage lower limit of 0.95 pu. Furthermore, the transmission line loading of the highest loaded line showed an increase from 71.7% to 80.1% of its rated capacity. Due to the considerably high increase in the voltage drop and transmission line loading, and by the fact that charging demand of dumb charging appeared at the systems peak hour, the highest level of EV penetration without exceeding any limitations was 10%.

However, the strategy of dual tariffs and smart charging showed improving results with a considerably higher share of EV. With the integration of these two strategies, the EV share could be increased to 14% for dual tariffs and 52% for smart charging. That is an increase of more than five times compared to the dumb charging and was a result of having the EV peaks shifted to the valley hours. With these three different levels of EV share, the voltage losses and transmission line ratings of the most affected lines were more or less equal, thus emphasising the benefits of having a controlled charging system. Another interesting investigation was how the power losses were distributed during the three study cases. Since loads of smart charging were distributed more uniformly throughout the day, it also reduced the high current peaks that would usually be present for dumb charging. By having the more uniformly distribution of EV load, the current peaks were shaved off, thus resulting in lower losses since losses are expressed as the square of the current.

By controlling the charging pattern with incentives, lower tariffs, or charging limitations, this could save the grid operators necessary grid investments. The respective studies showed how a controlled charging pattern would improve the power balance by moving the EV charging from peak hours to low demand hours. By now, most residential consumers are equipped with a smart metering system which gives a significant demand response, allowing vehicles and power grid to communicate in order to maintain a supply demand balance [20].

2.4 The Effect of Electrical Distancing of EV Charging

From a study carried out from Howard University, it showed how electrical distancing of EV charging stations, measured in ohms, would affect the voltage quality of the power grid [12]. The EV load was modelled as a time-varying load based on statistical methods and data based on vehicle user behavior. The two systems that were examined were a 13-bus system and 5-feeder test circuit.

For each study case there were three scenarios, represented as near bus, mid bus, and far bus, based on the electrical distancing from the feeder. The keynotes from the power flow of the 13-bus system considering an EV load of 360 kW, showed that the voltage limits were exceeded when the mid bus and far bus were examined, two hours and six hours of violation, respectively.

Looking at the results from the power flow of the 5-feeder bigger network where the EV penetration varied from 10% at 496 kW and to 40% at 1985 kW, it showed a great voltage deviation when comparing the near bus and far bus. For the near bus with 30 % EV penetration, no violations were exceeded, however, the far bus and 30% penetration expressed 17 hours of voltage violation of more than 5% voltage drop.

2.5 Challenges Related to Integration of Electric Taxis and Electric Busses

Up until now, the main field of research has been on EV. The introduction of electric taxis (ET) and electric buses (EB) in electric power grids could raise additional grid challenges. These vehicles will have higher consumption, thus the time during charging will be a more critical period [3].

A study carried out by [16], investigated the load impacts of regular battery charging and battery swapping stations (BSS), which is a station for customers to turn in a discharged battery and get a fully charged one in return. The results showed that the power demand peaks generated from fast electric vehicle charging were more critical than what generated from the swapping station. Considering implementation of large scale ET, an interesting challenge is the charging infrastructure, finding the most optimal place for a charging station in order to reduce downtime for the drivers. Moreover, the downtime coming from charging is not convenient for the drivers as they may have to turn down customers [2].

A study [5] investigated how energy storage systems (ESS) could benefit the EB's fast-charging system. The results showed that ESS reduced the total cost by 22.85% by shaving the peak loads and lowering the investment costs due to lower required ratings for transformers and other components. Furthermore, the ESS was also reducing the cost due to the purchase of electricity from the grid through price arbitrage. Likewise to ET, the implementation of EB [17] also have the characteristic regarding the time scheduled routes. This means that the EB still has to satisfy the customers' demand, thus charging the batteries has to be a part of the route or by having a scheduled period for charging. Considering EB on a larger scale, there are also challenges related to grid impacts due to the high power demand. Resulting problems associated with the heavy power demand from a source like high EB penetration could be power quality, harmonic pollution, and higher voltage fluctuations [32].

Chapter 3

Theory

3.1 Voltage Quality

NVE is responsible for water and energy management in Norway. They have made a report regarding the voltage quality and requirements for Norwegian utility companies. This report, Regulations regarding the Quality of Supply, states that supply voltage variations with mean values over 1 minute are to be within the limit of $\pm 10\%$ for voltages up to 1.0 kV. There are no regulations for the high-voltage (HV) quality, other than that the low-voltage (LV) has to be within the specified limit for the end-user [23].

3.2 Power Flow

Section 3.2.1 is extracted from a project report made prior to this thesis. The relevant background information on power flow are identical for both of these project, thus no new relevant literature is carried out for this specified section of the thesis [1].

3.2.1 Newton-Raphson Power Flow

Newton-Raphson is a wide application for solving nonlinear algebraic equations. The method is based on Newton's method which is an operation that starts of with an initial estimate for the unknown values, and by help of Taylor's series expansion the Newton-Raphshon solution is found through an iterative process [28].

The first step in order to solve a newton-Raphson power flow is to calculate the parameters that will be used throughout the iteration process. Admittance bus Y_{bus} can be expressed in terms of susceptance B and conductance G. The net current injection on each bus can then be calculated by help of Y_{bus} and the corresponding bus voltage V,

$$I_{bus} = Y_{bus} V_{bus} \tag{3.1}$$

Equation 3.1 can be made more general by representing it as in form of numbers of busses in the system.

$$I_k = \sum_{n=1}^{N} Y_{kn} V_n \tag{3.2}$$

N is number of busses and k is the specific bus number that are being examined. For the specific bus k, the complex power that are being transmitted can be expressed as

$$S_k = P_k + jQ_k = V_k I_k^* \tag{3.3}$$

Inserting equation 3.2 into equation 3.3, one can obtain the power balance equations, using rectangular coordinates G and jB from the Y_{bus}.

$$P_k = V_k \sum_{n=1}^{N} V_n (G_{kn} cos(\delta_k - \delta_n) + B_{kn} sin(\delta_k - \delta_n)) \tag{3.4}$$

$$Q_k = V_k \sum_{n=1}^{N} V_n (G_{kn} sin(\delta_k - \delta_n) - B_{kn} cos(\delta_k - \delta_n)) \qquad k = 1, 2, ..., N \tag{3.5}$$

The three vectors that are used in order to solve for the Newton-Raphson power flow problem are as follows, the vector x, the vector of power load y, and $f(x)$ which is the net injection computed from 3.4 and 3.5.

$$x = \begin{bmatrix} \delta \\ V \end{bmatrix} = \begin{bmatrix} \delta_2 \\ \vdots \\ \delta_N \\ V_2 \\ \vdots \\ V_N \end{bmatrix} ; \quad y = \begin{bmatrix} P \\ Q \end{bmatrix} = \begin{bmatrix} P_2 \\ \vdots \\ P_N \\ Q_N \\ \vdots \\ Q_N \end{bmatrix} ; \quad f(x) = \begin{bmatrix} P(x) \\ Q(x) \end{bmatrix} = \begin{bmatrix} P_2(x) \\ \vdots \\ P_N(x) \\ Q_2(x) \\ \vdots \\ Q_N(x) \end{bmatrix} \tag{3.6}$$

Bus 1 is used as slack bus in equation 3.6 and thus the already known slack bus voltage magnitude and angle are removed from this equation. By assuming a flat start i.e. forcing all voltage magnitudes to equal 1.0 pu and voltage angels equal zero, then $x(i)$ is found. The next step is to compute the mismatch vector $\Delta y(i)$

$$\Delta y(i) = \begin{bmatrix} \Delta P(i) \\ \Delta Q(i) \end{bmatrix} = \begin{bmatrix} P - P(x(i)) \\ Q - Q(x(i)) \end{bmatrix} \tag{3.7}$$

whereas P and Q are the specified loads in pu value, and the subtracting part is equal to $f(x)$in equation 3.6. In order to solve the last and final equation,

$$J(i) \Delta x(i) = \Delta y(i) \tag{3.8}$$

Jacobian $J(i)$ has to be calculated. The Jacobian is representing the partial derivatives of the power balance equation stated in expression 3.4 and 3.5 with respect to all the variables stated in x. By inverting $J(i)$, the resulting correction vector can be found as

$$\Delta x(i) = J^{-1}(i)\Delta y(i) \tag{3.9}$$

The first iteration is now finished. In order to start the next iteration, the voltage correction vector is added to the initial voltage magnitudes and angles, in this case the flat start values [14].

3.2.2 Current Injection

The current flowing in a transmission line can be expressed as the voltage drop over this specific line, times the admittance. For instance if there are two arbitrary buses i and j connected by a transmission line with admittance y_{ij}, the current flowing in this branch is found by equation 3.10 [28, p.251].

$$I_{ij} = I_l + I_{i0} = y_{ij}(V_i - V_j) + y_{i0}V_i \tag{3.10}$$

whereas the last term on the righ-hand side can be neglected if no shunt capacitance is considered.

Chapter 4

Power Grid Modelling in MATLAB

4.1 MATPOWER

MATPOWER [33] is an open source simulating package used in MATLAB® for power flow analysis, with the possibility of executing AC, DC or Optimal power flow. It is a tool that is easy to modify and user friendly for researchers and educators [34]. Throughout this thesis, MATPOWER will be used to produce the results given in chapter 7. The use of each MATPOWER functionality will be described in more detail in section 4.2.

4.2 MATLAB Modelling Description

4.2.1 MATLAB Overview

This section will give a brief overview of the MATLAB scripts that have been used, and the purpose of each of these. All of the different scripts used are summarized below,

- $runpf\_new.m$
- $Load\_flow.m$
- $System\_description.m$

runpf_new.m

This is a made script from MATPOWER called *runpf.m* consisting mainly of the function *runpf()* which is used in order to run a power flow. For this thesis it contains some additional information, hence the name new. Script *runpf_new.m* is attached to appendix C.3.

Load_flow.m

The purpose of this script is to run all the necessary power flows by the use of function *runpf()* which is found in *runpf_new.m*. Despite the fact that this study examines the behavior of a power system over a certain time period, one power flow has to be executed for each time interval that is being investigated. For this thesis, the interval is set to 24 to represent each hour through one day, thus *runpf()* is inserted into a loop for each of the intervals. The *Load_flow.m* script is showed in appendix C.1.

System_description.m

This is the script where all data for the given network is inserted, hence the data that has been presented in chapter 5. It consists of four sections regarding *base MVA*, *branch data*, *generator data* and *bus data*. For the specific system used in this thesis, only the key variables are specified since many of the remaining variables are not valid for a normal power flow, but rather used for optimal or DC power flow. Take note that *'casefile'* in section 4.2.2 is referred to this particular file. This script can be found in appendix C.2.

Base MVA

For this section there is only one possible variable, which is the system global MVA base.

Bus Data

The variables that are specified for the bus data of the given system illustrated in figure 5.1 are shown below.

- bus i: bus number
- type: type of bus, PV, PQ or swing bus
- Pd: real power demand (MW)
- Qd: reactive power demand (MVAr)
- Vm: voltage magnitude (pu)
- Va: voltage angle (degrees)
- base kV: base voltage (kV)

Pd and Qd are referred to the power demand of any specific load that is connected to bus i.

Generator Data

There are no physical generators present in the system. However, the slack bus in the system is in reality connected to an external grid. The external grid can be represented as a generator providing the main grid with the necessary power.

- bus: bus number
- Vg: voltage magnitude setpoint (pu)

Branch Data

The input variables used to model the transmission lines are represented below.

- fbus: from bus number
- tbus: to bus number
- r: resistance (pu)
- x: reactance (pu)

4.2.2 Running a Power Flow

As mentioned in section 4.2.1, power flow can be executed by the function called *runpf()*. In order to run a proper load flow in MATPOWER there are some additional inputs that will be needed, showed in expression 4.1.

$$runpf(casefile, mpopt, filename, result, other); \tag{4.1}$$

The first input *'casefile'*, is referred to as the script *System_description.m* described in the previous section. Upon running the power flow, a new file *'filename'* will be made, containing the results from the power flow. Likewise, it will also be created a new script *'result'* that consists of all the updated variables for branch, bus and generator data in a MATLAB format. It is also possible to include other optional inputs, expressed as *'other'*. There are some MATPOWER options, hence the name *'mpopt'* that will have to be specifically chosen. The expression below shows what options that are used throughout this thesis. The power flow algorithm, *'pf.alg'*, is restricted to Newton Raphson, *'NR'*, and the tolerance level of the power mismatch, *'pf.tol'*, is defined as *'1e-4'*.

$$mpopt = mpoption(pf.alg, NR, pf.tol, 1e-4); \tag{4.2}$$

4.2.3 Load Modelling

All the loads including the charging loads and the general loads that are used in the MATLAB model have been approached in a similar way. From appendix A.1, these expressed values of the general loads have been extracted from an excel sheet by simple integrated MATLAB functions. For each of the iterations described in section 4.2.1, the individual power demand from the general loads and the charging load for a an arbitrary hour is used in order to obtain the power values for that specific hour.

The battery storage that will be described in more details in section 5.5, is implemented in the MATLAB model in the same approach as for the remaining loads. When the battery will be implemented in section 6.6, it will be represented as one common load that includes the charging load and the charging and discharging of the battery, see table B.2 in appendix B. The battery supply and demand will be subtracted and added to the already existing EV charging load.

Chapter 5

System Description

In this chapter, a brief description of the system will be given. The purpose is to give insight in how the system is modelled, what area is being examined, how various components are estimated, how the EV load is obtained, and how the general loads in the system are modelled.

5.1 System Topology

The power system that will be examined in this thesis is illustrated in figure 5.1. As shown, the network is an 11 bus system with one feeder and seven loads and is visually represented as a radial network of 24kV. The system is developed based on the MV grid overview from NVE [31] of the rural area Vikhammer-Hommelvika, outside of Trondheim. From NVE's data of the electrical grid in the respective area, figure 5.1 is based on the location starting off from the transformer station with ID 14757 close to Hønstad. This transformer is fed from the regional power lines of 132kV and is transformed down to 24kV, which is the voltage level for this network. See figure 5.2 for a detailed overview of the area that has been investigated.

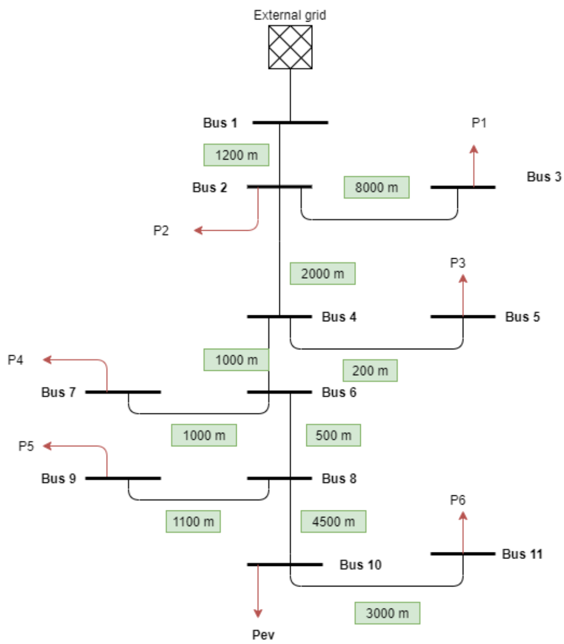

Figure 5.1: System overview

The reasoning for the chosen location is because it is a good representation of a rural area with both agriculture and spread out households, schools, and department stores. It also gives a representation of a power system consisting of long transmission lines, areas with lower consumption, and areas with higher consumption from service providers and neighborhoods and so forth. Another reasonable statement for the chosen location is that the charging load described later in section 5.2.1 is based on the traffic flow and the environment of a close by area.

As illustrated in figure 5.1, the system only consists of one feeder, which is visually expressed as the External grid. This means that all power that is being injected into the system is coming from this grid. By having only one feeder, one can study in detail the power quality, voltage deviations, and the current distribution, from start to end without having any additional feeding points.

5.2 Load Data

There are two different types of loads in this given network. P_{ev} is represented as the only charging station that will be used throughout this study. All the remaining loads from P1-P6 are loads represented general loads, including households, agriculture, schools, and department stores. In the sections below, a more detailed description of these two types of loads will be explained.

For this thesis, the reactive power for both the general and the charging load is defined by the same power factor. This power factor is set to $cos(\varphi) = 0.95$ to provoke some voltage fluctuations, and still being kept within the boundaries of a realistic power system. According to [28], the active and reactive power can be expressed as,

$$P = |V||I|cos(\varphi) \qquad Q = |V||I|sin(\varphi) \tag{5.1}$$

Combining these two equations, it gives a simplified expression of the reactive power Q, which is based on the power factor and also the active power. This equation is implemented in the MATLAB model to calculate all the corresponding reactive power demands.

$$Q = P * tan(cos^{-1}(\varphi)) \tag{5.2}$$

5.2.1 Charging Load

The charging station load is represented as P_{ev} in figure 5.2. The charging station is placed at a gas station close to the highway, which is a considerably good place regarding the traffic flow in the area. The station's location is far from the main feeder in order for the EV charging to have a greater impact on the power system, which is a significant part of this thesis. Another essential element for the chosen location is the charging load profiles, where these are based upon data from the same area as the system's topology, outside of Trondheim. These charging load profiles are generated from another study that focuses on demand modelling of high-power EV charging [13]. This modelling is based on elements like traffic flow, state of charge (SoC), queuing, number of outlets, output power, EV share rate. The load profiles are generated as minute-resolution and illustrate how the total charging power shifts over 24 hours. Despite the fact that this thesis uses hourly-based values, the load profiles that are generated are transformed into average power demand for each hour.

There are three user inputs needed to obtain the charging load profiles, charging output power per outlet, EV market share, and numbers of charging outlets. The model used to obtain the charging load profiles is generating 10 different profiles, which can be characterized as 10 arbitrary days. This model uses Poisson implementations, thus the outcome will have a stochastic effect on the number of vehicles entering and leaving the area. This means that even with similar inputs, the generated profiles will vary from one another.

Charging Output Power

The charging output power is limited to 150 kW per outlet due to the car roster used to generate load profiles are not capable of charging with higher power. Since this thesis examines the impact of high-power charging, it is reasonable to use the highest possible power output of 150kW all through this study.

Numbers of Charging Outlets

The number of charging outlets that are active will vary through different study cases and will be discussed in more detail in chapter 6.

EV Penetration

According to [9] it is assumed that in 2030 the EV share will be roughly 69% including plug-in hybrid, given that all new sold passenger cars in 2025 are zero-emission vehicles. The EV penetration level that will be used throughout this thesis is therefore set to 69%.

5.2.2 General Load Description

The general load profiles P1-P6 are created by using of a model made by SINTEF [8], general FASIT load profiles. These profiles are hourly-resolution profiles used to indicate the hourly demand for specific load groups throughout different seasons and different levels of demand. Each of these groups is representing a unique load group and can be temperature adjusted based on a chosen day with a specific set of temperature data. The equation used to express the power demand for each load in the system is given by equation 5.3.

$$P_{d,h} = A_{d,h}T_d + B_{d,h} \tag{5.3}$$

$P_{d,h}$ is characterized as the energy demand for day d and hour h. $A_{d,h}$ is a coefficient that will be multiplied with a temperature T_d, and together it will express the temperature adjusted energy demand. $B_{d,h}$ is a constant that is different for each load group and for each of the 24 hours. The values for A and B are found in appendix A for each of the 11 load groups.

There are four distinct types of each load group depending on seasonal variations and the day of the week, which are represented as high demand, low demand, weekday, and weekend. High demand is characterized as the winter months, January, February and December, while low demand is represented the remaining months. The temperature that will be used in all accounts for this thesis are two distinctive weather data set gathered from The Norwegian Meteorological Institute of Ranheim, which is the closest area with available weather data [24]. Two different days for high and low demand are chosen, 16. January 2019 and 16. June 2019, respectively. Tables 5.1 and 5.2 shows the weather data that is used for this thesis.

Table 5.1: Weather data of Ranheim 16. January 2019

Time period	**0000-0100**	**0100-0200**	**0200-0300**	**0300-0400**	**0400-0500**	**0500-0600**	**0600-0700**	**0700-0800**	**0800-0900**	**0900-1000**	**1000-1100**	**1100-1200**
Degree [$^\circ C$]	-8	-8,2	-9,2	-7,4	-7,8	-8,5	-7,6	-7,5	-7,5	-7,4	-6,3	-5,7
Time period	**1200-1300**	**1300-1400**	**1400-1500**	**1500-1600**	**1600-1700**	**1700-1800**	**1800-1900**	**1900-2000**	**2000-2100**	**2100-2200**	**2200-2300**	**2300-2400**
Degree [$^\circ C$]	-4,9	-4,2	-4	-4,2	-4,3	-4,9	-6,8	-6	-4,7	-4,6	-4,8	-4,8

Table 5.2: Weather data of Ranheim 16. June 2019

Time period	**0000-0100**	**0100-0200**	**0200-0300**	**0300-0400**	**0400-0500**	**0500-0600**	**0600-0700**	**0700-0800**	**0800-0900**	**0900-1000**	**1000-1100**	**1100-1200**
Degree [$^\circ C$]	11,1	11,2	11,2	11,4	12,9	14,9	15,8	15,7	17,8	18,7	19,4	22,1
Time period	**1200-1300**	**1300-1400**	**1400-1500**	**1500-1600**	**1600-1700**	**1700-1800**	**1800-1900**	**1900-2000**	**2000-2100**	**2100-2200**	**2200-2300**	**2300-2400**
Degree [$^\circ C$]	23,2	24	22,3	23,9	23,8	21,7	20,3	19,1	17,5	15,9	14,9	13,6

General Load Approximation

From NVE's grid overview, each of the six general loads has been roughly estimated by looking at the map and counting the number of consumers. The map of Vikhammer-

Hommelvika has been divided into six geographical areas represented by each of the loads, P1-P6. All the consumers in one area have been clustered together as one load. An overview of the specific area that has been investigated is shown in figure 5.2.

Figure 5.2: A geographical overview of the area that has been examined

Load P6 is characterized as a big load consisting of household consumers, agriculture, department stores, and a few schools. Likewise to P6, P1 is also a considerably big load with mostly the same type of consumers, except for department stores. These two loads are placed at each end of the network, one close to the main feeder and the other far away. On the other hand, P2-P5 are small loads in contrast to P1 and P6 and are distributed along the spine of the network. The size of each load will be summarized below.

- P1: 580 households, 30 agriculture, 4 schools
- P2: 16 households, 4 agriculture
- P3: 13 households, 7 agriculture
- P4: 20 households, 6 agriculture
- P5: 33 households, 10 agriculture
- P6: 510 households, 30 agriculture, 2 schools, 7 department stores

The total power consumption for each load is found in appendix A.1. These values are given in kW and are transformed into MW in the MATLAB model. These values are only represented as weekday loads due to the power demand for weekends is quite similar. On the other hand, the difference between high demand and low demand is quite some and can range up to 2 MW deviation for one specific hour. This gives us two distinctive load types that will be examined, weekday and high demand, and weekday and low demand.

5.3 Bus Data

Parts of the section below, including table 5.3, is retrieved from earlier work [1] with no new additional materials or information.

For each bus in a power system there are three distinguished bus types;

- Slack bus or swing bus, used as a reference bus
- PQ bus, load bus
- PV bus, bus with connected generating units

The swing bus has voltage magnitude and angle as input. For the swing bus it is convenient to have the voltage magnitude close to 1.0 pu and the voltage angle at zero degrees. When a power flow solution is computed, it gives the resultant active and reactive power for the slack bus. As of the PQ bus, the input parameters are active and reactive power. In contrast to the slack bus, the outputs are now voltage magnitude and angle. As the name implies, the input variables for the PV bus are active power and voltage magnitude [14]. Different bus types are summarized in 5.3.

Table 5.3: Bus types and their corresponding variables

Type of bus	Known	Unknown
$Slack$	V, δ	P, Q
PQ	P, Q	V, δ
PV	P, V	Q, δ

In figure 5.1, all buses are visually presented. Each of these buses will be considered as one of the mentioned bus types from table 5.3. There are no generator or shunt elements in the system, hence no PV bus present. Bus 1 is considered the slack bus, while all the remaining buses 2-11 are considered as PQ buses.

5.4 Branch Data

NVE's map only shows transmission lines of 24kV and upwards, meaning that the LV grid is not visible, thus the distances of the LV grid have been calculated using map scaling and estimates of cable routes. Likewise to the general loads, the distance of each transmission line has been clustered together as one big line for the specific areas. One thing to take into account is that there is no transformer present in the system for the sake of this thesis, thus LV transmission lines are not considered but instead included in the cluster of 24kV lines.

The transmission line data is gathered from REN data [26] for BLX overhead lines, which are used for all lines throughout this project. Although it is only one type of overhead line, the cross-section will vary depending on the location of the lines. From figure 5.1 all radials will have a lower cross-section due to the fact that they will not need to transmit as much power as the transmission lines that goes from the main feeder and to bus 10. Table 5.4 shows the resistance, reactance, and allowed current for the respective cross-sections of BLX overhead lines.

Table 5.4: Specification of BLX overhead line

Type	Resistance $[\Omega/km]$	Reactance $[\Omega/km]$	Allowed current $[A]$
BLX 50mm^2	0.633	0.375	260
BLX 95mm^2	0.337	0.354	390

Table 5.5 gives an overview of all the transmission line data present in the network, with its corresponding line type and cable length.

Table 5.5: Branch data

Type	From bus	To bus	Distance [km]
	2	3	8.0
	4	5	0.2
BLX $50mm^2$	6	7	1.0
	8	9	1.1
	10	11	3.0
Type	From bus	To bus	Distance [km]
	1	2	1.2
	2	4	2.0
BLX $95mm^2$	4	6	1.0
	6	8	0.5
	8	10	4.5

5.5 Battery Storage

In parts of this thesis, the implementation of battery storage will be investigated. The battery is equipped with a power control system with the intention of being able to adjust the amount of power that the battery will supply and consume for different time periods. In addition to that, for the simplicity of this thesis, the battery will have a unity power factor, meaning that when the battery is charging or discharging only the active power is taken into account. The functionality of the battery is to charge up during the time periods of low consumption, thus having excess power that can be supplied to the EV charging load when the demand is high.

For this purpose, the battery has to be modelled accordingly to the objectives described above. The battery will be implemented for the worst case scenario, hence case four from section 6.5. The size of the battery has been modified through a parameter study, whereas different parameters have been tested in order to achieve the best possible results. The parameters that have been tested are primarily the variables regarding when and how much the battery should charge and discharge for certain hours. Throughout this investigation, a battery that covered 40% of the total demand from the EV charging load seemed to fit the description and was therefore specifically chosen. Appendix B shows the supply and demand for the battery storage and the final modified load which includes EV charging,

5.6 Voltage Limit

As it has been described in section 3.1, there are no voltage limits for the MV grid. The only regulation for voltage quality is for it to be within $\pm 10\%$ regarding the LV for the end-users. This means that as long as the voltage is within this limit for the LV grid, there is no restriction for the MV grid.

For this thesis, there will be assumed a somewhat strict voltage limit of $\pm 5\%$. By having this limit, the variety of voltage levels found in chapter 7 can be related to this restriction. The reasoning for the chosen value of 5% is so that there can be a slight drop in the voltage, but at the same time it is not critical for the system. In addition to that, this also opens up for future grid expansion or higher forms of electric mobility charging, and still being able to keep the voltage within a reasonable limit.

Chapter 6

Case Studies

This chapter will present all the different study cases that will be investigated in this thesis, what the main characteristics are, and what separates one from the other. As it was described in section 5.2.2 the load profiles for all the general loads can be found in appendix A.1. The EV charging profiles that are not presented in chapter 7, can be found in appendix B.

6.1 Case Zero - Initial Condition

The first study case is considered as an initial case where no EV charging is present, hence P_{ev} from figure 5.1 is not connected. This case indicates how well the system responds to normal operating conditions and whether the system is under- or oversized. Since the system now operates under normal conditions, there are no active loads other than the general loads P1-P6 described in section 5.2. These loads are characterized as low or high demand loads based on seasonal variations, and both of these types will be investigated during this study.

- High demand
- Low demand

6.2 Case One - Two Charging Outlets Connected

The main adjustment compared to the first study case is the charging load P_{ev}, which is now connected to bus 10. In addition to this, the low demand months will not be included. The P_{ev} load is characterized as the power being consumed when vehicles are charging their batteries. According to section 5.2.1, the three inputs needed to obtain the load profiles are defined as charging power, numbers of charging outlets, and EV penetration. As already described, two of these inputs are already determined, hence the charging power of 150 kW and EV penetration level of 69%. The remaining input, numbers of charging outlets is set to two for this study case.

- 150 kW chargers, two charging outlets, 69% EV penetration, high demand

6.3 Case Two - Four Charging Outlets Connected

This study case is similar to case one, with the exception of charging outlets. The purpose of this case is to increase the power demand coming from EVs. This is done by adjusting the number of charging outlets to four, which increases the number of vehicles that can charge simultaneously, thus exposing the grid of higher consumption. Specific details of this study case are summarized below,

- 150 kW chargers, four charging outlets, 69% EV penetration, high demand

6.4 Case Three - Six Charging Outlets Connected and Increased Traffic Flow of 40%

Study case three is looking at the impact of six charging outlets when the traffic flow is increased by 40% and the EV penetration is still 69%. The increased traffic flow will increase the number of vehicles that are driving in and out of the area. This will also increase the total number of EVs on the road, thus a higher charging demand. However, there are expected to be more vehicles that would want to charge simultaneously, thus the number of charging outlets are increased to six outlets in order not to overload the charging station. Overloading in this context means that the time of queuing for charging becomes too long for the end-users. If the queuing is too long, customers will leave the charging station, thus increased traffic flow and higher EV penetration will have no greater impact on the total power demand. The two scenarios that will be analysed for case three are shown below.

- 150 kW chargers, six charging outlets, 69% EV penetration, 40% increased traffic flow, day 2
- 150 kW chargers, six charging outlets, 69% EV penetration, 40% increased traffic flow, day 7

Day 2 and day 7 are the two days with the highest power demand out of all 10 charging profiles that are being generated, see section 5.2.1 for a more detailed description about the generated charging profiles.

6.5 Case Four - Twenty Charging Outlets Connected and Increased Traffic Flow of 335%

For study case four, the number of charging outlets for the charging station is increased to 20 outlets. In addition to that, the traffic flow is increased to 335% for this study case.

This is the last study case regarding any new adjustments to the charging load and is therefore considered as a worst case scenario, regarding additional power demand. The traffic flow has increased drastically in order to achieve the worst case scenario. Thus, the number of charging outlets is chosen accordingly to the increased traffic flow, in order not to overload the station or by having excess power that will not be used. The two scenarios that are being investigated during this study case are summarized below.

- 150 kW chargers, 20 charging outlets, 69% EV penetration, 335% increased traffic flow, day 6
- 150 kW chargers, 20 charging outlets, 69% EV penetration, 335% increased traffic flow, day 10

6.6 Case Five - Measures for Grid Improvement

This case study will investigate two different strategies to mitigate the grid impacts from the EV charging load described in section 6.5, specifically, the charging load for day 10. The first strategy for improving the grid quality is to replace all transmission lines of type $BLX 50mm^2$ to $BLX 95mm^2$. The last strategy for grid improvements is the implementation of battery storage. This gives three scenarios that will be further investigated.

- Improvements of modified transmission lines
- Improvements of battery storage
- Improvements of modified transmission lines and implemented battery storage

Chapter 7

Results

This chapter will present all the results related to the study cases described in chapter 6. These results are obtained through Newton-Raphson power flow in MATLAB® by the use of MATPOWER. The important parts of each study will be emphasised, and the numerous study cases will be compared in order to retrieve the most useful data. The system description is illustrated in figure 5.1, which shows the location of all the components in the network.

7.1 Case Zero Results - Initial Condition

7.1.1 High Demand

The first results are expressed as general loads of high demand. Table 7.1 shows what loads that have been active in the analysis and also with its respective values. Take note that these values only express the highest demand hour out of 24 hours, to give a perspective on the size of these loads.

Table 7.1: Case zero - Active loads in the system, highest demand hour - high demand

Load	P1	P2	P3	P4	P5	P6	Pev
Value [kW]	2865	77	76	99	164	3477	-

Figure 7.1 shows how the voltage magnitude for the different buses is changing based on the general load profiles throughout the day. Take note that bus 1 is not shown since it is expressed as the slack bus, thus a having voltage magnitude of 1.0 pu no matter what. Bus 2-9, with the exception of bus 3, are not experiencing any significant voltage drop. The lowest voltage for the specified buses appears to be on bus 9 with a voltage drop of roughly 2%. Bus 3 is considered as the first radial from the main feeder and has voltage as low as 0.955 pu, which is closing in on the -5% voltage limit described in section 5.6. For bus 11, this limit is exceeded for roughly 8 hours, from 8-13 and 16-21. Bus 3, 10,

and 11 are all distinguished by long transmission lines, varying from 3-8 km from table 5.5. Despite transmission line 8-10 being 1.5 km longer than line 10-11, transmission line 10-11 is placed further away, thus resulting in a lower voltage level for bus 11.

From appendix A.1, most of the general load end-users are represented as customers going through the normal cycle of work routines and having a higher consumption during the morning and afternoon hours. This pattern is also reflected in the voltage magnitudes illustrated in figure 7.1.

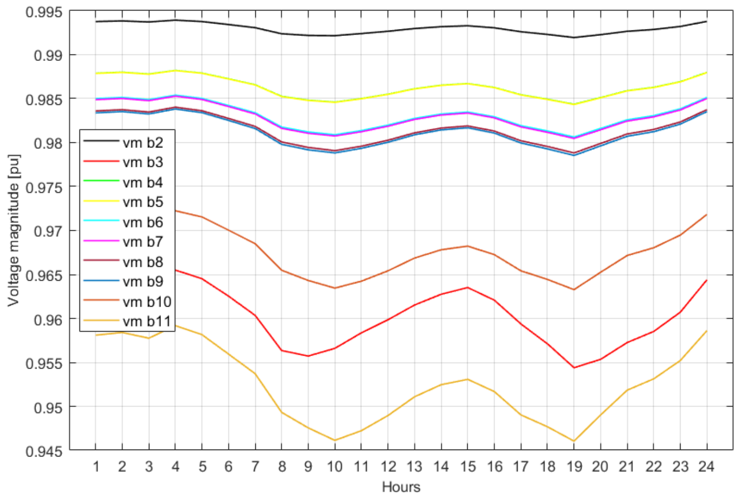

Figure 7.1: Case zero - Voltage magnitude - high demand

The most critical transmission line regarding the current values illustrated in figure 7.2, is line 1-2. This is the first transmission line, and it is also the spine for the remaining parts of the network, everything that flows to all remaining buses and branches has to flow through this line. Keeping that in mind, the magnitude of the current is not getting close to the limit of a $BLX95mm^2$ overhead line, referred to in table 5.4. At its worst, the current only reaches around 50% of the total line capacity. The second highest current magnitude is the current flowing in line 2-4 due to still having most of the power flowing through this line. From figure 7.2, the current that flows towards P1 is expressed as line 2-3 and is covering slightly above 40% of the current flowing in line 1-2, which makes P1 a significant load. Although the current value is considerably lower than for transmission line 1-2, it also has a lower current limit due to the lower cross-section, which adds up to 32% of its total capacity.

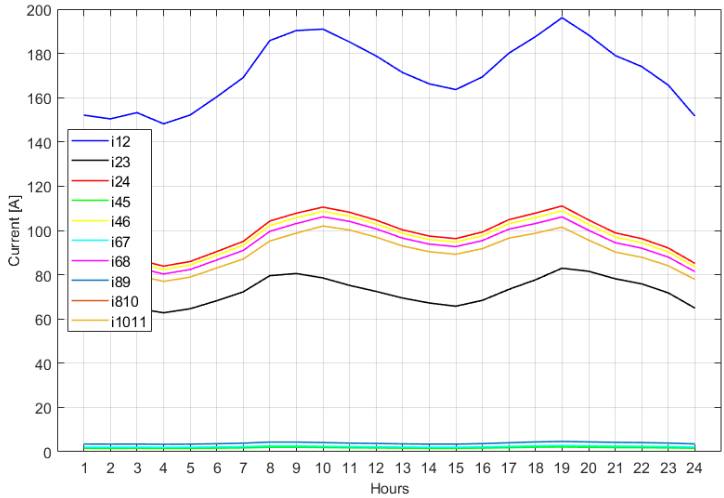

Figure 7.2: Case zero - Current distribution - high demand

The active and reactive transmission line losses are shown in table 7.2. These values are expressed as the total loss for 24 hours by each branch. Transmission line 2-3 has a considerably high loss compared to the other branches. Despite the fact that this line has a lower cross-section than some transmission lines and is tremendously longer than the remaining lines, it will commit to higher losses. Likewise to line 2-3, all the transmission lines of $BLX50mm^2$ have a substantially higher resistance than reactance, which is reflected in the active and reactive losses in table 7.2. Since P_{ev} is not active, thus no load connected to bus 10, it means that transmission lines 8-10 and 10-11 are transmitting more or less the same amount of power, with the only exception of transmission line losses. These two lines are of different cross-section, thus different impedance. Keeping that in mind, there is a noticeable difference in terms of cable length, which results in higher reactive losses for line 8-10 even though the reactance per km is lower.

Table 7.2: Case zero - Total power loss for 24 hours - high demand

	Line 1-2	Line 2-3	Line 2-4	Line 4-5	Line 4-6	Line 6-7	Line 6-8	Line 8-9	Line 8-10	Line 10-11	Total
Total active loss [MW]	0,860	1,895	0,466	0,000	0,225	0,000	0,107	0,001	0,886	1,110	5,551
Total reactive loss [MVAr]	0,904	1,123	0,490	0,000	0,236	0,000	0,112	0,000	0,931	0,657	4,454

The power injection of active and reactive power into the different buses is shown in table 7.3. Bus 1, which is the first bus in the system, shows how much of active and reactive power that is being injected from the main feeder and into the whole system for 24 hours. The active power that is being injected is almost three times the reactive power, which is reflected in the chosen power factor of 0.95, described in section 5.2. Given table 7.2, the amount of lost power compared to what is being injected, covers 3.7% and 8.7% for active and reactive power, respectively. The impedance of the $BLX95mm^2$ transmission line can explain the noticeably higher value of almost 10% for reactive losses. Since the resistance and reactance are more or less equal, the reactive losses will cover a larger percentage of what is being injected because the total reactive power in the system is in general lower.

Table 7.3: Case zero - Total power injection for 24 hours - high demand

Injection into	Bus 1	bus 2	bus 3	bus 4	bus 5	bus 6	bus 7	bus 8	bus 9	bus 10	bus 11
Active power [MW]	147,98	147,12	59,91	83,31	1,50	81,58	1,99	79,49	3,28	75,32	74,21
Reactive power [MVAr]	51,26	50,36	19,69	28,55	0,49	27,82	0,65	27,06	1,08	25,05	24,39

7.1.2 Low Demand

The results presented in this subsection are based on the low demand months, specifically the summer months. Comparing table 7.4 to table 7.1, one can see that there is a significant span in these numbers. Low demand months are only consuming half the power that is being consumed during the high demand months. This deviation can be a result of higher temperatures and less need for heating systems like electric heating, boilers, central heating and so forth.

Table 7.4: Case zero - Active loads in the system, highest demand hour - low demand

Load	P1	P2	P3	P4	P5	P6	Pev
Value [kW]	1217	36	37	47	78	1580	-

The buses connected to the small loads P2-P5 are not experiencing any noticeable drop in the voltage, as shown in figure 7.3. More specifically, the voltage drop on these buses does not even reach 1%. Looking at the voltage for the remaining buses, bus 11 which is the most affected bus, only has some hours that are below 2%. However, from figure 7.1, the voltage for buses 3, 10, and 11 are all exceeding 2% voltage drop for every hour. In addition to that, there are also a few hours where bus 8 and 9 are having voltages beneath 2%, which is considerably more in contrast to the almost 1% drop of figure 7.3. The lowest voltage peaks during low demand months are first found during the time period 10-11 and again observed during 22-23 with an even lower voltage, by the slightest difference of 0.0008 pu. On the other hand, the lower peaks of high demand are present from 09-10 and 18-19, with voltage drops more than twice the value of low demand.

As illustrated in figure 7.3, the voltage magnitude of bus 3 is varying by a tremendous amount during the 08-22. From 08-11 it behaves opposite, by having the voltage level raised, rather than reduced like for all the remaining buses. Not only that, but it is also increased by a greater amount than for the other buses. From 08-14 there is a considerable increase in the voltage for bus 3. This spike in the voltage is coming from the power drop of P1, which is directly tied up to bus 3, see appendix A.1. The power is dropping from 1024 kW to 356 kW, which adds up to a total drop of 668 kW. Looking at the power being consumed by P6 for the same period of time, it shows a power drop of 257 kW. Considering the percentage power drop of P1 and P6, it equals 65% and 18%, respectively, thus giving the voltage variations from figure 7.3. Another similar observation is how the voltage of bus 3 tends do decrease linearly from 17-22 by a significant amount. The voltage curve for bus 11, has a more gentle decrease during the specified hours. The power of P1 and P6 is now increased by 785 kW and 340 kW, respectively. This indicates an increase in the power consumed by 186% for P1 and 28% for P6.

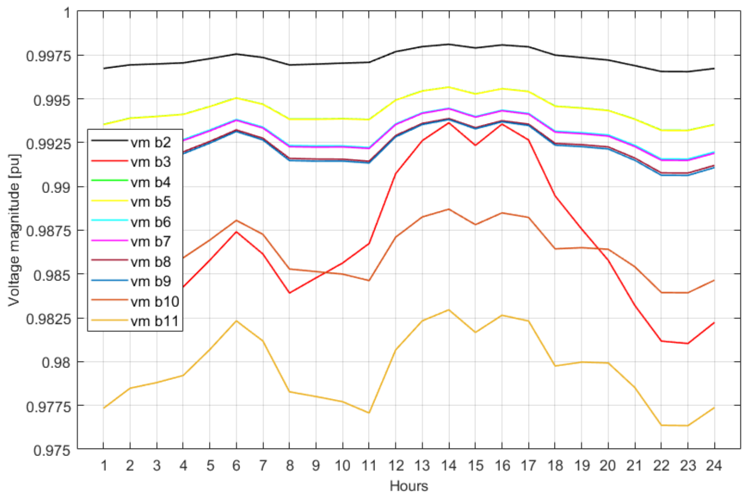

Figure 7.3: Case zero - Voltage magnitude - low demand

The current that flows through the different branches of the network in figure 7.4 is not close to any of the transmission line limits, referred to in table 5.4. Transmission line 1-2 is the highest loaded line with a current of 85A, which corresponds to roughly 22% of the cable rating. This covers almost half of the current flowing in this branch during high demand, illustrated in figure 7.2.

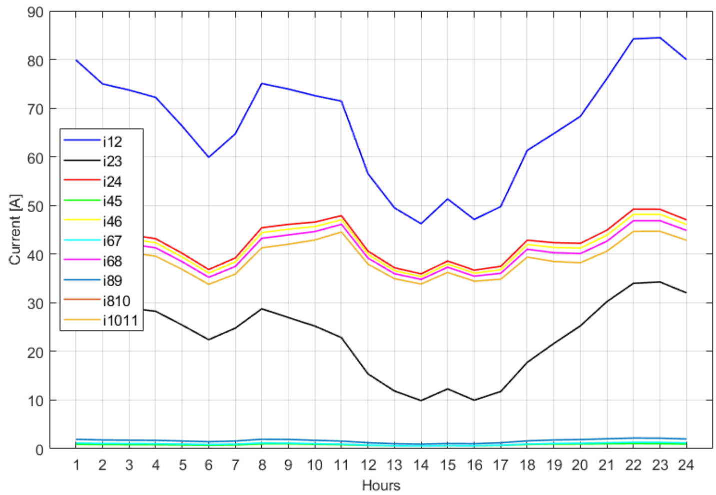

Figure 7.4: Case zero - Current distribution - low demand

Considering the power losses that are present in the system during low demand months are marginal. The active and reactive losses equal to 890 kW and 736 kVAr, five times as low as high demand. One interesting observation is the power losses coming from transmission line 2-3. From table 7.2, the highest loss came from this exact line, with values considerably higher than for the rest of the system. On the other hand, looking at how the system now behaves, there are marginal differences between the losses of line 2-3 and line 10-11, presented in table 7.5. Comparing the tables in appendix A.1, the total power consumed throughout one day has decreased more for P1 than what is has for P6, thus resulting in the more evenly losses for the corresponding transmission lines, as expressed in table 7.5.

Table 7.5: Case zero - Total power loss for 24 hours - low demand

	Line 1-2	Line 2-3	Line 2-4	Line 4-5	Line 4-6	Line 6-7	Line 6-8	Line 8-9	Line 8-10	Line 10-11	Total
Total active loss [MW]	0,134	0,221	0,089	0,000	0,043	0,000	0,020	0,000	0,170	0,212	0,890
Total reactive loss [MVAr]	0,141	0,131	0,094	0,000	0,045	0,000	0,022	0,000	0,178	0,126	0,736

The total power that is being injected into the system is presented in table 7.6, bus 1, specifically. Comparing this to the numbers given during high demand, it covers almost 40% of the total demand. Since P1 and P6 are the main contributors to the heavy power demand, they will have a more significant impact on the system. By adding up the power that flows to each of these loads, hence bus 3 and 11, it adds up to a total of 53.4 MW. If this number is compared to the total system injection of 57,9 MW, it covers 92% of the systems total injected active power.

Table 7.6: Case zero - Total power injection for 24 hours - low demand

Injection into	Bus 1	bus 2	bus 3	bus 4	bus 5	bus 6	bus 7	bus 8	bus 9	bus 10	bus 11
Active power [MW]	57,94	57,81	20,02	36,84	0,73	36,07	0,85	35,20	1,41	33,62	33,41
Reactive power [MVAr]	19,49	19,35	6,58	12,33	0,24	12,05	0,28	11,75	0,46	11,11	10,98

7.2 Case One Results - Two Charging Outlets Connected

The results presented in this section are the result gathered from the power flow when the charging station P_{ev} is connected to bus 10. The charging station now consists of two charging outlets of 150kW. By looking at the size of the charging load in table 7.7, one can see that this load is barely any bigger than the system's smallest load.

Table 7.7: Case one - Active loads in the system, highest demand hour

Load	P1	P2	P3	P4	P5	P6	Pev
Value [kW]	2865	77	76	99	164	3477	86

When that is said, the charging load has a relatively significant deviation, considering the high and low peaks, as shown in table 7.8. The highest power drawn from this load is 106 kW, while the lowest point is only 13 kW.

Table 7.8: Charging load demand with two charging outlets and 69% EV penetration

Time period	**0000-0100**	**0100-0200**	**0200-0300**	**0300-0400**	**0400-0500**	**0500-0600**	**0600-0700**	**0700-0800**	**0800-0900**	**0900-1000**	**1000-1100**	**1100-1200**
Power demand [kW]	34	28	26	13	22	24	44	96	106	89	70	76
Time period	**1200-1300**	**1300-1400**	**1400-1500**	**1500-1600**	**1600-1700**	**1700-1800**	**1800-1900**	**1900-2000**	**2000-2100**	**2100-2200**	**2200-2300**	**2300-2400**
Power demand [kW]	77	40	78	85	90	88	86	57	75	59	50	20

From table 7.8, the period from 08-10 expresses the most loaded hours. There is also a smaller peak found in the period 16-19. In figure 7.5, the charging load and all the general loads except P1 and P6 are shown. P2-P5 follows the same pattern most of the time, considering the upper and lower peak hours. Looking at the first and highest peak of the charging load, there is a similarity to the other loads by having higher power demand during the morning hours. The general loads have another peak around 18-20 with a slightly higher value. On the other hand, the lower top peak of the charging load is present when the demand from the general loads are on their way up. This gives a lower total load for these specific hours if all the loads were added, compared to having the peaks occurring at the same time. The major difference between the general loads and the charging load is the great variations throughout the day. The variations of low to high peak of P5 is 45 kW, which equals an increase of 38%. P_{ev}, on the other hand, is varying from 13 kW to 106 kW, equivalent to an increase of 715%.

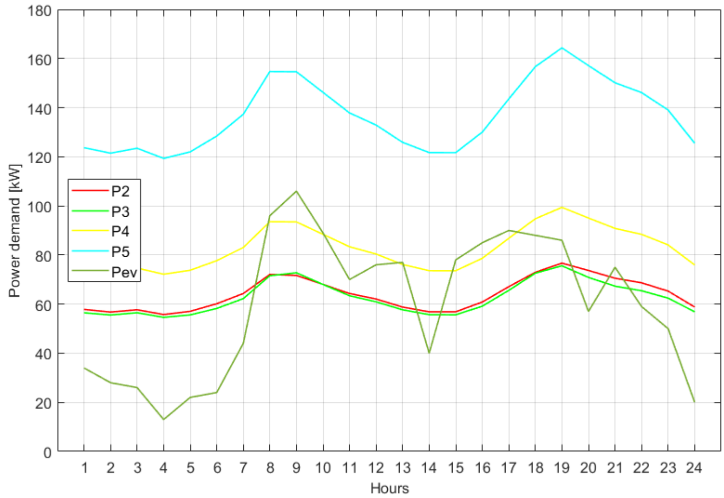

Figure 7.5: Case one - Power demand for all loads excluding P1 and P6

As seen in figure 7.6, there are only the smallest changes compared to the voltage magnitude expressed in case zero for high demand. Comparing the lowest and most critical voltage levels of figure 7.6 and figure 7.1, it gives a deviation of 0.0008 pu, or 0.08%, which is considerably low. The same goes for the current flowing in line 1-2, which only increases by 2.6 A. This is a relatively small amount compared to the almost 200 A that is flowing in figure 7.7.

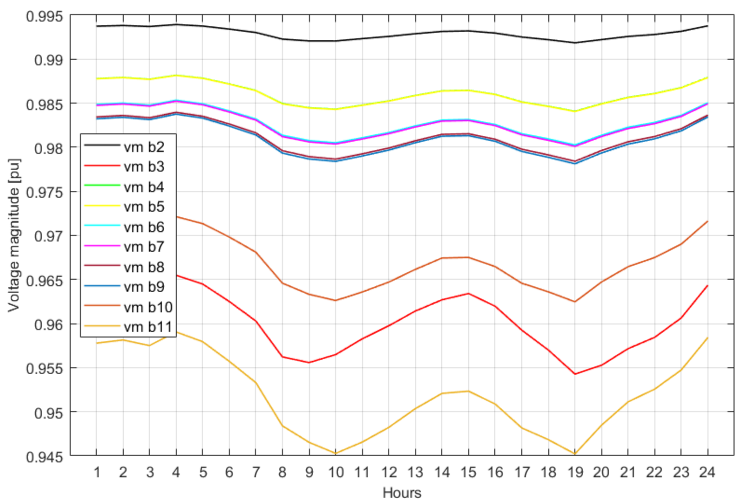

Figure 7.6: Case one - Voltage magnitude

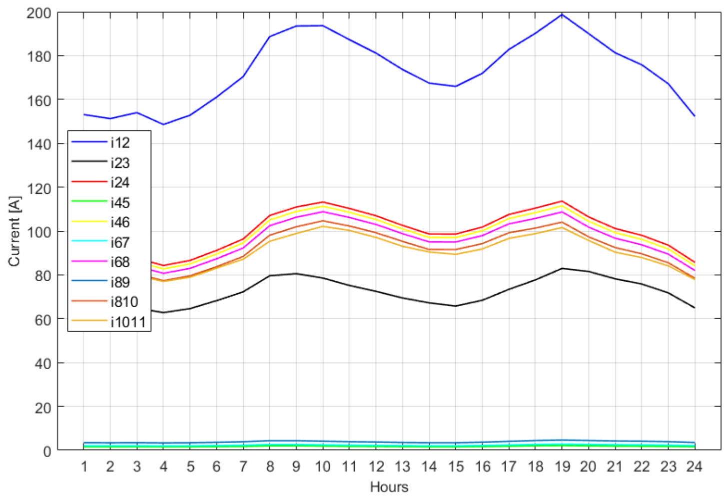

Figure 7.7: Case one - Current distribution

The total power loss for the power system is presented in table 7.9. When comparing table 7.9 and table 7.2, the charging load's minor impact is reflected in the additional power losses of 86 kW and 90 KVAr, which corresponds to an increase of 1.5% and 2%, respectively. Due to the relatively long transmission line 8-10, this is the line which will have the greatest impact on the power losses. Explicitly it is committing to roughly 42% of the additional losses coming from the EV charging load. Even though transmission line 2-3 is by far the longest, the power that is being consumed by the charging load is not flowing through this branch, thus not getting affected by the implementation of P_{ev}.

Table 7.9: Case one - Total power loss for 24 hours

	Line 1-2	Line 2-3	Line 2-4	Line 4-5	Line 4-6	Line 6-7	Line 6-8	Line 8-9	Line 8-10	Line 10-11	Total
Total active loss [MW]	0,879	1,896	0,484	0,000	0,234	0,000	0,111	0,001	0,922	1,111	5,637
Total reactive loss [MVAr]	0,923	1,123	0,508	0,000	0,245	0,000	0,117	0,000	0,969	0,658	4,544

The power that is now being injected into bus 1 from table 7.10, is 1% higher than for high demand of case zero, and corresponds to an increase of 1.52MW. Since P_{ev} is the only load separating case zero and case one, this increase of 1.52MW is reflected in the total power consumed by the charging load in addition to the increased losses of 86 kW.

Table 7.10: Case one - Total power injection for 24 hours

Injection into	Bus 1	bus 2	bus 3	bus 4	bus 5	bus 6	bus 7	bus 8	bus 9	bus 10	bus 11
Active power [MW]	149,50	148,62	59,91	84,79	1,50	83,06	1,99	80,96	3,28	76,75	74,21
Reactive power [MVAr]	51,82	50,90	19,69	29,07	0,49	28,34	0,65	27,57	1,08	25,52	24,39

7.3 Case Two Results - Four Charging Outlets Connected

As discussed in section 6.3, this case will investigate how the system responds to an increase of two additional charging outlets, giving four outlets in total. Figure 7.8 illustrates the power distribution of the charging load P_{ev3} and the small general loads.

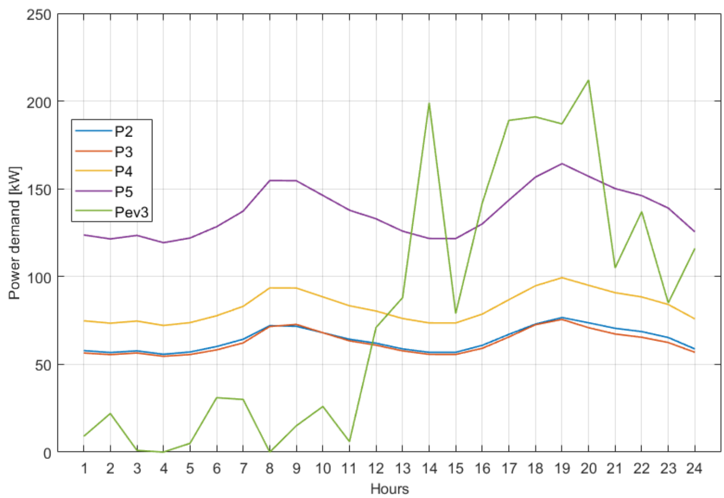

Figure 7.8: Case two - Power demand for all loads excluding P1 and P6

From table 7.11, one can see that the power demand of the charging load during the highest loaded hour is exceeding the values of all the small general loads, that is all loads except P1 and P6. The highest demand hour is considered as the hour with the highest total load in the system, and these values may not be the highest for each individual load for that specific hour. This is reflected in figure 7.8, whereas the charging load P_{ev3} has values greater than 187 kW, as referred to in table 7.11. The charging load now covers approximately 5% of the P6 load from table 7.11.

Table 7.11: Case two - Active loads in the system, highest demand hour

Load	P1	P2	P3	P4	P5	P6	P_{ev3}
Value [kW]	2865	77	76	99	164	3477	187

The top portion of the charging load P_{ev3} is present during the systems' high peak. Table 7.12 shows a high peak at 13-14 and a more significant peak from 17-20. All the general loads have their highest peak during 17-21, which is in the same period as the top portion of the charging load. When comparing table 7.12 and table 7.8, the charging load for case one tends to have a more stable but lower demand throughout the day, while P_{ev3} has a higher demand but is only active more or less half the day. The more evenly distributed charging load from figure 7.5 results in lower impact for the vulnerable time periods, in contrast to P_{ev3}, which is affecting these time periods even more.

Table 7.12: Charging load demand with four charging outlets and 69% EV penetration

Time period	**0000-0100**	**0100-0200**	**0200-0300**	**0300-0400**	**0400-0500**	**0500-0600**	**0600-0700**	**0700-0800**	**0800-0900**	**0900-1000**	**1000-1100**	**1100-1200**
Power demand [kW]	9	22	1	0	5	31	30	0	15	26	6	71
Time period	**1200-1300**	**1300-1400**	**1400-1500**	**1500-1600**	**1600-1700**	**1700-1800**	**1800-1900**	**1900-2000**	**2000-2100**	**2100-2200**	**2200-2300**	**2300-2400**
Power demand [kW]	88	199	79	142	189	191	187	212	105	137	85	116

When only two charging outlets are connected, that gives voltage values of 0.9453 pu and 0.9452 pu for each of the bottom peaks on bus 11 from figure 7.6. Figure 7.9 illustrates the resulting voltage behavior when four charging outlets are connected, with bottom peaks of 0.9459 pu and 0.9443 pu for bus 11. interestingly, the first lower peak has increased its voltage value when moving from two to four charging outlets. As discussed earlier, the power consumed by P_{ev} during case one is more evenly spread out, thus causing a higher power demand during this period and therefore a higher voltage drop. The lowest values for each of these studies of 0.9452 and 0.9443, can be represented as additional voltage drop compared to case zero, equivalent to 0.08% and 0.17% for case one and case two, respectively. This shows an increase in voltage drop by twice the value comparing case two to case one. This deviation is mostly because of how the two loads are differently distributed, but also the fact that four outlet charging station has an overall slightly higher consumption.

Regarding the assumed voltage limit of $\pm5\%$, there are some small variations in four charging outlets and case zero. In figure 7.9, looking at the first time period where the voltage is below 0.95, it tends to stay beneath this limit for an additional 30 minutes or so compared to figure 7.1. Likewise, for case zero, the voltage goes beneath the voltage limit again between 16 and 17, while as for case two the voltage limit is exceeded half an hour earlier. This roughly adds up to an additional one hour, where the voltage exceeds the limit of -5%.

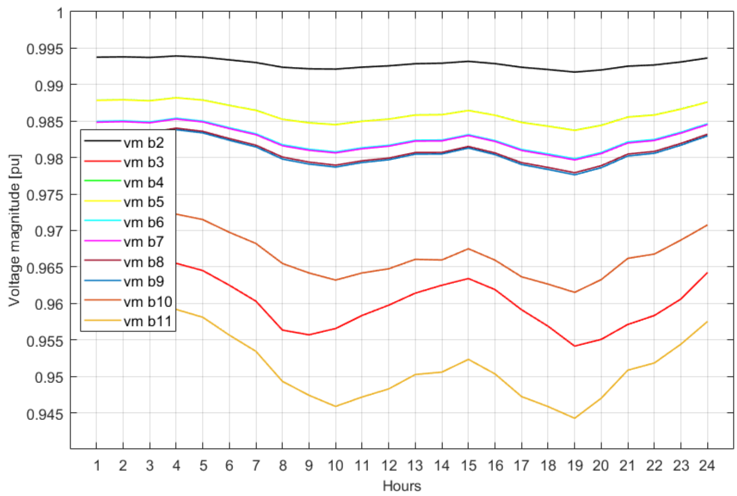

Figure 7.9: Case two - Voltage magnitude

Table 7.13 shows how much the current magnitude has increased for the heaviest loaded line during cases one and two, compared to the current that was flowing for high demand of case zero. Since the all-over effect of these two charging loads is relatively small, only the most crucial hours are presented. As discussed earlier, the voltage drop was slightly more than double when looking at the lower peak during 18-19, compared to case one. This is also reflected in table 7.13, where the current of the second peak is changing by twice the value. Likewise, the different power distribution of P_{ev} and P_{ev3} can describe the 2.6A compared to the 0.8A at 09-10.

Table 7.13: Increased current magnitude of line 1-2 for case one and two, compared to high demand of case zero.

	1st peak (09-10)	2nd peak (18-19)
Case one	2.6 A	2.6 A
Case two	0.8 A	5.6 A

If the injected power from table 7.14 is being compared to what is being injected during case zero, it shows an increase of 1.40%. From section 7.2, the increased injected power was 1% for case one. Thus the remaining percentage of 0.40% is what separates two and four charging outlets regarding the injected power.

Table 7.14: Case two - Total power injection for 24 hours

Injection into	Bus 1	bus 2	bus 3	bus 4	bus 5	bus 6	bus 7	bus 8	bus 9	bus 10	bus 11
Active power [MW]	150,05	149,16	59,91	85,32	1,50	83,59	1,99	81,49	3,28	77,26	74,21
Reactive power [MVAr]	52,03	51,10	19,69	29,26	0,49	28,52	0,65	27,75	1,08	25,69	24,39

7.4 Case Three Results- Six Charging Outlets and 40% Increased Traffic Flow

The presented results below are based on 40% increased traffic flow and also with a charging station consisting of six outlets. As figure 7.10a, illustrates there are two different charging loads present, characterized as P_{ev2} and P_{ev7}. As mentioned in section 5.2.1, the charging profiles generated consist of 10 profiles based on 10 arbitrary days, hence P_{ev2} and P_{ev7}. The total power demand from both of these charging profiles corresponds to a total value of 3367 kW and 3452 kW for P_{ev2} and P_{ev7}, respectively. There is not any noticeably difference between the total power demand for each of these loads, but there are some small variations regarding how the loads are distributed. As can be seen from figure 7.10b, the charging loads are still relatively small compared to the major general loads.

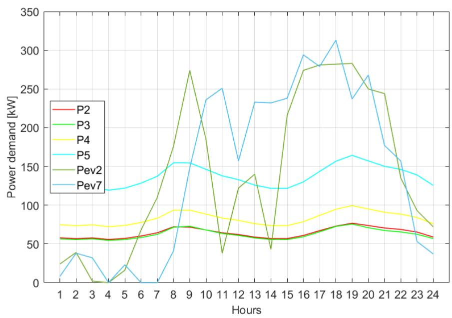

(a) Power demand, excluding P1 and P6

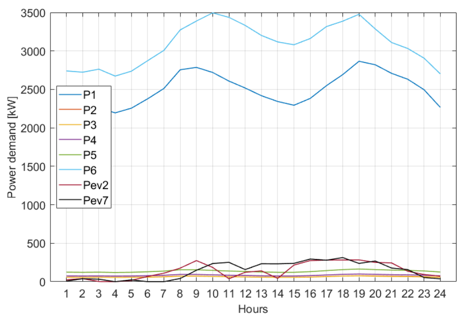

(b) Power demand, including P1 and P6

Figure 7.10: Case three - Power demand for all loads, six charging outlets and 40% increased traffic flow

The small variations of the charging load shown in figure 7.10a can also be reflected in table 7.15 and table 7.16. From 15-05, the power demand from these loads is approximately on the same level. For the remaining hours, these two curves are shifted by two hours, where P_{ev2} is facing a considerably high increase in power demand around 05 and P_{ev7} is having this increase around 07. After that, they are both undergoing some fluctuations in power, with P_{ev2} having a higher drop resulting in the slightly lower total power demand.

Table 7.15: Charging load demand with six charging outlets and 69% EV penetration, day 2

Time period	**0000-0100**	**0100-0200**	**0200-0300**	**0300-0400**	**0400-0500**	**0500-0600**	**0600-0700**	**0700-0800**	**0800-0900**	**0900-1000**	**1000-1100**	**1100-1200**
Power demand [kW]	24	39	2	0	16	68	110	176	274	185	38	122
Time period	**1200-1300**	**1300-1400**	**1400-1500**	**1500-1600**	**1600-1700**	**1700-1800**	**1800-1900**	**1900-2000**	**2000-2100**	**2100-2200**	**2200-2300**	**2300-2400**
Power demand [kW]	140	43	216	274	281	282	283	250	244	135	93	72

Table 7.16: Charging load demand with six charging outlets and 69% EV penetration, day 7

Time period	**0000-0100**	**0100-0200**	**0200-0300**	**0300-0400**	**0400-0500**	**0500-0600**	**0600-0700**	**0700-0800**	**0800-0900**	**0900-1000**	**1000-1100**	**1100-1200**
Power demand [kW]	8	38	32	0	23	0	0	41	148	236	251	157
Time period	**1200-1300**	**1300-1400**	**1400-1500**	**1500-1600**	**1600-1700**	**1700-1800**	**1800-1900**	**1900-2000**	**2000-2100**	**2100-2200**	**2200-2300**	**2300-2400**
Power demand [kW]	233	232	238	294	279	313	237	268	177	157	53	37

The voltage magnitudes of study case three considering both days of charging, are presented in figure 7.11. Even though that P1 and all the small general loads have their first high consuming peak during 08-09 from figure 7.10, the first lower peak of the systems voltage is occurring at 10 because of the impact of the bigger general load P6. The first top portion of P_{ev7} is during 09-11, which can be considered the same period as the first high peak of P6. Due to this, it will slightly decrease the overall voltage for this critical hour, compared to the voltage of figure 7.11a.

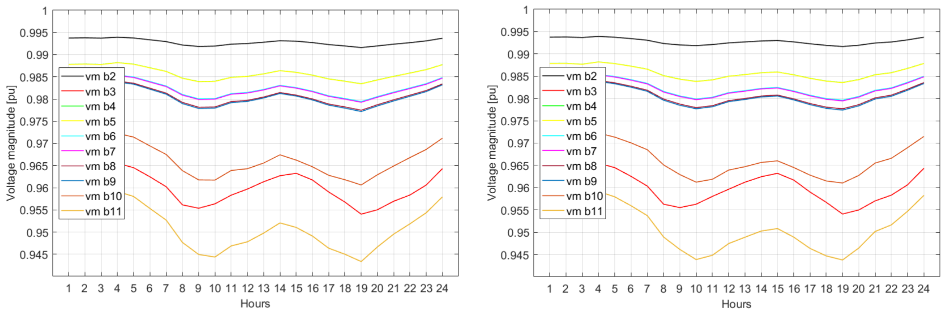

(a) Voltage magnitude for day 2

(b) Voltage magnitude for day 7

Figure 7.11: Case three - Voltage magnitude

When looking at the lowest voltage values of figure 7.11, which are present around 19, it shows a slightly lower voltage for day 2. This value is as low as 0.9433 pu, which equals a total voltage drop of 5.67%. From figure 7.1, the voltage drop when there was no active charging station was 5.4%. This adds up to a deviation of 0.27% comparing these two cases. Looking at table 7.15, the power demand from the charging station for this specific period is 283kW. Even though the power consumption coming from the charging load is getting higher than for two and four outlets, it still has a relatively small impact on the system's voltage quality, which is reflected in the 0.27%.

7.5 Case Four Results - Twenty Charging Outlets and 335% Increased Traffic Flow

The results that are investigated in this section have been changed drastically from the previous case studies. From a few charging outlets to 20 outlets, and from 40% to 335% increased traffic flow, but with EV penetration still being 69%. Likewise to case three, there will be different charging profiles presented, which are defined as separate days.

Due to the increased number of charging outlets and increased traffic flow, the power being consumed by the charging station is considerably higher than for previous cases. Figure 7.12 illustrates how the power of the charging stations is distributed throughout the day. It is visually representing two separate days, defined as P_{ev6} and P_{ev10}. P_{ev10} can be characterized as a big load which only stretches out over a certain time period. The majority of the power that is being consumed by this load is during the time 09-23, with relatively steep transitions from low to high, and high to low peak. In addition to that, this curve does not have a distinct peak value, but rather a flat top part spread over 9 hours. Curve P_{ev6}, on the other hand, has a more distinct top value, and also a more gradual increase from the lower parts and to the high peak.

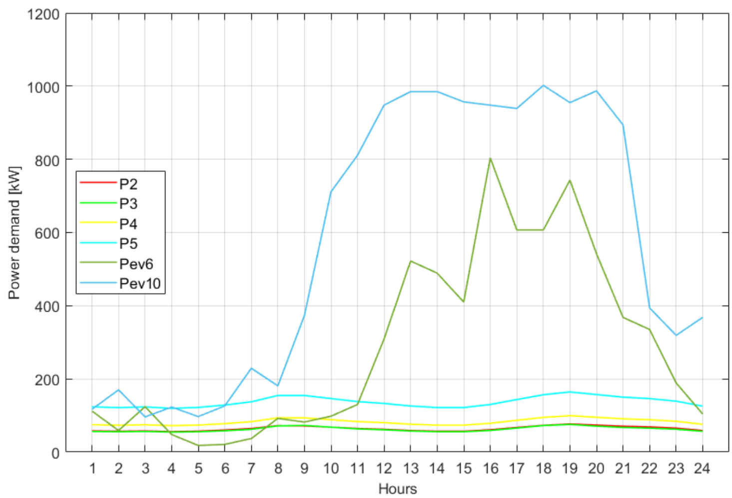

Figure 7.12: Case four - Power demand for all loads excluding P1 and P6, twenty charging outlets and 335% increased traffic flow

From figure 7.12, there is a high deviation between the values of the charging loads and the small general loads. The small general loads are now insignificant compared to the charging loads, with the highest value of 164 kW compared to the 1002 kW of P_{ev10} and 804 kW of P_{ev6}. Even the lower part of P_{ev10} is higher than the general load P5 for the majority of hours. As illustrated, the power demand from P_{ev6} is higher than P5 for the second half of the day, by a great amount. The power being consumed for day 10 is higher than the power for day 6 for every hour. During 08-22 this amount is something between 200-400 kW greater, except for the peak hour at 16.

Figure 7.13 represents the load distribution for all active loads in the system, including the big general loads of P1 and P6. This figure visually express how big the charging load P_{ev10} is compared to the small general loads, but at the same time it also shows that P_{ev10} is not quite yet at the same level as the two greater loads, P1 and P6. The high peaks present around 19 for P1 and P6 have values of 2866 kW and 3477 kW, respectively. The 955 kW top of P_{ev10} at 19 is equivalent to 33% of P1 and 27% of P6. When that is said, there are relatively significant differences between the top and bottom of P1 and P6. As mentioned earlier, the top part of P_{ev10} is evenly distributed, which makes this charging load cover a more substantial portion of the big general loads during the lower consuming hours. Specifically, it covers 42% and 31% of P1 and P6, respectively, during the low demand hour at 15.

P_{ev6}, on the contrary, covers 26% of P1 and 21% of P6 during the high peak hour. Unlike day 10, P_{ev6} does not have a flat high peak, but rather a curved distribution that has a clear separation between the low and high peak hours around 15 and 19. Since the power consumed by P_{ev6} decreases at the same time as for the big general loads and by a higher factor, the charging load during low demand hour will cover a lower percentage of P1 and P6 compared to the high demand hour. More specifically, it covers 18% and 13% of P1 and P6, respectively. This clearly shows that P_{ev10} is considerably greater than P_{ev6}, which can also be seen in appendix B.

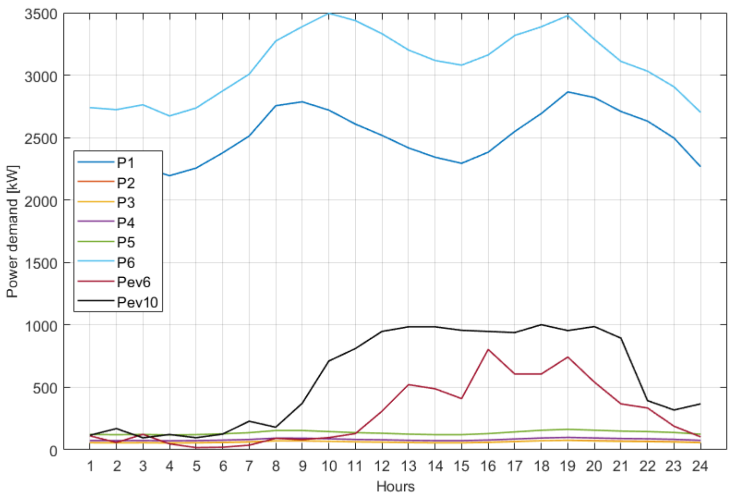

Figure 7.13: Case four - Power demand for all loads, twenty charging outlets and 335% increased traffic flow

Bus 3 will barely be affected at all during EV implementation, due to this bus being connected to a separate radial than the charging load. This radial is connected to bus 2 through line 2-3, thus being mostly affected by what happens prior to bus 2, i.e., transmission line 1-2, see figure 5.1. However, buses 5, 7, and 9 are also connected to separate radials. These radials are further away from the main feeder, meaning that the charging load will have a greater impact on these buses. Likewise to bus 3, the buses connected to the separate radials are mostly affected by the adjustments that occur prior to the respective buses. Table 7.17, express how much the voltage has changed for each bus on the different radials when looking at the lowest peak at 19 from figure 7.14a, compared to the high demand of case zero. As shown in this table, the additional voltage drop that comes from the implementation of the charging station will increase as further away the bus gets from the main feeder, due to longer distances for the additional power to travel, thus higher voltage drop.

Table 7.17: Increased voltage drop of the different radials as a result of the charging load P_{ev10}. It is compared to high demand of case zero

	[pu] drop	[%] drop
Bus 3	0.0013	0.13
Bus 5	0.0031	0.31
Bus 7	0.0042	0.42
Bus 9	0.0046	0.46

Figure 7.14a illustrates the voltage level for all the respective buses in the system when bus 10 is being exposed to EV charging. These are the results that are based on the power consumed by P_{ev10}. Looking at the most critical bus, which is bus 11, the voltage exceeds 5% voltage drop for the majority of the day. More precisely, it is below 0.95 pu from around 08 and to 22, resulting in a total of 14 hours. Even though the total power in the system has now increased, none of the remaining buses are exceeding the voltage limit of $\pm 5\%$.

The voltage for day 6 is illustrated in figure 7.14b. Looking at how the power of P_{ev6} is distributed in figure 7.13, at 10 the power consumed by the charging load is barely anything. From here on, the power consumed by P1 and P6 are decreasing linearly until 15. However, the power from the charging load is increasing for the first few hours of this same period. This opposing behavior of the general loads and the charging load will to some degree even each other out, which will limit the voltage variations of these two loads during this period of time. This results in the more evenly distributed voltage curve during 09-13 for day 6.

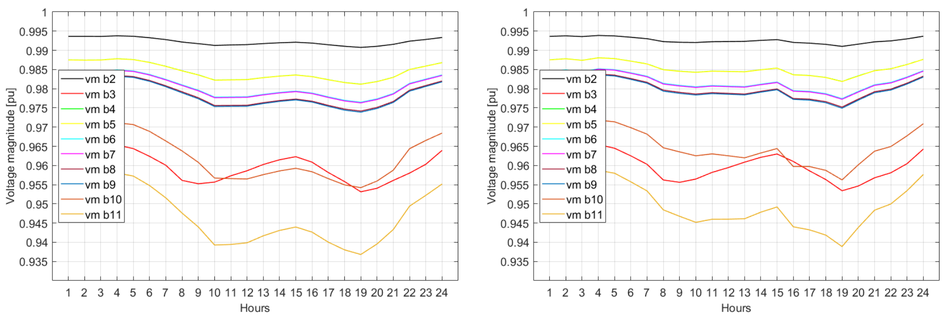

(a) Voltage magnitude for day 10 **(b)** Voltage magnitude for day 6

Figure 7.14: Case four - Voltage magnitude

The voltage for bus 11 in figure 7.14a has its lowest value of 0.9368 pu, which corresponds to a percentage voltage drop of 6.32%. The voltage drop for the high demand of case zero was 5.4%, which indicates that the voltage drop that is coming solely from the P_{ev10} in case four represents 0.92%. Without the charging load active, i.e., case zero, the voltage of bus 10 during high demand peak hour was 0.9633 pu, while for case four this value is

0.9542 pu. This gives a deviation of 0.91%, considering the additional percentage voltage drop. Because all the power that P_{ev10} is consuming is going to bus 10, that means transmission line 10-11 will not transmit any additional power during case four than it has to transmit during case zero. As a result of this, the additional voltage losses coming from P_{ev10} for bus 10 and 11 are more or less the same, 0.91% and 0.92%, respectively.

Figure 7.15 visually expresses the voltage losses coming from P_{ev10} alone, for buses extending from the main feeder and all the way to bus 11. As shown in the figure, the buses closest to the main feeder have a lower voltage drop because the voltage is dropping over fewer and shorter transmission lines. On the contrary, the greater deviation in the voltage drop of bus 2 and bus 4, and bus 8 and bus 11, are explained by the longer transmission lines 2-4 and 8-10 reflected in table 5.5. Take note that bus 10 is not shown because the additional voltage drop is quite similar to bus 11.

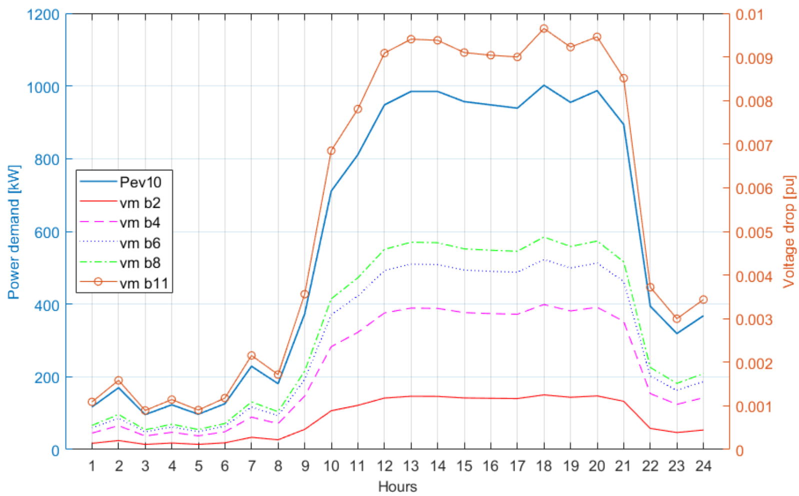

Figure 7.15: Case four - Additional voltage drop as a result of charging load P_{ev10}, compared to high demand of case zero. The P_{ev10} load is related to the left y-axis, while the remaining voltage curves are referred to the right y-axis

As seen from figure 7.16, the current that is flowing past bus 10 hence the current in transmission line 10-11, does not change with any noticeable amount when comparing the current for day 6 and day 10. As it has been discussed earlier, none of the additional power that is being consumed by the charging load is flowing past the correlating bus. The 212 kW that is separated by P_{ev6} and P_{ev10} during the high demand hour of 19 is accountable for the 6.5A difference from figure 7.16a and figure 7.16b, considering the current flowing in line 1-2.

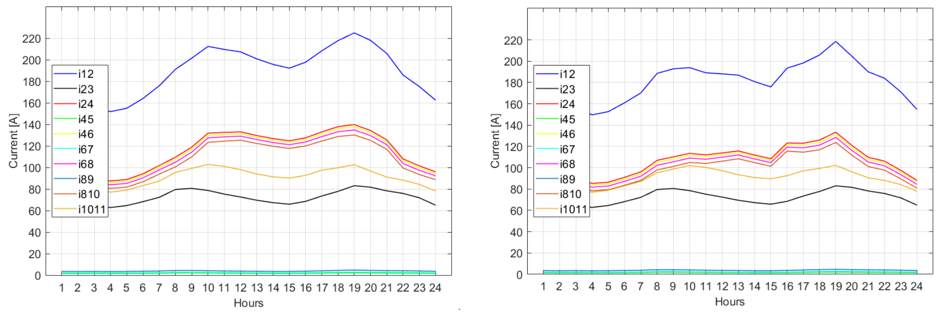

(a) current distribution for day 10 **(b)** current distribution for day 6

Figure 7.16: Case four - Current distribution

The total power that is being injected into the network is expressed in table 7.18 and table 7.19, whereas the system is exposed to charging of P_{ev6} and P_{ev10}. From case zero, the total injected power was 147.98 MW, which is now equal to roughly 155.27MW and 162.62MW for day 6 and day 10, respectively. This gives an increase of 7.29MW and 14.64MW for the two respective days compared to case zero, similar to an increase of 4.9% and 9.9%.

Table 7.18: Case four - Total power injection for 24 hours, day 6

Injection into	Bus 1	bus 2	bus 3	bus 4	bus 5	bus 6	bus 7	bus 8	bus 9	bus 10	bus 11
Active power [MW]	155,27	154,32	59,91	90,42	1,50	88,65	1,99	86,53	3,28	82,17	74,21
Reactive power [MVAr]	53,97	52,97	19,69	31,07	0,49	30,30	0,65	29,51	1,08	27,31	24,40

Table 7.19: Case four - Total power injection for 24 hours, day 10

Injection into	Bus 1	bus 2	bus 3	bus 4	bus 5	bus 6	bus 7	bus 8	bus 9	bus 10	bus 11
Active power [MW]	162,62	161,57	59,91	97,57	1,50	95,75	1,99	93,61	3,28	89,04	74,21
Reactive power [MVAr]	56,73	55,63	19,69	33,62	0,49	32,80	0,65	31,99	1,08	29,57	24,40

The additional reactive power injected due to the two different charging alternatives are accountable for 5.3% and 10.7% for day 6 and day 10, respectively, when compared to what is being injected table in 7.3. This indicates that the percentage increase in reactive power is slightly higher than the percentage increase in active power.

The active and reactive losses are presented in table 7.20 and table 7.21. During the high demand of case zero shown in table 7.2, the active and reactive losses were equal to 5.551 MW and 4.454 MVAr. Comparing this to the losses during case four, it gives an increase of 0.440 MW and 0.459 MVAr for day 6. Likewise, for day 10, the power losses have increased by 0.923 MW and 0.962 MVAr, expressing the slightly higher reactive losses for both days. Even though the resistance is considerably higher than the reactance for $BLX50mm^2$ referred to in table 5.4; this type is only active at the radials, i.e., line 2-3, 4-5, 6-7, 8-9, and 10-11, thus not valid for the segment of the charging load. However,

$BLX95mm^2$, which is the type used for all the remaining transmission lines, has a slightly higher reactance than resistance. This type is used for the transmission lines that can be considered as the pathway for the charging load, thus resulting in higher reactive losses compared to the active losses.

Table 7.20: Case four - Total power loss for 24 hours, day 6

	Line 1-2	Line 2-3	Line 2-4	Line 4-5	Line 4-6	Line 6-7	Line 6-8	Line 8-9	Line 8-10	Line 10-11	Total
Total active loss [MW]	0,951	1,897	0,556	0,000	0,269	0,000	0,129	0,001	1,072	1,116	5,991
Total reactive loss [MVAr]	0,999	1,124	0,584	0,000	0,282	0,000	0,135	0,000	1,126	0,661	4,913

Table 7.21: Case four - Total power loss for 24 hours, day 10

	Line 1-2	Line 2-3	Line 2-4	Line 4-5	Line 4-6	Line 6-7	Line 6-8	Line 8-9	Line 8-10	Line 10-11	Total
Total active loss [MW]	1,048	1,898	0,654	0,000	0,317	0,000	0,152	0,001	1,278	1,124	6,474
Total reactive loss [MVAr]	1,101	1,125	0,687	0,000	0,333	0,000	0,160	0,000	1,343	0,666	5,416

7.6 Case Five Results - Measures for Grid Improvement

7.6.1 Increased Cross-section

In this section, alternative strategies for grid improvements for case four with P_{ev10} active will be investigated. First off, the cross-section for some of the transmission lines will be increased in order to reduce the power losses and voltage drop. As discussed in section 5.4, there are two types of transmission lines present in the system, $BLX95mm^2$ and $BLX50mm^2$. All lines represented as $BLX50mm^2$ are now being swapped to $BLX95mm^2$, meaning that all transmission lines are now of the same cross-section.

Figure 7.17 illustrates the results from the cross-section transformation for the most affected buses, hence bus 3 and bus 11. These results are expressed as voltage magnitude, more specifically, it is a comparison to case four, described in section 7.5. For the remaining buses, they are barely having any improvements at all due to the low consuming loads P2-P5. Thus these buses are not included in figure 7.17. *Modified* represents the results when the transmission lines are exposed to a higher cross-section, and *case four* are the results presented in section 7.5.

As can be seen from this figure, the voltage variations resulting from the increased cross-section are noticeably high. Looking at how the voltage level is changing for bus 3 when transmission line 2-3 is exposed to a higher cross-section, it is changing from 0.9531 pu to 0.9686 pu during the highest demand hour at 19. This gives a deviation of 1.55%, which is quite high, considering that the highest voltage drop at bus 3 for case four is 4.69%. The voltage increase compared to figure 7.1 of case zero is 1.42% for bus 3, which is relatively close to the increase of 1.55%. This small deviation of 0.13% is found in table 7.17 and is referred to as the additional voltage drop as a result of the implemented charging load P_{ev10}.

For bus 11, the lowest voltage is now 0.9441 pu taking into account the modified lines, which gives an increase of 0.73% compared to case four. As can be seen from figure 7.17, the increase on bus 3 is more than twice the size of the increase for bus 11. From table 5.5, the transmission line 2-3 is considerably longer than line 10-11, by almost three times. The effect of increasing the cross-section, i.e., reducing the impedance, will have a more significant impact on longer transmission lines, and therefore bus 3 is having greater improvements than bus 11.

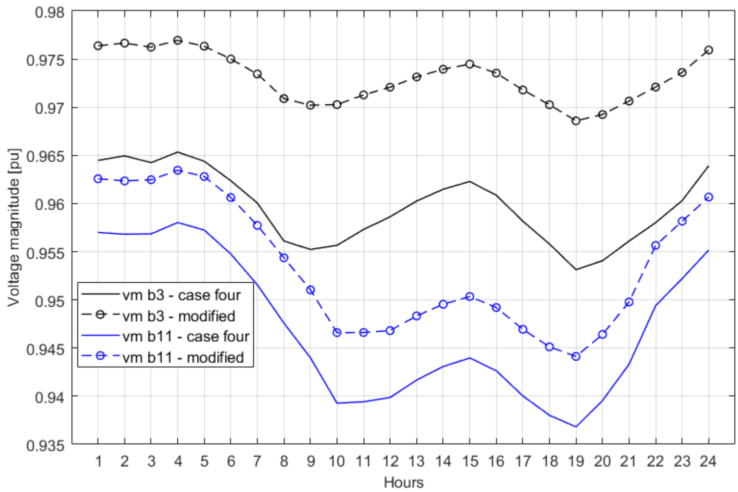

Figure 7.17: Case five - Voltage magnitude comparison of case four and increased cross section

Table 7.22 is expressing all the losses in the system with the modified transmission lines. By changing the transmission lines, the resistive part of the distribution line is reduced by almost twice the value, see table 5.4. The reactance on the other hand, does not have any significant reduction. It is only reduced by 5.6% in contrast to the almost 50% reduction for the resistance. This is reflected in total power losses for 24 hours from table 7.22, where the active and reactive power losses have been reduced by 1.494MW and 0.185MVAr, compared to case four from table 7.21. Transmission lines 2-3 and 10-11 are the longest modified lines. They are contributing to 1.449 MW and 0.139 MVAr, equivalent to 97% and 75% of the reduced losses.

Table 7.22: Case five - Total power loss for 24 hours with modified transmission lines

	Line 1-2	Line 2-3	Line 2-4	Line 4-5	Line 4-6	Line 6-7	Line 6-8	Line 8-9	Line 8-10	Line 10-11	Total
Total active loss [MW]	1,031	0,983	0,647	0,000	0,314	0,000	0,151	0,000	1,264	0,590	4,980
Total reactive loss [MVAr]	1,083	1,032	0,680	0,000	0,330	0,000	0,158	0,000	1,327	0,620	5,231

A more detailed description of the power losses can be found in figure 7.18, illustrating how the power losses are changing for each hour for line 2-3 and 10-11. All the solid lines are represented as power losses for case four, while the dashed lines are the results with the modified transmission lines. This figure clearly shows that the active power losses coming from transmission line 2-3 are considerably greater than for line 10-11, due to its longer transmission line. As for the reactive power, there are no significant differences between case four and the modified case. Take note that the different shapes of line 2-3 and 10-11 are a result of the distinct power demands of load P1 and P6, illustrated in figure 7.13. As for the current, the increased cross-section only contributes to a reduction of approximately 2A for the heaviest loaded line compared to case four. Figure 7.23 illustrates the current distribution for modified transmission lines.

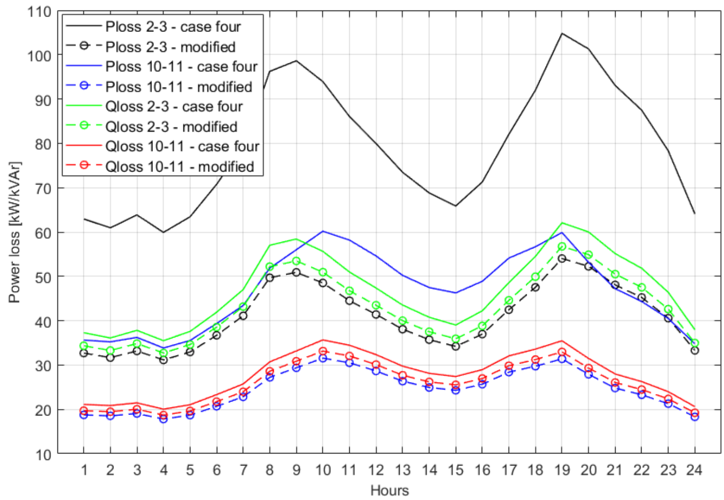

Figure 7.18: Case five - Power losses for transmission line 2-3 and 10-11, comparison of case four and increased cross section

7.6.2 Implementation of Battery Storage

Secondly, battery storage is implemented to improve the grid quality. This is a battery that will be handled as a power supply, with the ability to consume and supply power in certain situations. As described in section 5.5, the battery used for this thesis has a unity power factor and is equipped with a power control system, making it possible to regulate the charging of the battery. The battery is charged up during the systems' low demand hours and discharged while the total demand is high. More particular, it is being operated as a peak-shaving supply, meaning that it will supply the system with additional power in order to reduce the top peaks in the system. For this thesis's sake, the battery will be placed at bus 10, along with the charging load P_{ev10}, to reduce the heavily impacted time periods. The battery will cover 40% of the total demand of the EV charging load, equivalent to 5486kW.

Figure 7.19 illustrates how the EV charging load combined with battery storage is distributed for 24 hours. The grey area is referred to as *Battery charging* and is characterized as the time period when the battery is charging up. As illustrated, the battery is charging, i.e., consuming power from the grid during the period 24-06 with a constant active power of 1000 kW the majority of the time. Looking at figure 7.13, this specific time period is considered as the low demand period for the entire system. On the other hand, the green shaded area *Battery discharging* is representing the amount of power that is being supplied by the battery. The red shaded area expresses how much of the original charging load P_{ev10} is being shaved off by the battery. The solid black line is equivalent to the charging load P_{ev10} from figure 7.12. The solid blue line represents of the modified load consisting of battery storage and EV charging, see section 4.2.3 for more details.

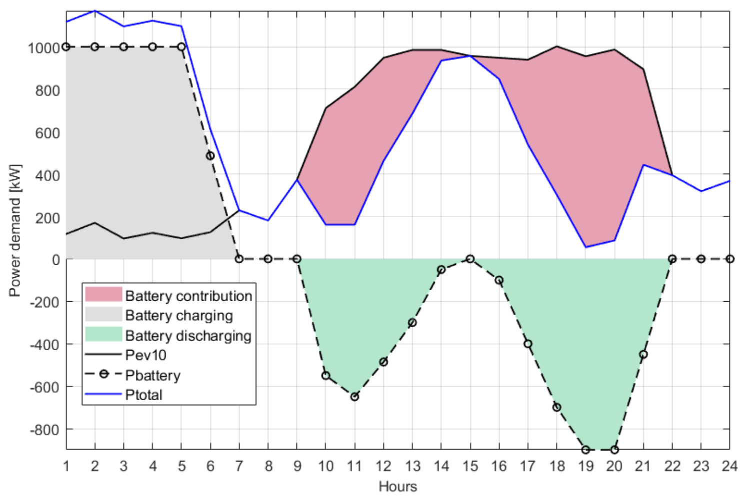

Figure 7.19: Case five - Power demand from modified charging load, including the battery charging and discharging

The results from battery implementation and modified transmission lines are presented in figure 7.20. Figure 7.20a shows the voltage magnitude with the implementation of battery storage, while figure 7.20b expresses the results of both battery storage and increased cross-section, $50mm^2 \rightarrow 95mm^2$.

With the implementation of the battery alone, the original lowest voltage point at 19 is now 0.9434 pu. Comparing this to the voltage of 0.9441 pu that was found from the modified transmission lines from figure 7.17, it gives a deviation of 0.0007 pu, which is considerably low. On the other hand, looking at the higher voltage peak of 15, the results are quite diverse from these two strategies. Since the power supplied from the battery in figure 7.19 for this specific hour is zero, there will be no improving effects during this time period. Thus the voltage is the same for battery implementation as for case four, 0.9440 pu. However, the voltage improvements for the modified lines is 0.64% or 0.0064 pu for the higher voltage peak of 15, compared to case four. This means that the deviation between battery implementation and increased cross-section is also going to be 0.0064 pu, which is more than nine times the deviation during the lowest peak hour at 19. Looking at the voltage improvements when some lines are exposed to higher cross-section and with an implemented battery storage, the voltage curve has been shifted by approximately 0.7% compared to figure 7.20a. When both strategies for grid improvements are applied, the voltage level is kept within the limits of $\pm 5\%$ except for two hours being slightly underneath by 0.0001 and 0.0002 pu.

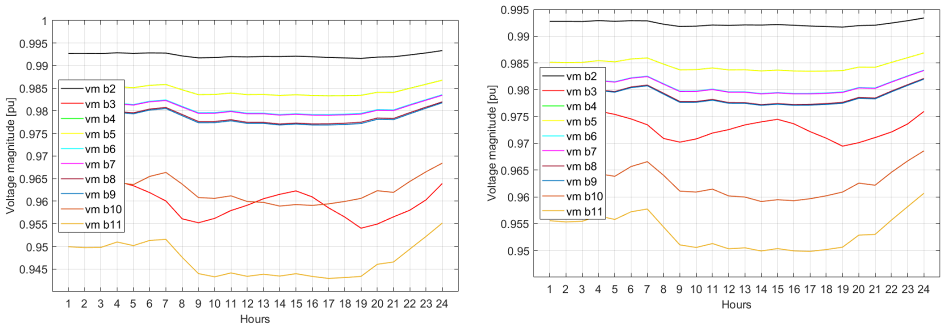

(a) Voltage magnitude with implemented battery

(b) Voltage magnitude with modified transmission lines and implemented battery

Figure 7.20: Case five - Voltage magnitude

Figure 7.21 expresses the different voltage levels for some of the study cases that have been investigated throughout this thesis. At first sight, one can see that the voltage magnitude during the low demand months is relatively high compared to the remaining voltage curves, thus having a great potential for vehicle charging. As seen from this figure, the voltage level during case five the with modified cross-section and battery storage is considerably higher than for the remaining buses, even for the high demand of case zero. This indicates that even with a charging load P_{ev10} of roughly 13MW and with the implementation of two alternatives for grid mitigation, the voltage level can be raised above the initial case where no EV charging was active, for the majority of hours.

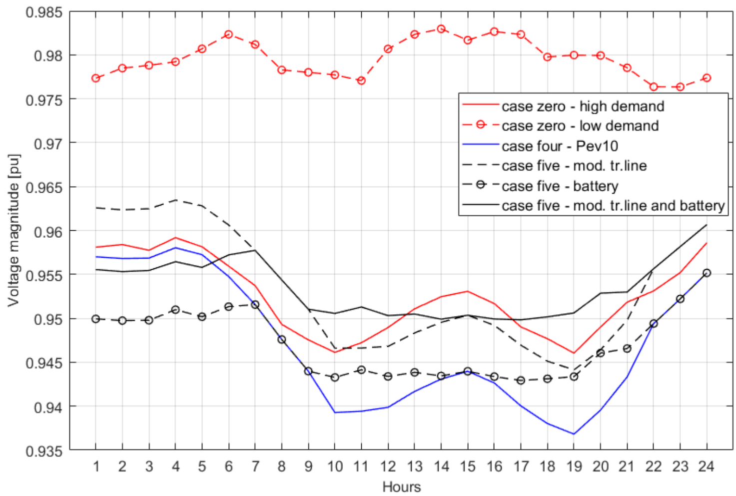

Figure 7.21: Case five - Voltage magnitude for bus 11 when the system is being exposed to EV charging and different strategies to of grid improvement

As shown in figure 7.22, the current is now more evenly distributed along the top part of the curve, compared to figure 7.2. During the high demand of case zero, the current reached up to a value of 196.1A, which is equal to 199,5A for this modified case, but for a different time period. Even though the current has a slightly higher top value for case five, the additional charging load P_{ev10} of 13MW has to be taken into consideration. With battery storage, the high demand hours of 10 and 19 have been shaved off accordingly to figure 7.19, thus resulting in a uniformly current distribution.

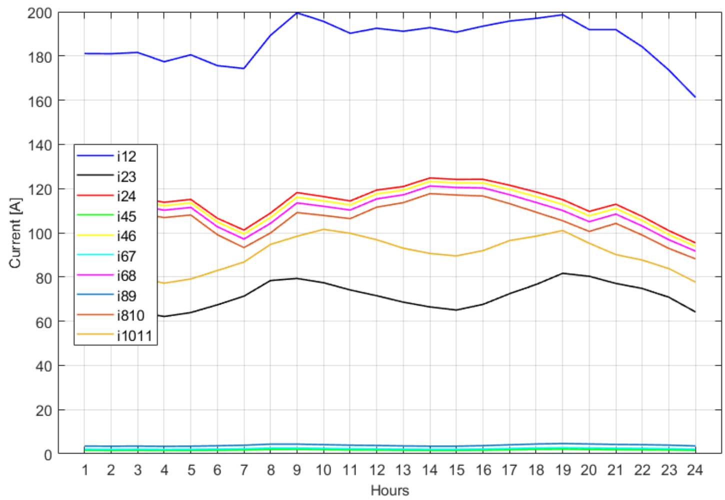

Figure 7.22: Case five - Current distribution with increased cross section in addition to battery storage

The variation in power losses either if the battery storage is active or not, are minimal. As it was presented in table 7.22, the total active losses were 4.980MW through one day. The active power losses when battery storage is added on top of this, gives 4.915MW from table 7.23, which shows the considerably small improvements of 0.065MW coming from the battery. This power difference can be investigated in more detail to determine what time periods are to be considered as substantial contributors.

Table 7.23: Case five - Total power loss for 24 hours with modified transmission lines and battery storage

	Line 1-2	Line 2-3	Line 2-4	Line 4-5	Line 4-6	Line 6-7	Line 6-8	Line 8-9	Line 8-10	Line 10-11	Total
Total active loss [MW]	1,018	0,983	0,634	0,000	0,307	0,000	0,147	0,000	1,236	0,589	4,915
Total reactive loss [MVAr]	1,069	1,032	0,666	0,000	0,323	0,000	0,155	0,000	1,299	0,619	5,163

Figure 7.23 shows how the power loss for transmission line 1-2 is changing with the current variations from the two strategies for grid improvements. The shaded area of this figure is illustrating the amount of active power that is separating the two alternatives. From figure 7.19, the first few hours of battery charging is increasing the total demand by roughly 1000kW for each hour, thus giving higher losses during these hours, hence the green area of figure 7.23. On the contrary, in the afternoon-evening hours, the total demand is decreasing due to the discharging of the battery, thus giving lower losses, hence the grey area. Since the total active power losses through 24 hours have been reduced by 0.065MW with the implementation of battery storage, that indicates that the grey area is slightly bigger than the green area.

When the battery is connected, the current flow in the system is lower during the high demand hours, and higher during the low demand hours, due to charging and discharging of the battery. The power loss is expressed as the current squared times the impedance. Thus the current peaks that are shaved off due to battery discharge will have a greater impact on the power losses than compared to the power losses coming from the increasing current when the battery is charging up. Take note that figure 7.23 is only representing the heaviest loaded line, referred to as transmission line 1-2.

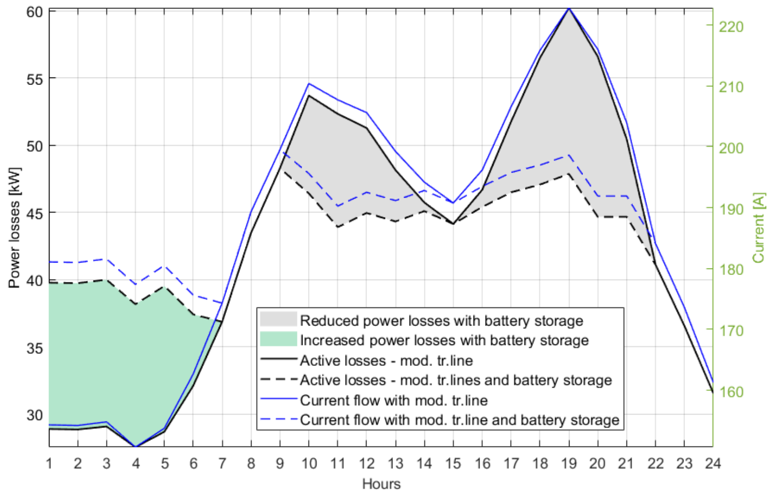

Figure 7.23: Case five - Active power losses as a result of varying current distribution for transmission line 1-2. Comparison of modified transmission lines and implementation of battery storage

Chapter 8

Discussion

According to the Paris Agreement, the temperature has to be reduced to below $2°C$. Norway which is considered as a pioneer within the electrification of transportation, has made a goal of reducing greenhouse gas emission by 40% by 2030. The transport sector is responsible for almost a third of Norway's total greenhouse gas emissions. Thus the transition towards electrified mobility has a crucial role in reaching this climate goal. With more research and new developments, smarter and more advanced ways of charging will be available, making electric cars a more viable alternative. However, this is also causing issues related to the power system, whether the capacity of existing grids are capable of handling this increase, or what measures have to be done in order to mitigate the grid impacts, focusing on the supply voltage variations . This thesis collaborates with SINTEF's project, Grid and Charging Infrastructure of the Future (FuChar), to investigate the grid impacts of high-power charging.

8.1 Validation of the Modelled Power System

The general loads used for this thesis are based on general load FASIT profiles, which are made by SINTEF. These profiles are estimates of how the load profiles from each diverse consumer group are distributed hourly throughout a day. Theses general load profiles could have been made more precise for this thesis by making them fit the yearly consumption coming from individual end-user, thus being scaled on actual data of customers from DSO's NIS system. Due to not having access to a customer overview like this, none of the general profiles were scaled accordingly. This means that all load profiles within each load group were the same, thus the total demand for each load group was only dependent on the number of customers. This prevents each load from being characterized by different levels of consumption, which would have been a reasonable way to model the loads more realistically. Another aspect considering the reliability of the loads is simply the fact that the number of loads has been approximated by the naked eye, from NVE's transmission line overview. As the name implies, this map only showed transmission lines, lines $\geq 24kV$

explicitly. Thus none of the buildings expressed in this geographical map showed where and how they were connected to the grid. This gives some uncertainty in the general load data, whether the approach used to estimate the number of loads and also the type of load has been done reasonably.

The goal of this thesis has been to investigate how a considerable amount of EV charging would affect the MV grid, thus the modelling of the charging profiles itself has not been a part of this thesis. The charging profiles that were generated for this thesis were based on the same area as for the modelled power system. This gives the reason to believe that the modelled network and the generated profiles give the best possible representation of this area. The charging profiles were based on numerous factors like SoC, charging duration, queuing, and more, which gives a good representation of realistic EV charging behavior. The total power demand from the charging station was limited by a few elements. First off, the car pool that was used to generate the charging profiles were restricted to a charging power of 150kW. As of today, due to new research and technology, some cars are capable of charging with power up to 350kW, which would have increased the power demand by quite some. Secondly, the area that was being investigated was a rural area meaning that the traffic flow would be lower than compared to an urban area. From the results of four charging outlets, the number of outlets was already limited by the traffic flow. In order to transition to six outlets, the traffic flow had to be increased for the two additional chargers to have any effect at all.

The purpose of the assumed voltage limit of $\pm 5\%$ was so that the power system would have spare capacity for future expansion like new customers, other alternatives for EV charging, or simply just an increase in the systems power demand. Despite this, a low tolerance level of $\pm 5\%$ is therefore assumed to be a reasonable limit for this thesis.

From the results presented, it is important to emphasise that the model is not based on actual data of customers, transmission lines or loads. Thus the assumptions and simplifications that have been present for this thesis might have caused a slight deviation compared to the physical system itself. When that is said, this area is mainly used as an outline to develop a network that could be analysed. Even though there will be some uncertainties in the data compared to the real system, it has not limited the purpose of this thesis to any high degree.

8.2 Validation of the Results

Validating the accuracy and reliability of the results that have been presented in this thesis, it is hard to tell whether the results are reasonable or not. There is no exact outline to follow for a power system, due to its large pool of impacting variables that will have to be considered. When that is said, the results that have been expressed in this thesis have some characteristics that could be tied up to a real power system. These could be high voltage fluctuations, a considerable difference in power demand for summer and winter months, higher consuming hours in the afternoon, periods where the values are close to or exceeding the threshold.

As it was described in the initial case study results, the voltage had a tendency to exceed the limit of -5% for some hours, even without EV charging implemented. This gave some interesting possibilities of how to improve the voltage quality when the system was to be exposed to an even higher total power demand when considering the implementation of EV charging. From the last study case regarding different strategies for grid improvements, the results that were presented showed some significant improvements for the voltage quality. With the implementation of battery storage and increased cross-sections for some transmission lines, the voltage was kept above the minimum limit of -5%. Keep in mind that the voltage was already exceeding this threshold without EV charging or alternatives for grid improvements.

The strategy of increased cross-section raises the question about utility cost, how much will the cost of increased cross-section be compared to the cost related to higher losses. As from a DSO point of view, this deep dive into the economic aspects has not been considered in this thesis. When that is said, the increased cross-section is also a realistic alternative regarding future expansion of the power grid, where some components would eventually have to be upgraded in order for the system to handle an increase in power demand, regardless of EV charging. The battery that was implemented had its purpose of shaving off the high peaks that were occurring during high demand hours. From the results, the battery which was modelled to take 40% of the total EV charging load, fulfilled its purpose by reducing the high peaks of 10 and 19 and instead distributed the load more evenly throughout the day. In reality, there would have been losses tied up to the battery and EV charging, but for the simplicity of this thesis, both the battery and EV charging was assumed to have 100% efficiency.

The various current values that were found throughout the investigation of this thesis were not considered as critical. Looking at the case zero during the high demand months, the current almost reached a 50% value of the transmission line's capacity, for the most affected line. Likewise, the results from the worst case scenario, case four, indicated an increase of 29A compared to case zero. Since this type of line has a limit of 390A, the 29A is equal to 7.4% of the line's total capacity. Depending on which power grid is being investigated, an increase of 7.4% may be critical for systems that are already heavily loaded. For the system modelled in this thesis, this increase is almost negligible since the lines are far from reaching a threshold. This indicates that the cross-section used for this thesis can be considered oversized. When that is said, this thesis has not been looking at the economic aspects of transmission lines. Thus the measure for grid improvements only studies how different cross-sections are affecting the supply voltage variation in the grid.

Looking at the outcome of the first two cases where EV charging was implemented, the reduced grid quality due to EV charging were minimal. Considering two charging outlets of 150kW, it gave an additional voltage drop of 0.0008 pu compared to the initial study case. Furthermore, when four charging outlets were being investigated, the voltage was 0.0017 pu lower than the initial case. Even with six charging outlets and a slight increase in the traffic flow, the additional voltage drop turned out to be 0.0027 pu. As these results express, none of these charging alternatives had any considerable impact on the voltage quality. However, in order for these profiles to be implemented in this thesis, they had to be converted into hourly-resolution profiles, thus being expressed as mean values for each individual hour. Due to this transformation, the high peaks from EV charging may have been shaved off, which implies that these high consuming periods might not have appeared as high peaks in the power flow model. This could have caused the systems total power demand to be slightly lower than the actual value for some hours, thus it may have caused a slight mismatch in the results.

Another interesting observation is how the EV charging profiles corresponds to the power demand from the general loads. For the various EV charging profiles that have been presented, the majority of the profiles followed the same power demand pattern as for the general loads. This means that the most critical hour of 19, where the system's power demand is at its highest, will be exposed to significantly higher demand with EV charging. Without any form of controlled charging or energy storage, highly loaded power systems with values close to different limits will most likely have the EV power demand interfere with the system's total capacity for specific periods.

Chapter 9

Conclusion

In this thesis, implementation of large scale EV in the MV grid has been investigated to find out how the modelled power system is responding to this increased power consumption, and to what extent different strategies can mitigate the impacts of EV charging. Throughout the study cases that have been presented in this thesis, a variety of charging alternatives expressed as different levels of power consumption have been investigated. In addition to that, two different strategies for grid improvements have been tested, increased cross-section and battery storage, respectively. The results of this analysis have been retrieved through power flows that have been executed in MATLAB®.

The impacts from two, four, and six charging outlets of 150kW had considerably small impacts on the power system. Even though the high-power charging of 150kW can be considered as a high level of charging, the power demand from the charging station is limited by the number of charging outlets. By increasing the number of charging outlets and the traffic flow remarkably, the results were quite different. With this alternative of charging, the voltage was below the limit of -5% for 14 hours, which is referred to as an additional 6 hours compared to the initial case with no EV charging. By implementing battery storage and increasing the cross-section of some transmission lines, the voltage was kept within the boundaries of $\pm 5\%$ throughout the whole day, with the exceptions of two hours where it was barely underneath the limit. It is concluded that even with a large EV scale and with its high power consumption, the supply voltage variations can be improved by a considerable amount by using smart and already developed strategies for grid improvements. Even though the voltage limit was already exceeded before the implementation of EV charging, the network could still handle a large EV share as long as measures were done to mitigate these impacts. However, the economic aspects are also something that has to be considered if these strategies are implemented in an actual power system.

The majority of the loads in the system were distributed more or less in the same way throughout the day, which emphasise the distinct separation of high and low demand hours. With these clear separations between high and low demand, a strategy like battery storage reduced the heavily loaded hours by moving some of the load to off-peak hours. This strategy for grid improvement was essential in order to keep the supply voltage variations within limits, regardless of EV charging. With the great deviation of high and low demand months, and if these low demand months were considered throughout a year, the system would have been more facilitated for a higher share of EV.

Chapter 10

Further Work

The work that has been done in this thesis could be expanded in several ways. The most valuable improvement is to obtain real data from the DSO of the examined area. Not only does this provide the DSO with relevant information regarding the impacts of EV charging, but it could also be used to validate the data that has been gathered throughout this thesis. In addition to that, it could indicate whether the assumptions and simplifications that have been carried out in this thesis is an appropriate way of modelling a network.

Another interesting approach is to investigate the economic aspects of increased the cross-section and implemented battery storage. As it has been mentioned, a major issue related to increasing the cross-section is how the economic benefits of reduced losses are compared to the price of reinvesting in the new transmission lines, and which of these alternatives are most cost-effective considering a future expansion with increasing power demand. The battery used for storage could also be investigated in more detail, by creating an algorithm that could keep track of when to charge and discharge in order to reduce the losses by as much as possible. In general, various strategies of grid improvement could be examined to find the most optimal and highly cost-effective alternative.

Smart charging which is also considered as a way of mitigating the grid impacts from EVs, could be reviewed. This strategy could be simulated through signal response, where the grid and the EVs are communicating to avoid overloading for specific hours. This means that instead of having a high share of EVs that are charging during high demand hours, they could be moved to the valley hours where the systems' total power consumption is lower. Thus taking advance of the spare capacity in the grid and also making room for a larger portion of EV.

Bibliography

[1] T. Aarnes. High-power electric charging in the norwegian distribution grid. Project report in TET5500, Faculty of Information Technology and Electrical Engineering, NTNU - Norwegian University of Science and Technology, December 2019.

[2] J. Asamer, M. Reinthaler, M. Ruthmair, M. Straub, and J. Puchinger. Optimizing charging station locations for urban taxi providers. *Transportation Research Part A: Policy and Practice*, 85:233 – 246, 2016.

[3] J.-M. Clairand, P. Guerra-Terán, X. Serrano Guerrero, M. Gonzalez, and G. Escrivá. Electric vehicles for public transportation in power systems: A review of methodologies. *Energies*, 12:3114, 08 2019.

[4] C. H. Dharmakeerthi, N. Mithulananthan, and T. K. Saha. Overview of the impacts of plug-in electric vehicles on the power grid. In *2011 IEEE PES Innovative Smart Grid Technologies*, pages 1–8, 2011.

[5] H. Ding, Z. Hu, and Y. Song. Value of the energy storage system in an electric bus fast charging station. *Applied Energy*, 157:630 – 639, 2015.

[6] A. O. Eggen and H. Vefsnmo. *FASIT kravspesifikasjon - versjon 2019*. SINTEF Energi AS, 2018.

[7] N. elbilforening. Ladestasjoner. `https://elbil.no/elbilstatistikk/ladestasjoner/`. Online; accessed 09-June-2020.

[8] A. M. F. Flataker, M. Z. Degefa, B. N. Torsæter, and K. Berg. Coordinated voltage control in the distribution grid, 2020. SINTEF Energi AS / Energisystemer.

[9] L. Fridstrøm. Framskriving av kjøretøyparken i samsvar med nasjonalbudsjettet 2019, 2019.

[10] C. N. Garrett Fitzgerald. Evgo fleet and tariff analysis, phase 1: California, 2017.

[11] C. Hedegaard and I. Kreutzer. Better growth, lower emissions - the norwegian government's strategy for green competitiveness.
`https://www.regjeringen.no`.
Online; accessed 10-June-2020.

[12] A. Ihekwaba and C. Kim. Analysis of electric vehicle charging impact on grid voltage regulation. In *2017 North American Power Symposium (NAPS)*, pages 1–6, 2017.

[13] E. Ivarsøy. Demand modeling of high-power electric vehicle charging. Project report in TET5500, Faculty of Information Technology and Electrical Engineering, NTNU - Norwegian University of Science and Technology, December 2019.

[14] M. S. S. J. Duncan Glover, Thomas J. Overbye. *Power System Analysis and Design*. 6 edition, 2016.

[15] P. Kasten, J. Bracker, M. Haller, and J. Purwanto. Assessing the status of electrification of the road transport passenger vehicles and potential future implications for the environment and european energy system. Technical report, 2016.

[16] B. Liao, L. Li, B. Li, J. Mao, J. Yang, F. Wen, and M. A. Salam. Load modeling for electric taxi battery charging and swapping stations: Comparison studies. In *2016 IEEE 2nd Annual Southern Power Electronics Conference (SPEC)*, pages 1–6, 2016.

[17] Y. Lin, K. Zhang, Z.-J. M. Shen, B. Ye, and L. Miao. Multistage large-scale charging station planning for electric buses considering transportation network and power grid. *Transportation Research Part C: Emerging Technologies*, 107:423 – 443, 2019.

[18] J. A. P. Lopes, F. J. Soares, and P. M. R. Almeida. Integration of electric vehicles in the electric power system. *Proceedings of the IEEE*, 99(1):168–183, 2011.

[19] E. Lorentzen, P. Haugneland, C. Bu, and E. Hauge. Charging infrastructure experiences in norway - the worlds most advanced ev market. In *EVS30 International Battery, Hybrid and Fuel Cell Electric Vehicle Symposium*, 2017.

[20] D. McCarthy and P. Wolfs. The hv system impacts of large scale electric vehicle deployments in a metropolitan area. In *2010 20th Australasian Universities Power Engineering Conference*, pages 1–6, 2010.

[21] M. Metcalf. Epic 1.25 – develop a tool to map the preferred locations for dc fast charging, based on traffic patterns and pge's distribution system, to address ev drivers' needs while reducing the impact on pge's distribution grid, 2016.

[22] D. H. Michael Nicholas. Lessons learned on early electric vehicle fast-charging deployments, 2018.

[23] Norges vassdrags- og energidirektorat. *Forskrift om leveringskvalitet i kraftsystemet*, 2004.

[24] M. i. NRK. Ranheim værvarsel. `https://www.yr.no/nb/historikk/graf/1-2411165/Norge/Tr%C3%B8ndelag/Trondheim/Ranheim`.
Online; accessed 14-April-2020.

[25] G. A. Putrus, P. Suwanapingkarl, D. Johnston, E. C. Bentley, and M. Narayana. Impact of electric vehicles on power distribution networks. In *2009 IEEE Vehicle Power and Propulsion Conference*, pages 827–831, 2009.

[26] RENBLAD NR 8041. *Distribusjonsnett - Tekniske verdier*, 2011.

[27] S. A. A. Rizvi, A. Xin, A. Masood, S. Iqbal, M. U. Jan, and H. Rehman. Electric vehicles and their impacts on integration into power grid: A review. In *2018 2nd IEEE Conference on Energy Internet and Energy System Integration (EI2)*, pages 1–6, 2018.

[28] H. Saadat. *Power System Analysis*. PSA Publishing, United States of America, 3 edition, 2010.

[29] SSB. Transport står for 30 prosent av klimautslippene i norge. https://www.ssb.no/natur-og-miljo/artikler-og-publikasjoner/transport-star-for-30-prosent-av-klimautslippene-i-norge. Online; accessed 10-June-2020.

[30] B. Torsæter. Fuchar - grid and charging infrastructure of the future. https://www.sintef.no/en/projects/fuchar/. Online; accessed 11-June-2020.

[31] N. vassdrags-og energidirektorat. Nve kartkatalog - nettanlegg. https://temakart.nve.no/link/?link=nettanlegg. Online; accessed 14-April-2020.

[32] Y. Yang, Q. Jia, X. Guan, X. Zhang, Z. Qiu, and G. Deconinck. Decentralized ev-based charging optimization with building integrated wind energy. *IEEE Transactions on Automation Science and Engineering*, 16(3):1002–1017, 2019.

[33] R. D. Zimmerman and C. E. Murillo-Sánchez. Matpower, June 2019.

[34] R. D. Zimmerman and C. E. Murillo-Sánchez. Matpower user's manual, June 2019.

Appendix

A

General FASIT Load Profiles

These are the FASIT load profiles from SINTEF [6] which illustrated the 11 different load groups and their respective value.

Navn	Måned	Dag	AB	01 0000-0100	02 0100-0200	03 0200-0300	04 0300-0400	05 0400-0500	06 0500-0600	07 0600-0700	08 0700-0800	09 0800-0900	10 0900-1000	11 1000-1100	12 1100-1200	13 1200-1300	14 1300-1400	15 1400-1500	16 1500-1600	17 1600-1700	18 1700-1800	19 1800-1900	20 1900-2000	21 2000-2100	22 2100-2200	23 2200-2300	24 2300-2400	SUM 0000-2400
Jordbruk	**høylast**	**hverdag**	**A**	-0,051	-0,051	-0,051	-0,052	-0,051	-0,050	-0,050	-0,052	-0,061	-0,062	-0,062	-0,066	-0,062	-0,063	-0,065	-0,061	-0,057	-0,064	-0,061	-0,059	-0,063	-0,065	-0,065	-0,067	**-1,411**
Jordbruk	**høylast**	**hverdag**	**B**	2,116	2,100	2,091	2,098	2,068	2,070	2,283	3,076	3,415	2,940	2,579	2,423	2,338	2,270	2,256	2,333	2,711	3,236	3,131	2,581	2,367	2,271	2,189	2,105	**59,047**
Jordbruk	**høylast**	**helg**	**A**	-0,026	-0,026	-0,030	-0,027	-0,028	-0,029	-0,028	-0,026	-0,038	-0,049	-0,043	-0,039	-0,037	-0,035	-0,056	-0,046	-0,046	-0,046	-0,027	-0,031	-0,035	-0,036	-0,038	-0,035	**-0,857**
Jordbruk	**høylast**	**helg**	**B**	2,151	2,149	2,138	2,149	2,120	2,111	2,279	2,846	3,402	3,018	2,573	2,376	2,311	2,217	2,199	2,301	2,623	3,207	3,059	2,604	2,400	2,336	2,248	2,186	**59,003**
Jordbruk	**lavlast**	**hverdag**	**A**	0,003	0,002	0,002	0,002	0,001	0,002	-0,002	-0,002	-0,004	-0,002	0,006	0,009	0,006	0,011	0,014	0,006	-0,004	-0,004	0,007	0,016	0,016	0,008	0,004	0,001	**0,098**
Jordbruk	**lavlast**	**hverdag**	**B**	1,865	1,852	1,841	1,827	1,818	1,795	1,970	2,702	3,108	2,732	2,405	2,237	2,125	2,064	2,044	2,149	2,522	3,014	2,926	2,438	2,195	2,111	2,006	1,914	**53,660**
Jordbruk	**lavlast**	**helg**	**A**	-0,006	-0,007	-0,007	-0,008	-0,010	-0,007	-0,011	-0,009	-0,019	-0,027	-0,018	-0,006	-0,007	-0,007	-0,008	-0,009	-0,016	-0,022	-0,007	-0,004	-0,004	-0,006	-0,010	-0,010	**-0,245**
Jordbruk	**lavlast**	**helg**	**B**	1,873	1,853	1,837	1,831	1,817	1,807	1,944	2,517	3,055	2,779	2,378	2,162	2,093	2,019	1,999	2,106	2,430	3,009	2,825	2,377	2,126	2,047	1,975	1,892	**52,751**
Husholdning	**høylast**	**hverdag**	**A**	-0,056	-0,058	-0,059	-0,061	-0,063	-0,068	-0,068	-0,080	-0,070	-0,066	-0,062	-0,065	-0,061	-0,060	-0,060	-0,060	-0,059	-0,062	-0,061	-0,056	-0,058	-0,054	-0,055	-0,056	**-1,478**
Husholdning	**høylast**	**hverdag**	**B**	2,536	2,442	2,423	2,412	2,458	2,558	2,837	3,038	2,987	2,913	2,887	2,809	2,715	2,668	2,685	2,904	3,201	3,369	3,491	3,536	3,470	3,401	3,191	2,799	**69,730**
Husholdning	**høylast**	**helg**	**A**	-0,056	-0,057	-0,050	-0,054	-0,057	-0,056	-0,054	-0,057	-0,059	-0,054	-0,054	-0,056	-0,049	-0,046	-0,050	-0,048	-0,054	-0,058	-0,057	-0,052	-0,056	-0,057	-0,061	-0,065	**-1,317**
Husholdning	**høylast**	**helg**	**B**	2,643	2,468	2,421	2,404	2,425	2,456	2,520	2,609	2,811	3,093	3,213	3,187	3,132	3,097	3,109	3,237	3,274	3,355	3,464	3,533	3,496	3,338	3,187	2,830	**71,302**
Husholdning	**lavlast**	**hverdag**	**A**	-0,082	-0,085	-0,086	-0,087	-0,089	-0,092	-0,094	-0,101	-0,100	-0,099	-0,099	-0,099	-0,097	-0,098	-0,103	-0,107	-0,109	-0,114	-0,117	-0,116	-0,110	-0,103	-0,096	-0,088	**-2,371**
Husholdning	**lavlast**	**hverdag**	**B**	2,445	2,343	2,315	2,304	2,321	2,389	2,618	2,901	2,945	2,915	2,865	2,793	2,691	2,682	2,753	2,992	3,192	3,341	3,408	3,433	3,409	3,346	3,167	2,793	**68,361**
Husholdning	**lavlast**	**helg**	**A**	-0,087	-0,084	-0,084	-0,086	-0,087	-0,091	-0,091	-0,091	-0,092	-0,096	-0,103	-0,106	-0,104	-0,102	-0,108	-0,112	-0,116	-0,118	-0,120	-0,116	-0,110	-0,100	-0,095	-0,088	**-2,387**
Husholdning	**lavlast**	**helg**	**B**	2,580	2,378	2,324	2,307	2,305	2,342	2,379	2,470	2,680	2,944	3,118	3,147	3,043	3,013	3,121	3,208	3,276	3,337	3,407	3,424	3,397	3,299	3,139	2,816	**69,454**
Industri-1	**høylast**	**hverdag**	**A**	0,000	0,000	0,000	0,000	0,000	0,000	0,000	0,000	0,000	0,000	0,000	0,000	0,000	0,000	0,000	0,000	0,000	0,000	0,000	0,000	0,000	0,000	0,000	0,000	**0,000**
Industri-1	**høylast**	**hverdag**	**B**	107,133	106,377	112,671	125,561	123,883	149,508	210,079	281,420	301,317	304,861	306,550	305,595	303,247	297,228	284,303	241,682	208,777	185,799	157,850	144,596	129,745	118,621	114,933	111,846	**4733,582**
Industri-1	**høylast**	**helg**	**A**	0,000	0,000	0,000	0,000	0,000	0,000	0,000	0,000	0,000	0,000	0,000	0,000	0,000	0,000	0,000	0,000	0,000	0,000	0,000	0,000	0,000	0,000	0,000	0,000	**0,000**
Industri-1	**høylast**	**helg**	**B**	107,286	102,043	100,498	100,635	99,890	99,892	103,752	104,773	110,019	119,227	123,649	126,109	123,465	123,772	119,859	115,739	115,594	115,150	112,861	112,816	111,567	110,379	110,164	108,648	**2677,787**
Industri-1	**lavlast**	**hverdag**	**A**	0,000	0,000	0,000	0,000	0,000	0,000	0,000	0,000	0,000	0,000	0,000	0,000	0,000	0,000	0,000	0,000	0,000	0,000	0,000	0,000	0,000	0,000	0,000	0,000	**0,000**
Industri-1	**lavlast**	**hverdag**	**B**	104,767	97,558	96,979	103,395	103,837	103,557	128,651	190,887	273,450	295,530	300,267	302,200	302,231	299,898	294,786	279,434	224,146	190,067	170,029	151,208	138,950	125,529	113,548	110,230	**4501,134**
Industri-1	**lavlast**	**helg**	**A**	0,000	0,000	0,000	0,000	0,000	0,000	0,000	0,000	0,000	0,000	0,000	0,000	0,000	0,000	0,000	0,000	0,000	0,000	0,000	0,000	0,000	0,000	0,000	0,000	**0,000**
Industri-1	**lavlast**	**helg**	**B**	102,693	95,583	94,579	93,518	93,080	93,274	98,590	99,517	103,657	112,609	116,219	118,420	115,529	115,706	113,198	110,192	109,004	108,388	106,635	105,765	104,348	103,586	103,264	102,731	**2520,085**
Industri-2	**høylast**	**hverdag**	**A**	0,000	0,000	0,000	0,000	0,000	0,000	0,000	0,000	0,000	0,000	0,000	0,000	0,000	0,000	0,000	0,000	0,000	0,000	0,000	0,000	0,000	0,000	0,000	0,000	**0,000**
Industri-2	**høylast**	**hverdag**	**B**	111,846	107,133	106,377	112,671	125,561	123,883	210,079	281,420	301,317	304,861	305,595	305,595	305,595	305,595	305,595	305,595	305,595	305,595	305,595	305,595	305,595	305,595	305,595	284,303	**6042,186**
Industri-2	**høylast**	**helg**	**A**	0,000	0,000	0,000	0,000	0,000	0,000	0,000	0,000	0,000	0,000	0,000	0,000	0,000	0,000	0,000	0,000	0,000	0,000	0,000	0,000	0,000	0,000	0,000	0,000	**0,000**
Industri-2	**høylast**	**helg**	**B**	107,286	102,043	100,498	100,635	99,890	99,892	104,773	110,019	119,227	123,465	123,465	123,465	123,465	123,465	123,465	123,465	123,465	123,465	123,465	123,465	123,465	123,465	123,465	115,739	**2788,512**
Industri-2	**lavlast**	**hverdag**	**A**	0,000	0,000	0,000	0,000	0,000	0,000	0,000	0,000	0,000	0,000	0,000	0,000	0,000	0,000	0,000	0,000	0,000	0,000	0,000	0,000	0,000	0,000	0,000	0,000	**0,000**
Industri-2	**lavlast**	**hverdag**	**B**	104,767	97,558	96,979	103,395	103,837	103,557	190,887	273,450	295,530	300,267	302,231	302,231	302,231	302,231	302,231	302,231	302,231	302,231	302,231	302,231	302,231	302,231	302,231	279,434	**5878,664**
Industri-2	**lavlast**	**helg**	**A**	0,000	0,000	0,000	0,000	0,000	0,000	0,000	0,000	0,000	0,000	0,000	0,000	0,000	0,000	0,000	0,000	0,000	0,000	0,000	0,000	0,000	0,000	0,000	0,000	**0,000**
Industri-2	**lavlast**	**helg**	**B**	102,693	95,583	94,579	93,518	93,080	93,274	99,517	103,657	112,609	116,219	116,219	116,219	116,219	116,219	116,219	116,219	116,219	116,219	116,219	116,219	116,219	116,219	116,219	110,192	**2625,768**
Industri-3	**høylast**	**hverdag**	**A**	0,000	0,000	0,000	0,000	0,000	0,000	0,000	0,000	0,000	0,000	0,000	0,000	0,000	0,000	0,000	0,000	0,000	0,000	0,000	0,000	0,000	0,000	0,000	0,000	**0,000**
Industri-3	**høylast**	**hverdag**	**B**	304,861	304,861	304,861	304,861	304,861	304,861	304,861	304,861	304,861	304,861	304,861	304,861	304,861	304,861	304,861	304,861	304,861	304,861	304,861	304,861	304,861	304,861	304,861	304,861	**7316,664**
Industri-3	**høylast**	**helg**	**A**	0,000	0,000	0,000	0,000	0,000	0,000	0,000	0,000	0,000	0,000	0,000	0,000	0,000	0,000	0,000	0,000	0,000	0,000	0,000	0,000	0,000	0,000	0,000	0,000	**0,000**
Industri-3	**høylast**	**helg**	**B**	123,649	123,649	123,649	123,649	123,649	123,649	123,649	123,649	123,649	123,649	123,649	123,649	123,649	123,649	123,649	123,649	123,649	123,649	123,649	123,649	123,649	123,649	123,649	123,649	**2967,576**
Industri-3	**lavlast**	**hverdag**	**A**	0,000	0,000	0,000	0,000	0,000	0,000	0,000	0,000	0,000	0,000	0,000	0,000	0,000	0,000	0,000	0,000	0,000	0,000	0,000	0,000	0,000	0,000	0,000	0,000	**0,000**
Industri-3	**lavlast**	**hverdag**	**B**	302,231	302,231	302,231	302,231	302,231	302,231	302,231	302,231	302,231	302,231	302,231	302,231	302,231	302,231	302,231	302,231	302,231	302,231	302,231	302,231	302,231	302,231	302,231	302,231	**7253,544**
Industri-3	**lavlast**	**helg**	**A**	0,000	0,000	0,000	0,000	0,000	0,000	0,000	0,000	0,000	0,000	0,000	0,000	0,000	0,000	0,000	0,000	0,000	0,000	0,000	0,000	0,000	0,000	0,000	0,000	**0,000**
Industri-3	**lavlast**	**helg**	**B**	116,219	116,219	116,219	116,219	116,219	116,219	116,219	116,219	116,219	116,219	116,219	116,219	116,219	116,219	116,219	116,219	116,219	116,219	116,219	116,219	116,219	116,219	116,219	116,219	**2789,256**
Varehandel	**høylast**	**hverdag**	**A**	-2,612	-2,617	-2,594	-2,581	-2,696	-2,782	-2,786	-2,751	-2,867	-3,604	-4,008	-3,938	-3,910	-3,873	-3,651	-3,415	-3,589	-3,228	-2,871	-3,149	-2,724	-2,948	-2,639	-2,761	**-74,594**
Varehandel	**høylast**	**hverdag**	**B**	110,838	112,498	110,461	110,690	110,832	113,092	117,935	128,397	144,894	164,127	170,017	167,751	165,096	164,520	164,238	162,386	161,509	152,737	142,092	121,101	114,631	111,380	110,273	109,250	**3240,745**
Varehandel	**høylast**	**helg**	**A**	-1,914	-1,892	-2,094	-1,880	-1,847	-1,745	-1,442	-1,704	-3,217	-3,599	-4,055	-4,110	-3,713	-2,869	-1,773	-2,035	-2,125	-2,122	-2,103	-1,897	-1,934	-1,963	-1,781	-2,058	**-55,872**
Varehandel	**høylast**	**helg**	**B**	109,361	111,910	109,971	111,174	111,817	113,420	117,961	122,651	128,003	132,506	132,730	128,448	126,059	120,693	115,034	106,718	105,483	107,015	111,133	107,470	110,712	110,149	112,517	111,258	**2774,193**
Varehandel	**lavlast**	**hverdag**	**A**	-1,755	-1,756	-1,635	-1,698	-1,706	-1,837	-1,880	-1,934	-1,811	-2,223	-1,625	-1,557	-1,424	-1,191	-1,129	-1,120	-1,401	-1,197	-1,643	-1,573	-1,894	-1,625	-1,609	-1,627	**-38,850**
Varehandel	**lavlast**	**hverdag**	**B**	103,191	104,025	102,465	102,636	103,285	105,903	108,848	119,050	133,031	155,064	163,238	163,159	161,355	159,878	158,227	157,515	156,175	146,592	134,103	115,270	109,813	106,609	103,688	103,144	**3076,264**
Varehandel	**lavlast**	**helg**	**A**	-1,734	-1,696	-1,552	-1,655	-1,752	-1,919	-1,961	-1,818	-1,996	-1,957	-1,622	-1,374	-1,303	-1,189	-1,402	-1,503	-1,467	-1,484	-1,533	-1,479	-1,851	-1,689	-1,737	-1,740	**-39,413**
Varehandel	**lavlast**	**helg**	**B**	101,924	102,297	100,746	101,358	102,657	104,326	107,030	111,590	118,848	126,857	128,552	126,623	125,302	119,634	110,033	101,573	100,982	101,975	103,401	100,893	102,497	103,972	104,275	104,586	**2611,931**
Kontor	**høylast**	**hverdag**	**A**	-0,846	-0,472	-0,333	0,667	1,941	1,612	2,740	2,459	-3,175	-4,386	-4,770	-5,197	-5,173	-5,239	-4,945	-4,526	-1,359	-0,581	-0,176	-1,250	-1,718	-1,181	-1,039	-0,971	**-37,918**
Kontor	**høylast**	**hverdag**	**B**	111,846	107,133	106,377	112,671	125,561	123,883	149,508	210,079	281,420	301,317	304,861	306,550	305,595	303,247	297,228	284,303	241,682	208,777	185,799	157,850	144,596	129,745	118,621	114,933	**4733,582**
Kontor	**høylast**	**helg**	**A**	-0,623	-0,206	-0,234	-0,227	-0,168	-0,147	-0,536	-0,739	-0,940	-1,641	-1,701	-1,667	-1,416	-1,181	-0,783	-0,770	-0,892	-0,818	-0,701	-0,600	-0,615	-0,538	-0,685	-0,700	**-18,528**
Kontor	**høylast**	**helg**	**B**	107,286	102,043	100,498	100,635	99,890	99,892	103,752	104,773	110,019	119,227	123,649	126,109	123,465	123,772	119,859	115,739	115,594	115,150	112,861	112,816	111,567	110,379	110,164	108,648	**2677,787**
Kontor	**lavlast**	**hverdag**	**A**	-1,271	-0,953	-0,846	-0,982	-1,045	-1,070	-1,395	-0,494	-2,470	-2,876	-2,842	-2,777	-2,804	-2,853	-3,021	-3,934	-2,237	-1,476	-1,172	-0,714	-0,738	-0,809	-1,074	-1,381	**-41,234**
Kontor	**lavlast**	**hverdag**	**B**	104,767	97,558	96,979	103,395	103,837	103,557	128,651	190,887	273,450	295,530	300,267	302,200	302,231	299,898	294,786	279,434	224,146	190,067	170,029	151,208	138,950	125,529	113,548	110,230	**4501,134**
Kontor	**lavlast**	**helg**	**A**	-1,348	-0,969	-0,962	-0,915	-0,987	-1,084	-1,432	-1,319	-0,973	-0,902	-0,898	-0,936	-0,930	-0,888	-0,891	-1,057	-1,074	-1,099	-1,166	-1,142	-1,062	-1,022	-1,033	-1,324	**-25,413**
Kontor	**lavlast**	**helg**	**B**	102,693	95,583	94,579	93,518	93,080	93,274	98,590	99,517	103,657	112,609	116,219	118,420	115,529	115,706	113,198	110,192	109,004	108,388	106,635	105,765	104,348	103,586	103,264	102,731	**2520,085**
Hotell	**høylast**	**hverdag**	**A**	-4,106	-4,058	-4,236	-4,330	-4,532	-4,617	-4,234	-4,617	-5,064	-4,488	-4,283	-3,877	-3,787	-3,839	-3,995	-3,668	-3,956	-4,294	-4,744	-4,942	-4,934	-5,009	-4,798	-4,293	**-104,701**
Hotell	**høylast**	**hverdag**	**B**	216,687	209,124	201,458	198,723	199,205	203,251	218,231	244,470	262,273	266,783	267,072	265,913	262,562	261,495	261,050	261,827	264,649	272,076	279,040	279,096	274,564	265,588	250,640	234,789	**5920,566**
Hotell	**høylast**	**helg**	**A**	-4,706	-4,560	-4,646	-4,489	-4,519	-4,758	-4,582	-4,410	-4,839	-4,730	-4,256	-3,748	-3,697	-3,490	-4,035	-3,889	-3,933	-4,721	-5,026	-5,108	-5,050	-5,142	-4,944	-4,119	**-107,397**
Hotell	**høylast**	**helg**	**B**	225,935	217,868	207,254	202,275	200,316	202,241	214,011	234,967	256,995	266,560	265,687	265,389	262,569	261,965	262,643	263,581	265,399	269,624	274,650	273,177	268,588	258,711	245,202	230,078	**5895,685**
Hotell	**lavlast**	**hverdag**	**A**	-5,323	-5,267	-5,115	-5,129	-5,150	-5,104	-5,014	-5,184	-5,333	-5,234	-5,058	-5,145	-5,113	-5,119	-5,125	-5,181	-5,384	-5,467	-5,540	-5,387	-5,385	-5,560	-5,486	-5,486	**-126,289**
Hotell	**lavlast**	**hverdag**	**B**	191,258	182,741	175,994	174,114	175,180	182,153	197,359	220,234	234,579	237,352	237,268	236,398	233,302	233,171	233,139	233,717	236,153	240,649	244,797	243,813	240,310	233,812	220,905	205,791	**5244,189**
Hotell	**lavlast**	**helg**	**A**	-5,864	-5,780	-5,462	-5,372	-5,363	-5,371	-5,310	-5,149	-5,318	-5,421	-5,345	-5,500	-5,468	-5,356	-5,502	-5,378	-5,513	-5,672	-5,584	-5,582	-5,451	-5,494	-5,682	-5,779	**-131,716**
Hotell	**lavlast**	**helg**	**B**	200,431	191,319	181,591	176,715	175,813	181,644	194,863	210,667	227,700	236,132	236,373	235,924	233,558	232,553	234,276	234,023	234,692	238,121	239,328	237,387	230,530	223,295	214,036	201,862	**5202,833**
Skole	**høylast**	**hverdag**	**A**	-2,406	-2,275	-2,520	-2,359	-2,263	-1,573	-0,432	-1,002	-0,808	-1,223	-1,285	-1,267	-1,341	-1,290	-2,398	-3,000	-3,109	-3,291	-3,337	-3,221	-3,126	-2,915	-2,693	-2,611	**-51,745**
Skole	**høylast**	**hverdag**	**B**	90,975	92,555	93,319	97,401	100,160	107,593	118,490	127,714	152,261	152,257	146,396	140,209	140,976	137,878	120,907	106,039	100,785	97,829	100,798	102,293	99,948	96,100	91,335	91,078	**2705,296**
Skole	**høylast**	**helg**	**A**	-2,046	-2,219	-2,129	-2,137	-1,916	-2,097	-2,113	-2,079	-1,831	-2,187	-2,485	-2,561	-2,789	-2,823	-2,900	-2,788	-2,820	-2,820	-2,861	-2,843	-2,522	-2,274	-2,152	-2,380	**-57,772**
Skole	**høylast**	**helg**	**B**	93,737	93,344	94,770	96,034	97,918	97,476	96,776	97,898	97,067	94,645	91,294	89,591	86,184	83,887	81,472	80,833	82,390	86,195	89,821	89,171	88,184	88,463	89,548	90,062	**2176,760**
Skole	**lavlast**	**hverdag**	**A**	-3,289	-3,412	-3,540	-3,592	-4,046	-4,858	-5,068	-5,711	-6,078	-5,733	-5,391	-5,224	-5,203	-4,959	-4,658	-4,732	-4,861	-4,312	-4,144	-3,822	-3,299	-3,275	-3,230	-3,278	**-105,715**
Skole	**lavlast**	**hverdag**	**B**	84,052	84,903	86,994	88,498	95,165	111,333	122,419	135,004	156,726	157,593	152,734	147,327	146,370	142,703	130,443	122,671	116,353	104,874	104,661	101,155	93,028	89,456	85,122	83,330	**2742,914**
Skole	**lavlast**	**helg**	**A**	-3,174	-3,187	-3,259	-3,425	-3,370	-3,612	-3,582	-3,776	-3,765	-3,588	-3,595	-3,489	-3,447	-3,586	-3,184	-3,287	-3,550	-3,562	-3,690	-3,530	-3,096	-3,324	-3,464	-3,443	**-82,985**
Skole	**lavlast**	**helg**	**B**	84,693	84,943	84,586	86,371	86,733	88,448	88,908	90,522	91,141	90,915	89,190	88,167	87,499	86,313	85,602	86,315	88,010	89,817	90,431	89,337	86,423	85,152	84,314	84,520	**2098,350**
Helse og sosial	**høylast**	**hverdag**	**A**	-31,718	-31,907	-32,174	-32,463	-32,419	-33,301	-32,433	-39,244	-34,096	-34,919	-32,243	-31,967	-34,731	-32,266	-37,343	-34,895	-33,017	-34,646	-34,131	-34,149	-34,001	-33,953	-32,634	-32,445	**-807,095**
Helse og sosial	**høylast**	**hverdag**	**B**	1050,539	1043,606	1040,771	1038,470	1043,435	1050,765	1145,913	1420,601	1621,464	1618,141	1683,880	1603,700	1526,940	1513,810	1442,782	1296,273	1211,546	1179,073	1186,771	1152,486	1109,456	1083,735	1058,074	1046,175	**30168,406**
Helse og sosial	**høylast**	**helg**	**A**	-30,022	-30,907	-30,497	-30,624	-31,235	-31,274	-30,235	-34,664	-31,964	-33,849	-31,399	-31,067	-32,771	-30,149	-30,484	-28,418	-28,417	-30,194	-29,921	-31,371	-31,665	-31,547	-30,392	-29,635	**-742,701**
Helse og sosial	**høylast**	**helg**	**B**	1039,390	1029,484	1030,721	1027,828	1025,552	1032,908	1101,055	1230,824	1281,727	1296,001	1306,403	1261,292	1197,546	1189,458	1170,654	1145,819	1127,694	1124,559	1142,658	1116,746	1081,119	1055,262	1034,463	1026,381	**27075,544**
Helse og sosial	**lavlast**	**hverdag**	**A**	-31,226	-31,162	-31,217	-31,315	-31,366	-31,581	-32,462	-36,925	-34,616	-32,223	-33,852	-33,557	-32,432	-33,151	-35,414	-34,425	-34,158	-33,817	-32,966	-32,313	-32,169	-31,939	-31,814	-31,734	**-787,834**
Helse og sosial	**lavlast**	**hverdag**	**B**	1047,507	1037,610	1035,683	1033,279	1035,930	1047,169	1130,662	1446,266	1621,148	1643,134	1701,602	1622,837	1564,323	1552,950	1499,838	1332,750	1239,387	1208,894	1199,303	1161,024	1139,271	1118,694	1092,305	1065,910	**30577,476**
Helse og sosial	**lavlast**	**helg**	**A**	-29,496	-29,856	-29,391	-29,349	-29,517	-30,075	-31,127	-33,476	-32,424	-31,189	-30,931	-29,626	-28,963	-29,541	-29,624	-30,166	-30,902	-31,106	-30,794	-30,278	-30,004	-29,462	-29,143	-29,106	**-725,546**
Helse og sosial	**lavlast**	**helg**	**B**	1039,224	1033,371	1027,648	1023,069	1026,746	1042,150	1094,224	1235,552	1273,124	1307,542	1317,396	1268,146	1226,543	1223,759	1186,703	1152,404	1138,119	1125,825	1134,554	1111,511	1096,046	1079,375	1058,400	1033,577	**27255,008**
Elkjel	**høylast**	**hverdag**	**A**	-17,284	-16,503	-19,098	-20,426	-21,075	-22,487	-22,774	-30,221	-33,447	-31,141	-30,605	-29,259	-27,927	-24,043	-22,417	-22,746	-20,257	-18,875	-19,221	-17,485	-18,361	-18,044	-17,744	-16,849	**-538,289**
Elkjel	**høylast**	**hverdag**	**B**	447,849	441,503	425,235	432,638	436,285	447,855	515,413	589,043	638,532	643,454	639,390	638,104	631,699	616,415	604,132	599,550	586,420	550,348	556,456	533,238	509,749	490,718	467,521	448,024	**12889,571**
Elkjel	**høylast**	**helg**	**A**	-3,924	-3,800	-6,290	-9,357	-10,456	-11,601	-8,443	-9,612	-12,750	-12,313	-17,663	-9,099	-8,365	-4,835	-1,756	0,098	2,143	1,704	-1,596	-4,106	-5,822	-6,207	-7,921	-8,198	**-160,169**
Elkjel	**høylast**	**helg**	**B**	425,988	431,453	415,589	418,182	422,411	423,669	452,001	457,269	472,189	485,759	485,811	503,571	500,573	492,582	465,295	465,527	462,820	464,741	469,174	468,971	460,731	457,984	456,365	452,749	**11011,404**
Elkjel	**lavlast**	**hverdag**	**A**	-20,190	-20,829	-19,613	-20,432	-20,445	-20,301	-20,618	-24,521	-28,737	-30,052	-30,569	-31,194	-31,482	-31,041	-30,251	-30,796	-30,298	-27,853	-26,904	-24,365	-22,993	-21,568	-20,516	-19,796	**-605,364**
Elkjel	**lavlast**	**hverdag**	**B**	420,315	416,822	393,742	399,727	401,357	409,795	479,844	544,315	600,589	620,049	621,963	617,173	609,829	596,422	582,623	583,795	577,699	546,821	538,112	511,956	495,302	476,396	458,466	433,298	**12336,410**
Elkjel	**lavlast**	**helg**	**A**	-18,114	-18,272	-17,438	-18,262	-18,079	-18,437	-18,785	-19,126	-20,399	-21,303	-21,766	-22,782	-22,901	-23,581	-22,038	-22,396	-22,811	-22,649	-22,204	-22,510	-22,039	-21,768	-21,358	-21,645	**-500,663**
Elkjel	**lavlast**	**helg**	**B**	394,262	387,472	370,409	373,321	372,444	377,563	418,830	423,674	439,092	459,483	475,782	487,929	485,269	484,283	460,815	458,179	461,110	461,939	463,260	467,822	462,565	458,246	453,674	443,967	**10541,390**

A.1 General Load Demand

These tables are showing the power demand for 24 hours of loads P1-P6 for both high and low demand months. These numbers are retrieved from the FASIT profiles in appendix A, with its corresponding weather data from table 5.1 and 5.2 and the number of consumers summarized in section 5.2.2.

Table A.1: General load demand for high demand months

	01	02	03	04	05	06	07	08	09	10	11	12	13	14	15	16	17	18	19	20	21	22	23	24	SUM
	0000-0100	0100-0200	0200-0300	0300-0400	0400-0500	0500-0600	0600-0700	0700-0800	0800-0900	0900-1000	1000-1100	1100-1200	1200-1300	1300-1400	1400-1500	1500-1600	1600-1700	1700-1800	1800-1900	1900-2000	2000-2100	2100-2200	2200-2300	2300-2400	0000-2400
High demand weekday P1 [kW]	2247,332	2212,594	2262,982	2194,686	2255,872	2377,584	2512,187	2754,936	2786,419	2720,005	2608,062	2517,81	2417,504	2342,822	2293,976	2382,712	2549,024	2692,532	2865,696	2820,286	2709,162	2631,788	2495,976	2266,565	59918,51
High demand weekday P2 [kW]	57,84	56,7544	57,6936	55,7456	57,0536	60,156	64,3128	72,072	71,682	68,0176	64,32	62,0688	58,7896	56,8584	56,864	60,8528	67,0996	72,9632	76,676	73,692	70,534	68,6704	65,284	58,7912	1534,792
High demand weekday P3 [kW]	56,46	55,5562	56,4768	54,6038	55,6028	58,233	62,2404	71,556	72,7635	68,0098	63,396	60,9279	57,6733	55,7022	55,637	59,1524	65,6038	72,5936	75,596	70,881	67,2955	65,4322	62,422	56,8676	1500,683
High demand weekday P4 [kW]	74,824	73,4612	74,6772	72,1648	73,7828	77,69	83,054	93,556	93,475	88,4208	83,3696	80,3852	76,1288	73,6076	73,596	78,6552	86,8306	94,7536	99,3908	95,05	90,8306	88,408	84,106	75,9156	1986,133
High demand weekday P5 [kW]	123,712	121,4628	123,4734	119,3202	121,9882	128,438	137,3054	154,714	154,621	146,2342	137,8568	132,9155	125,8767	121,706	121,685	130,04	143,5661	156,6984	164,3494	157,126	150,1368	146,1302	139,025	125,5034	3283,885
High demand weekday P6 [kW]	2740,144	2723,644	2762,651	2673,059	2736,816	2873,31	3007,635	3273,025	3388,713	3494,869	3436,519	3331,766	3201,222	3117,3362	3080,122	3161,617	3317,479	3387,405	3476,615	3285,973	3109,936	3031,898	2906,184	2702,117	74220,05

Table A.2: General load demand for low demand months

	01	02	03	04	05	06	07	08	09	10	11	12	13	14	15	16	17	18	19	20	21	22	23	24	SUM
	0000-0100	0100-0200	0200-0300	0300-0400	0400-0500	0500-0600	0600-0700	0700-0800	0800-0900	0900-1000	1000-1100	1100-1200	1200-1300	1300-1400	1400-1500	1500-1600	1600-1700	1700-1800	1800-1900	1900-2000	2000-2100	2100-2200	2200-2300	2300-2400	0000-2400
Low demand weekday P1 [kW]	1137,309	1049,766	1029,33	1006,767	907,0954	801,0952	884,5544	1024,357	960,9544	899,3276	815,9884	551,5414	426,1156	355,988	441,5024	359,2028	422,1728	636,0064	773,2762	901,0192	1076,152	1207,494	1217,176	1138,621	20022,81
Low demand weekday P2 [kW]	32,15	29,7536	29,0824	28,3944	26,09	23,5904	25,8784	31,7272	30,7872	27,7976	25,196	19,4252	16,1064	14,592	16,7224	16,1248	19,272	25,584	28,7988	30,4528	33,644	36,2856	36,048	33,2496	636,7528
Low demand weekday P3 [kW]	33,2405	31,2038	30,6172	30,0072	28,064	26,0102	28,2952	35,7931	36,4026	32,6903	29,927	24,9176	21,5772	20,586	22,4227	21,6979	24,759	31,764	34,9044	35,0314	36,617	37,8753	37,035	34,2438	725,6824
Low demand weekday P4 [kW]	42,0858	39,0664	38,2164	37,3428	34,4434	31,3128	34,2864	42,3296	41,5208	37,4416	34,0164	26,7174	22,3972	20,568	23,2592	22,4484	26,5168	34,9072	39,0666	40,8096	44,53	47,5952	47,1256	43,4896	851,4932
Low demand weekday P5 [kW]	69,6314	64,647	63,2434	61,8006	57,0147	51,8486	56,7664	70,1109	68,813	62,0481	56,3792	44,3273	37,1818	34,17	38,6133	37,2691	43,9954	57,8896	64,7667	67,6102	73,722	78,7559	77,9638	71,9506	1410,519
Low demand weekday P6 [kW]	1520,759	1449,524	1429,083	1402,766	1307,992	1201,646	1274,577	1462,407	1487,896	1518,554	1575,574	1346,676	1242,18	1204,572	1287,788	1224,85	1238,823	1397,015	1365,148	1356,072	1438,357	1578,547	1579,621	1516,506	33406,93

Appendix B

Charging Load Profiles for EV and Battery Storage

These tables are expressing the power consumed by the charging load and the implemented battery storage. Keep in mind that this is just an more precise overview of the figures that can be found in chapter 7.5 and chapter 7.6.

Table B.1: EV charging load profiles for case four, for day 6 and day 10

	01	02	03	04	05	06	07	08	09	10	11	12	13	14	15	16	17	18	19	20	21	22	23	24	SUM
	0000-0100	0100-0200	0200-0300	0300-0400	0400-0500	0500-0600	0600-0700	0700-0800	0800-0900	0900-1000	1000-1100	1100-1200	1200-1300	1300-1400	1400-1500	1500-1600	1600-1700	1700-1800	1800-1900	1900-2000	2000-2100	2100-2200	2200-2300	2300-2400	0000-2400
$P_{ev6}[kW]$	112	59	124	48	18	21	37	92	82	98	130	309	522	489	410	804	607	607	743	542	368	335	189	104	6850
$P_{ev10}[kW]$	117	170	96	123	97	126	229	181	373	711	811	948	985	985	957	948	939	1002	955	987	894	394	319	368	13715

Table B.2: Power demand for $P_{battery}$ and P_{total}

	01	02	03	04	05	06	07	08	09	10	11	12	13	14	15	16	17	18	19	20	21	22	23	24	SUM
	0000-0100	0100-0200	0200-0300	0300-0400	0400-0500	0500-0600	0600-0700	0700-0800	0800-0900	0900-1000	1000-1100	1100-1200	1200-1300	1300-1400	1400-1500	1500-1600	1600-1700	1700-1800	1800-1900	1900-2000	2000-2100	2100-2200	2200-2300	2300-2400	0000-2400
$P_{battery}[kW]$	1000	1000	1000	1000	1000	486	0	0	0	-550	-650	-486	-300	-50	0	-100	-400	-700	-900	-900	-450	0	0	0	0
$P_{total}[kW]$	1117	1170	1096	1123	1097	612	229	181	373	161	161	462	685	935	957	848	539	302	55	87	444	394	319	368	13715

Appendix C

MATLAB Code

The listings below represent all the MATLAB scripts that were described in chapter 4. These are the most significant scripts that have been used in this thesis. The remaining scripts that are not shown, are used for extracting load data from excel sheet, making tables, graphic illustration and plots.

C.1 Load_flow.m File

This is the script use to run a power flow for each individual hour, for 24 hours.

```
%% Running power flows

mpopt = mpoption('pf.alg', 'NR', 'pf.tol', 1e-4);
for i = 1:24

    %The last inputs P1(i) - P_batt(i), are optional inputs. For
    %this thesis, they are expressing the general loads, EV
    %charging load and battery storage load. These variables are
    %retrieved from an excel sheet, expressing the power demand for
    %each load. The power demand for all various loads have been
    %presented throughout this thesis.
    pf= runpf_new('system_description', mpopt, 'output', ...
        'result_description', P1(i), P2(i), P3(i), P4(i), P5(i), ...
        P6(i), Pev20_10(i), Pev20_10_batt(i), P_batt(i));

    %Retriving PD data - active power demand
    pd{1,i}  =   pf.bus(:,3);

    %Retriving VM data - voltage magnitude
    vm{1,i}  =   pf.bus(:,8);

    %Retriving QD data - reactive power demand
    qd{1,i}  =   pf.bus(:,4);

```

```
    %Retriving VA data - voltage angle
    va{1,i}  =   pf.bus(:,9);

    %Retriving P_FROM data - active power out from bus X
    p_from{1,i}=   pf.branch(:,14);

    %Retriving P_TO data - active power in to bus X
    p_to{1,i}  =   pf.branch(:,16);

    %Retriving Q_FROM data - reactive power out from bus X
    q_from{1,i}=   pf.branch(:,15);

    %Retriving Q_TO data - reactive power in to bus X
    q_to{1,i}  =   pf.branch(:,17);

end
```

C.2 System_description.m File

This MATPOWER script contains all the data regarding the network's specifications. Take note that some of the inputs are only used for DC or optimal PF, thus not valid for this thesis. In addition to that, some values have been changed during the different study cases that have been examined, thus not all values used for this thesis are shown. See a more detailed description in section 4.2.1.

```
function mpc = case_test
%CASE9    Power flow data for 9 bus, 3 generator case.
%   Please see CASEFORMAT for details on the case file format.
%
%   Based on data from p. 70 of:
%
%   Chow, J. H., editor. Time-Scale Modeling of Dynamic Networks with
%   Applications to Power Systems. Springer-Verlag, 1982.
%   Part of the Lecture Notes in Control and Information Sciences book
%   series (LNCIS, volume 46)
%
%   which in turn appears to come from:
%
%   R.P. Schulz, A.E. Turner and D.N. Ewart, "Long Term Power System
%   Dynamics," EPRI Report 90-7-0, Palo Alto, California, 1974.

%   MATPOWER


%% MATPOWER Case Format : Version 2
mpc.version = '2';

%%-----  Power Flow Data  -----%%
%% system MVA base
mpc.baseMVA = 10;

%% bus data
%   bus_i   type    Pd  Qd  Gs  Bs  area    Vm  Va  baseKV  zone    ...
    Vmax    Vmin
mpc.bus = [
    1   3   0       0       0   0   1   1   0   22  1   1.1 0.9;
    2   1   0       0       0   0   1   1   0   22  1   1.1 0.9;
    3   1   0       0       0   0   1   1   0   22  1   1.1 0.9;
    4   1   0       0       0   0   1   1   0   22  1   1.1 0.9;
    5   1   0       0       0   0   1   1   0   22  1   1.1 0.9;
    6   1   0       0       0   0   1   1   0   22  1   1.1 0.9;
    7   1   0       0       0   0   1   1   0   22  1   1.1 0.9;
    8   1   0       0       0   0   1   1   0   22  1   1.1 0.9;
    9   1   0       0       0   0   1   1   0   22  1   1.1 0.9;
    10  1   0       0       0   0   1   1   0   22  1   1.1 0.9;
    11  1   0       0       0   0   1   1   0   22  1   1.1 0.9;
];

%% generator data
%   bus Pg  Qg  Qmax    Qmin    Vg  mBase   status  Pmax    Pmin    ...
    Pc1 Pc2 Qc1min  Qc1max  Qc2min  Qc2max  ramp_agc    ramp_10 ...
    ramp_30 ramp_q  apf
```

```
mpc.gen = [
     1    0.0 0.0 300 -300     1.00     100 1    10   1    0    0    0    0    ...
          0    0    0    0    0    0    0;
];

%% branch data
%    fbus     tbus     r    x    b    rateA    rateB    rateC    ratio    ...
     angle    status   angmin   angmax
mpc.branch = [
     1    2    0.337    0.354    0    250  250  250  0    0    1    -360    360;
     2    3    0.633    0.375    0    250  250  250  0    0    1    -360    360;
     2    4    0.337    0.354    0    150  150  150  0    0    1    -360    360;
     4    5    0.633    0.375    0    300  300  300  0    0    1    -360    360;
     4    6    0.337    0.354    0    150  150  150  0    0    1    -360    360;
     6    7    0.633    0.375    0    250  250  250  0    0    1    -360    360;
     6    8    0.337    0.354    0    250  250  250  0    0    1    -360    360;
     8    9    0.633    0.375    0    250  250  250  0    0    1    -360    360;
     8    10   0.337    0.354    0    250  250  250  0    0    1    -360    360;
     10   11   0.633    0.375    0    250  250  250  0    0    1    -360    360;
];

%95mm 0.337   0.354
%50mm 0.633   0.375

%% Tr.line length
%    fbus     tbus     km
length = [
     1    2    1.2;
     2    3    8.0;
     2    4    2.0;
     4    5    0.2;
     4    6    1.0;
     6    7    1.0;
     6    8    0.5;
     8    9    1.1;
     8    10   4.5;
     10   11   3.0;
];

% Find transmission lines with no transformer connected
LINE = find(mpc.branch(:,9) ==0);

% Converting from [ohm/km] to [ohm]
mpc.branch(LINE, 3) = mpc.branch(LINE, 3).*length(LINE, 3)
mpc.branch(LINE, 4) = mpc.branch(LINE, 4).*length(LINE, 3)

%Converting resistance/reactance to pu values
zref = (mpc.bus(1,10)).^2./(mpc.baseMVA)     %Impedance base value
mpc.branch (LINE, 3) = (mpc.branch(LINE,3))/(zref);
mpc.branch (LINE, 4) = (mpc.branch(LINE,4))/(zref);
```

C.3 Runpf_new.m File

This is the MATPOWER file that contains all the necessary data in order to execute a power flow, with some small modifications for this thesis.

```

function [MVAbase, bus, gen, branch, success, et] = ...
    runpf_test(casedata, mpopt, fname, solvedcase, last1, last2, ...
    last3, last4, last5, last6, ev1,ev2, ev3)
%RUNPF  Runs a power flow.
%   [RESULTS, SUCCESS] = RUNPF(CASEDATA, MPOPT, FNAME, SOLVEDCASE)
%
%   Runs a power flow (full AC Newton's method by default), optionally
%   returning a RESULTS struct and SUCCESS flag.
%
%   Inputs (all are optional):
%       CASEDATA : either a MATPOWER case struct or a string containing
%           the name of the file with the case data (default is ...
    'case9')
%           (see also CASEFORMAT and LOADCASE)
%       MPOPT : MATPOWER options struct to override default options
%           can be used to specify the solution algorithm, output ...
    options
%           termination tolerances, and more (see also MPOPTION).
%       FNAME : name of a file to which the pretty-printed output will
%           be appended
%       SOLVEDCASE : name of file to which the solved case will be ...
    saved
%           in MATPOWER case format (M-file will be assumed unless the
%           specified name ends with '.mat')
%
%   Outputs (all are optional):
%       RESULTS : results struct, with the following fields:
%           (all fields from the input MATPOWER case, i.e. bus, branch,
%               gen, etc., but with solved voltages, power flows, etc.)
%           order - info used in external <-> internal data conversion
%           et - elapsed time in seconds
%           success - success flag, 1 = succeeded, 0 = failed
%       SUCCESS : the success flag can additionally be returned as
%           a second output argument
%
%   Calling syntax options:
%       results = runpf;
%       results = runpf(casedata);
%       results = runpf(casedata, mpopt);
%       results = runpf(casedata, mpopt, fname);
%       results = runpf(casedata, mpopt, fname, solvedcase);
%       [results, success] = runpf(...);
%
%       Alternatively, for compatibility with previous versions of ...
    MATPOWER,
%       some of the results can be returned as individual output ...
    arguments:
%
%       [baseMVA, bus, gen, branch, success, et] = runpf(...);
%
```

```
%   If the pf.enforce_q_lims option is set to true (default is ...
    false) then, if
%   any generator reactive power limit is violated after running ...
    the AC power
%   flow, the corresponding bus is converted to a PQ bus, with Qg ...
    at the
%   limit, and the case is re-run. The voltage magnitude at the bus ...
    will
%   deviate from the specified value in order to satisfy the ...
    reactive power
%   limit. If the reference bus is converted to PQ, the first ...
    remaining PV
%   bus will be used as the slack bus for the next iteration. This may
%   result in the real power output at this generator being ...
    slightly off
%   from the specified values.
%
%   Examples:
%       results = runpf('case30');
%       results = runpf('case30', mpoption('pf.enforce_q_lims', 1));
%
%   See also RUNDCPF.

%   MATPOWER
%   Copyright (c) 1996-2019, Power Systems Engineering Research ...
    Center (PSERC)
%   by Ray Zimmerman, PSERC Cornell
%   Enforcing of generator Q limits inspired by contributions
%   from Mu Lin, Lincoln University, New Zealand (1/14/05).
%
%   This file is part of MATPOWER.
%   Covered by the 3-clause BSD License (see LICENSE file for details).
%   See https://matpower.org for more info.

%%-----  initialize  -----

%% Retrieving the general load and the EV charging values
%Converting the active power demand to MW (standard for Matpower)
p1 = last1.*10.^-3;
p2 = last2.*10.^-3;
p3 = last3.*10.^-3;
p4 = last4.*10.^-3;
p5 = last5.*10.^-3;
p6 = last6.*10.^-3;
pev = ev1.*10.^-3;          %Avtive power of Charging load

%Converting the reactive power demand to MW (standard for Matpower)
q1 = p1.*tan(acos(0.95));
q2 = p2.*tan(acos(0.95));
q3 = p3.*tan(acos(0.95));
q4 = p4.*tan(acos(0.95));
q5 = p5.*tan(acos(0.95));
q6 = p6.*tan(acos(0.95));
qev = pev.*tan(acos(0.95)); %Reactive power of charging load

%This is the load simulating the resulting power demand when both ...
    EV and
```

```
%battery are combined in to 1 load. Even tho the same formula is ...
     applied
%above, it is applied here once more WITHOUT the reactive part, since
%battery has a unity power factor
% pev = ev2.*10.^-3;


%% define named indices into bus, gen, branch matrices
[PQ, PV, REF, NONE, BUS_I, BUS_TYPE, PD, QD, GS, BS, BUS_AREA, VM, ...
    VA, BASE_KV, ZONE, VMAX, VMIN, LAM_P, LAM_Q, MU_VMAX, MU_VMIN] ...
         = idx_bus;
[F_BUS, T_BUS, BR_R, BR_X, BR_B, RATE_A, RATE_B, RATE_C, ...
    TAP, SHIFT, BR_STATUS, PF, QF, PT, QT, MU_SF, MU_ST, ...
    ANGMIN, ANGMAX, MU_ANGMIN, MU_ANGMAX] = idx_brch;
[GEN_BUS, PG, QG, QMAX, QMIN, VG, MBASE, GEN_STATUS, PMAX, PMIN, ...
    MU_PMAX, MU_PMIN, MU_QMAX, MU_QMIN, PC1, PC2, QC1MIN, QC1MAX, ...
    QC2MIN, QC2MAX, RAMP_AGC, RAMP_10, RAMP_30, RAMP_Q, APF] = idx_gen;








%% default arguments
if nargin < 4
    solvedcase = '';                %% don't save solved case
    if nargin < 3
        fname = '';                 %% don't print results to a file
        if nargin < 2
            mpopt = mpoption;       %% use default options
            if nargin < 1
                casedata = 'case9'; %% default data file is 'case9.m'
            end
        end
    end
end

%% options
qlim = mpopt.pf.enforce_q_lims;         %% enforce Q limits on gens?
dc = strcmp(upper(mpopt.model), 'DC');  %% use DC formulation?


%% read data
mpc = loadcase(casedata);

%% add zero columns to branch for flows if needed
if size(mpc.branch,2) < QT
  mpc.branch = [ mpc.branch zeros(size(mpc.branch, 1), ...
       QT-size(mpc.branch,2)) ];
end

%% convert to internal indexing
mpc = ext2int(mpc, mpopt);
[baseMVA, bus, gen, branch] = deal(mpc.baseMVA, mpc.bus, mpc.gen, ...
    mpc.branch);
```

```
%% Converting the PD (power deamand) values of each PV bus
bus(3,PD)=p1;
bus(2,PD)=p2;
bus(5,PD)=p3;
bus(7,PD)=p4;
bus(9,PD)=p5;
bus(11,PD)=p6;
bus(10,PD)=pev;

bus(3,QD)=q1;
bus(2,QD)=q2;
bus(5,QD)=q3;
bus(7,QD)=q4;
bus(9,QD)=q5;
bus(11,QD)=q6;
bus(10,QD)=qev;

if ¬isempty(mpc.bus)
    %% get bus index lists of each type of bus
    [ref, pv, pq] = bustypes(bus, gen);

    %% generator info
    on = find(gen(:, GEN_STATUS) > 0);      %% which generators are on?
    gbus = gen(on, GEN_BUS);                %% what buses are they at?

    %%-----  run the power flow  -----
    t0 = tic;
    its = 0;            %% total iterations
    if mpopt.verbose > 0
        v = mpver('all');
        fprintf('\nMATPOWER Version %s, %s', v.Version, v.Date);
    end
    if dc                                   %% DC formulation
        if mpopt.verbose > 0
          fprintf(' -- DC Power Flow\n');
        end
        %% initial state
        Va0 = bus(:, VA) * (pi/180);

        %% build B matrices and phase shift injections
        [B, Bf, Pbusinj, Pfinj] = makeBdc(baseMVA, bus, branch);

        %% compute complex bus power injections (generation - load)
        %% adjusted for phase shifters and real shunts
        Pbus = real(makeSbus(baseMVA, bus, gen)) - Pbusinj - bus(:, ...
            GS) / baseMVA;

        %% "run" the power flow
        [Va, success] = dcpf(B, Pbus, Va0, ref, pv, pq);
        its = 1;

        %% update data matrices with solution
        branch(:, [QF, QT]) = zeros(size(branch, 1), 2);
        branch(:, PF) = (Bf * Va + Pfinj) * baseMVA;
        branch(:, PT) = -branch(:, PF);
        bus(:, VM) = ones(size(bus, 1), 1);
```

```
        bus(:, VA) = Va * (180/pi);
        %% update Pg for slack generator (1st gen at ref bus)
        %% (note: other gens at ref bus are accounted for in Pbus)
        %%      Pg = Pinj + Pload + Gs
        %%      newPg = oldPg + newPinj - oldPinj
        refgen = zeros(size(ref));
        for k = 1:length(ref)
            temp = find(gbus == ref(k));
            refgen(k) = on(temp(1));
        end
        gen(refgen, PG) = gen(refgen, PG) + (B(ref, :) * Va - ...
            Pbus(ref)) * baseMVA;
    else                                    %% AC formulation
        alg = upper(mpopt.pf.alg);
        switch alg
            case 'NR-SC'
                mpopt = mpoption(mpopt, 'pf.current_balance', 0, ...
                    'pf.v_cartesian', 1);
            case 'NR-IP'
                mpopt = mpoption(mpopt, 'pf.current_balance', 1, ...
                    'pf.v_cartesian', 0);
            case 'NR-IC'
                mpopt = mpoption(mpopt, 'pf.current_balance', 1, ...
                    'pf.v_cartesian', 1);
        end
        if mpopt.verbose > 0
            switch alg
                case 'NR'
                    solver = 'Newton';
                case 'NR-SC'
                    solver = 'Newton-SC';
                case 'NR-IP'
                    solver = 'Newton-IP';
                case 'NR-IC'
                    solver = 'Newton-IC';
                case 'FDXB'
                    solver = 'fast-decoupled, XB';
                case 'FDBX'
                    solver = 'fast-decoupled, BX';
                case 'GS'
                    solver = 'Gauss-Seidel';
                case 'PQSUM'
                    solver = 'Power Summation';
                case 'ISUM'
                    solver = 'Current Summation';
                case 'YSUM'
                    solver = 'Admittance Summation';
                otherwise
                    solver = 'unknown';
            end
            fprintf(' -- AC Power Flow (%s)\n', solver);
        end
        switch alg
            case {'NR', 'NR-SC', 'NR-IP', 'NR-IC'}  %% all 4 ...
                variants supported
            otherwise                       %% only power balance, ...
                polar is valid
```

```
                if mpopt.pf.current_balance || mpopt.pf.v_cartesian
                    error('runpf: power flow algorithm ''%s'' only ...
                        supports power balance, polar ...
                        version\nI.e. both ''pf.current_balance'' ...
                        and ''pf.v_cartesian'' must be set to 0.');
                end
        end
        if have_zip_loads(mpopt)
            if mpopt.pf.current_balance || mpopt.pf.v_cartesian
                warnstr = 'Newton algorithm (current or cartesian ...
                    versions) do';
            elseif strcmp(alg, 'GS')
                warnstr = 'Gauss-Seidel algorithm does';
            else
                warnstr = '';
            end
            if warnstr
                warning('runpf: %s not support ZIP load model. ...
                    Converting to constant power loads.', warnstr);
                mpopt = mpoption(mpopt, 'exp.sys_wide_zip_loads', ...
                                struct('pw', [], 'qw', []));
            end
        end

        %% initial state
        % V0    = ones(size(bus, 1), 1);            %% flat start
        V0  = bus(:, VM) .* exp(1j * pi/180 * bus(:, VA));
        vcb = ones(size(V0));           %% create mask of ...
            voltage-controlled buses
        vcb(pq) = 0;                    %% exclude PQ buses
        k = find(vcb(gbus));            %% in-service gens at v-c buses
        V0(gbus(k)) = gen(on(k), VG) ./ abs(V0(gbus(k))).* V0(gbus(k));

        if qlim
            ref0 = ref;                         %% save index and ...
                angle of
            Varef0 = bus(ref0, VA);             %%   original ...
                reference bus(es)
            limited = [];                       %% list of indices ...
                of gens @ Q lims
            fixedQg = zeros(size(gen, 1), 1);   %% Qg of gens at Q ...
                limits
        end

        %% build admittance matrices
        [Ybus, Yf, Yt] = makeYbus(baseMVA, bus, branch);

        repeat = 1;
        while (repeat)
            %% function for computing V dependent complex bus power ...
                injections
            %% (generation - load)
            Sbus = @(Vm)makeSbus(baseMVA, bus, gen, mpopt, Vm);

            %% run the power flow
            switch alg
                case {'NR', 'NR-SC', 'NR-IP', 'NR-IC'}
```

```
                if mpopt.pf.current_balance
                    if mpopt.pf.v_cartesian     %% current, ...
                        cartesian
                        newtonpf_fcn = @newtonpf_I_cart;
                    else                        %% current, polar
                        newtonpf_fcn = @newtonpf_I_polar;
                    end
                else
                    if mpopt.pf.v_cartesian     %% power, cartesian
                        newtonpf_fcn = @newtonpf_S_cart;
                    else                        %% default - ...
                        power, polar
                        newtonpf_fcn = @newtonpf;
                    end
                end
                [V, success, iterations] = newtonpf_fcn(Ybus, ...
                    Sbus, V0, ref, pv, pq, mpopt);
            case {'FDXB', 'FDBX'}
                [Bp, Bpp] = makeB(baseMVA, bus, branch, alg);
                [V, success, iterations] = fdpf(Ybus, Sbus, V0, ...
                    Bp, Bpp, ref, pv, pq, mpopt);
            case 'GS'
                [V, success, iterations] = gausspf(Ybus, ...
                    Sbus([]), V0, ref, pv, pq, mpopt);
            case {'PQSUM', 'ISUM', 'YSUM'}
                [mpc, success, iterations] = radial_pf(mpc, mpopt);
            otherwise
                error('runpf: ''%s'' is not a valid power flow ...
                    algorithm. See ''pf.alg'' details in ...
                    MPOPTION help.', alg);
        end
        its = its + iterations;

        %% update data matrices with solution
        switch alg
            case {'NR', 'NR-SC', 'NR-IP', 'NR-IC', 'FDXB', ...
                'FDBX', 'GS'}
                [bus, gen, branch] = pfsoln(baseMVA, bus, gen, ...
                    branch, Ybus, Yf, Yt, V, ref, pv, pq, mpopt);
            case {'PQSUM', 'ISUM', 'YSUM'}
                bus = mpc.bus;
                gen = mpc.gen;
                branch = mpc.branch;
        end

        if success && qlim      %% enforce generator Q limits
            %% find gens with violated Q constraints
            mx = find( gen(:, GEN_STATUS) > 0 ...
                    & gen(:, QG) > gen(:, QMAX) + ...
                        mpopt.opf.violation );
            mn = find( gen(:, GEN_STATUS) > 0 ...
                    & gen(:, QG) < gen(:, QMIN) - ...
                        mpopt.opf.violation );

            if ¬isempty(mx) || ¬isempty(mn)  %% we have some Q ...
                limit violations
                %% first check for INFEASIBILITY
```

```
        infeas = union(mx', mn')';  %% transposes ...
            handle fact that
            %% union of scalars is a row vector
        remaining = find( gen(:, GEN_STATUS) > 0 & ...
                        ( bus(gen(:, GEN_BUS), ...
                            BUS_TYPE) == PV | ...
                          bus(gen(:, GEN_BUS), ...
                              BUS_TYPE) == REF ));
        if length(infeas) == length(remaining) && ...
            all(infeas == remaining) && ...
                (isempty(mx) || isempty(mn))
            %% all remaining PV/REF gens are violating ...
                AND all are
            %% violating same limit (all violating Qmin ...
                or all Qmax)
            if mpopt.verbose
                fprintf('All %d remaining gens exceed ...
                    their Q limits : INFEASIBLE ...
                    PROBLEM\n', length(infeas));
            end
            success = 0;
            break;
        end

        %% one at a time?
        if qlim == 2    %% fix largest violation, ...
            ignore the rest
            [junk, k] = max([gen(mx, QG) - gen(mx, QMAX);
                             gen(mn, QMIN) - gen(mn, QG)]);
            if k > length(mx)
                mn = mn(k-length(mx));
                mx = [];
            else
                mx = mx(k);
                mn = [];
            end
        end

        if mpopt.verbose && ¬isempty(mx)
            fprintf('Gen %d at upper Q limit, ...
                converting to PQ bus\n', mx);
        end
        if mpopt.verbose && ¬isempty(mn)
            fprintf('Gen %d at lower Q limit, ...
                converting to PQ bus\n', mn);
        end

        %% save corresponding limit values
        fixedQg(mx) = gen(mx, QMAX);
        fixedQg(mn) = gen(mn, QMIN);
        mx = [mx;mn];

        %% convert to PQ bus
        gen(mx, QG) = fixedQg(mx);      %% set Qg to ...
            binding limit
        gen(mx, GEN_STATUS) = 0;        %% temporarily ...
            turn off gen,
```

```
                    for i = 1:length(mx)            %% (one at a ...
                        time, since
                        bi = gen(mx(i), GEN_BUS);   %%  they may be ...
                            at same bus)
                        bus(bi, [PD,QD]) = ...      %% adjust load ...
                            accordingly,
                            bus(bi, [PD,QD]) - gen(mx(i), [PG,QG]);
                    end
                    if length(ref) > 1 && any(bus(gen(mx, GEN_BUS), ...
                        BUS_TYPE) == REF)
                        error('runpf: Sorry, MATPOWER cannot ...
                            enforce Q limits for slack buses in ...
                            systems with multiple slacks.');
                    end
                    bus(gen(mx, GEN_BUS), BUS_TYPE) = PQ;    %% & ...
                        set bus type to PQ

                    %% update bus index lists of each type of bus
                    ref_temp = ref;
                    [ref, pv, pq] = bustypes(bus, gen);
                    %% previous line can modify lists to select new ...
                        REF bus
                    %% if there was none, so we should update bus ...
                        with these
                    %% just to keep them consistent
                    if ref ≠ ref_temp
                        bus(ref, BUS_TYPE) = REF;
                        bus( pv, BUS_TYPE) = PV;
                        if mpopt.verbose
                            fprintf('Bus %d is new slack bus\n', ref);
                        end
                    end
                    limited = [limited; mx];
                else
                    repeat = 0; %% no more generator Q limits violated
                end
            else
                repeat = 0;     %% don't enforce generator Q ...
                    limits, once is enough
            end
        end
        if qlim && ¬isempty(limited)
            %% restore injections from limited gens (those at Q limits)
            gen(limited, QG) = fixedQg(limited);    %% restore Qg ...
                value,
            for i = 1:length(limited)               %% (one at a ...
                time, since
                bi = gen(limited(i), GEN_BUS);      %%  they may be ...
                    at same bus)
                bus(bi, [PD,QD]) = ...              %% re-adjust load,
                    bus(bi, [PD,QD]) + gen(limited(i), [PG,QG]);
            end
            gen(limited, GEN_STATUS) = 1;               %% and turn ...
                gen back on
            if ref ≠ ref0
                %% adjust voltage angles to make original ref bus ...
                    correct
```

```
                bus(:, VA) = bus(:, VA) - bus(ref0, VA) + Varef0;
            end
        end
    end
else
    t0 = tic;
    success = 0;
    its = 0;
    if mpopt.verbose
        fprintf('Power flow not valid : MATPOWER case contains no ...
            connected buses');
    end
end
mpc.et = toc(t0);
mpc.success = success;
mpc.iterations = its;

%%-----  output results  -----
%% convert back to original bus numbering & print results
[mpc.bus, mpc.gen, mpc.branch] = deal(bus, gen, branch);
results = int2ext(mpc);

%% zero out result fields of out-of-service gens & branches
if ¬isempty(results.order.gen.status.off)
  results.gen(results.order.gen.status.off, [PG QG]) = 0;
end
if ¬isempty(results.order.branch.status.off)
  results.branch(results.order.branch.status.off, [PF QF PT QT]) = 0;
end

if fname
    [fd, msg] = fopen(fname, 'at');
    if fd == -1
        error(msg);
    else
        if mpopt.out.all == 0
            printpf(results, fd, mpoption(mpopt, 'out.all', -1));
        else
            printpf(results, fd, mpopt);
        end
        fclose(fd);
    end
end
printpf(results, 1, mpopt);

%% save solved case
if solvedcase
    savecase(solvedcase, results);
end

if nargout == 1 || nargout == 2
    MVAbase = results;
    bus = success;
elseif nargout > 2
    [MVAbase, bus, gen, branch, et] = ...
        deal(results.baseMVA, results.bus, results.gen, ...
            results.branch, results.et);
```

```
% else  %% don't define MVAbase, so it doesn't print anything



end




function TorF = have_zip_loads(mpopt)
if (¬isempty(mpopt.exp.sys_wide_zip_loads.pw) && ...
        any(mpopt.exp.sys_wide_zip_loads.pw(2:3))) || ...
        (¬isempty(mpopt.exp.sys_wide_zip_loads.qw) && ...
        any(mpopt.exp.sys_wide_zip_loads.qw(2:3)))
    TorF = 1;
else
    TorF = 0;
end
```

NTNU

Norwegian University of
Science and Technology